Neuroanatomical and Functional Characterization of the Motor Circuitry Controlling *Drosophila* Taste Behavior

Inauguraldissertation

zur
Erlangung der Würde eines Doktors der Philosophie
vorgelegt der
Philosophisch-Naturwissenschaftlichen Fakultät
der Universität Basel

von

Olivia Schwarz

aus Ueken, Schweiz

Basel, 2018

Genehmigt von der Philosophisch-Naturwissenschaftlichen Fakultät

auf Antrag von

Prof. Dr. Silvia Arber
Dr. Jan Pielage
Prof. Dr. Heinrich Reichert

Basel, den 23. Februar 2016

Prof. Dr. Jörg Schibler

„All truths are easy to understand once they are discovered; the point is to discover them"

Galileo Galilei

Contents

1. Summary

The human nervous system consists of an immense number of neurons that are highly interconnected with each other. Circuit neuroscience aims to understand how neurons are connected into functional ensembles that allow us to perceive the world with all our senses, to produce a variety of behaviors und to perform sophisticated mental tasks.

In this study, we are using the *Drosophila melanogaster* gustatory system as a model to study the principles underlying the connectivity and function of a simple sensory-motor circuit. In the adult fly, attractive and aversive substances are detected by gustatory sensory neurons that relay taste information to the primary gustatory center, the subesophageal zone (SEZ). Sweet stimuli evoke a robust and highly stereotypic motor behavior, the proboscis extension response (PER) towards the food source. This behavior can be assessed in a noninvasive manner to test for the integrity of the circuit. In addition, the proboscis extension response is an ideal behavioral model to study the neuronal control underlying the generation of a stereotypic, sequential movement in an intact animal. So far, the neuronal ensembles forming the sensory-motor circuitry within the SEZ are largely unknown.

We performed a combined behavioral and morphological screen of Gal4 driver lines to identify genetic control elements allowing the selective manipulation of individual neurons within the taste circuit. We were able to identify and functionally characterize five motoneurons, each one controlling one particular sequential step of the proboscis extension response. Furthermore, we could demonstrate that the activation of a motoneuron controlling a preceding step is neither a requirement nor the trigger for the initiation of the subsequent step. Thus, we conclude that the different steps of the PER motor sequence are mutually independent suggesting that the temporal orchestration of motoneuron activity is entirely controlled by interneurons within the central nervous system. A promising line to represent such an interneuron was identified in a second screen but needs further investigation.

The combination of opto- and thermogenetic tools with classical genetic approaches will allow us to test this assumption and to further unravel the principles underlying information processing and motor control of the taste circuitry. The concept of centrally coordinated motor control to produce stereotypic, serial behavior like the PER might be applicable to other sequential motor programs across species such as reaching or grasping in mammals.

2. Introduction

2.1. History of Circuit Neuroscience

The nervous system of a human being is presumably the most complex structure in the animal kingdom. Already more than two thousand years ago philosophers argued whether the seat of the soul lies within the brain or the heart. Ever since, the nervous system kept the attention from scientists but only the development of new techniques mainly in the 19th century led to first attempts to understand its structure and function. As a consequence of the new findings, the commonly accepted *reticular theory*, which stated that the entire nervous system is a continuous structure, lost acceptance.

The pioneering work of Santiago Ramón y Cajal in the late 19th century led to the discovery that neurons are the building blocks of the nervous system and the concept of the *neuron doctrine* (Ramón y Cajal, 1888; Ramón y Cajal, 1899). This groundbreaking finding on its own strongly implied that neurons must be connected to each other. Using the Golgi method Ramón y Cajal described a huge variety of morphologically different neuron types and created excellent depictions of their connectivity in several different structures of the central nervous system (Figure 1). This was basically the origin that laid the foundation for modern neuroscience and opened an immense number of questions, some of which we are still facing today.

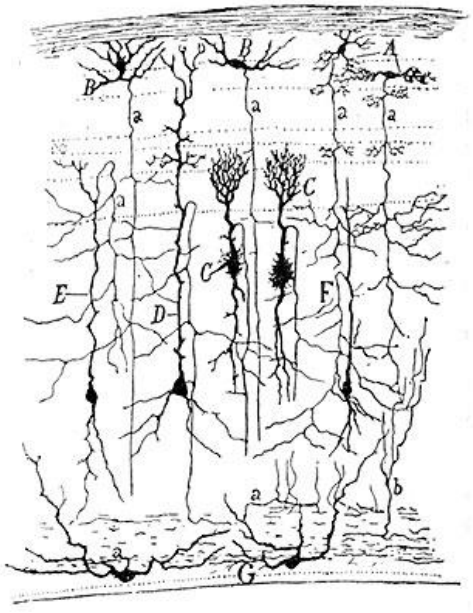

Figure 1. Drawing from Ramón y Cajal showing a section through the optic tectum of a sparrow (1905)

One of the biggest challenges in neuroscience is to unravel how neurons are specifically connected into functional circuits that allow an animal to perceive the world and take appropriate actions. The term "neuronal circuit" is used to describe a network of interconnected neurons. A circuit can consist of only two to up to 100 billion neurons if the entire nervous system of a human being is considered as a neuronal network (Meinertzhagen, 2010). Neuronal circuits form the physiological basis for sensory perception, information processing, and motor control which together form sensory-motor systems. Furthermore, the control of body homeostasis (Hamada et al., 2008), the change of motivational states to fit an animal's needs (Asahina et al., 2014; Stockinger et al., 2005), the ability to feel and express emotions (Wang and Anderson, 2010; Wang et al., 2008), the control of the circadian clock (Nitabach and Taghert, 2008),and also higher cognitive functions such as learning and memory (Davis, 2005), all depend on functional neuronal circuits.

In the nervous system, individual neurons or groups of the same type of neurons constitute the basic functional and structural units of a circuit. These units connect to each other via synapses and the connectivity pattern among these units is a major determinant of the circuit properties. That the connectivity of a neuronal network is tightly linked to its function was demonstrated by the impressive work of Roger Sperry in the middle of the 20th century. He cut the optic nerve of a frog and rotated the eye by 180° (Sperry, 1943). After spontaneous regeneration, the frog fails to catch a prey, as its attack was now targeted to the diametrically opposed direction. This experiment nicely showed that the appropriate connectivity of retinal ganglion cells onto neurons in the tectum, i.e. the restoration of the retinotopy, is required for the proper function of the retinotectal circuitry. The wiring diagram is not the only factor that defines circuit function; also the strength of each connection and the synaptic characteristics determine how neuronal circuits process information.

2.2 Development of Neuroscientific Tools

In the second half of the 20th century neuroscientific tools and techniques advanced rapidly. Further improved cell staining methods and better light microscopes as well as the development of immunohistochemistry and electron microscopy extensively increased our knowledge about the anatomy and connectivity of the nervous system in a variety of vertebrate and invertebrate species. In *Caenorhabditis elegans* for example, it was possible to successfully reconstruct the entire connectome, i.e. the complete wiring diagram of all 302

neurons present in this animal (White et al., 1986). However, functional characteristics for many of these neurons are still largely lacking.

w techniques emerged to study the functional properties of neurons. Electrophysiological recordings allowed monitoring neuronal activity at a single cell level with a very high temporal resolution (Gilbert and Wiesel, 1979; Hubel and Wiesel, 1959; Kuffler, 1953; Lee et al., 2006; Wilson and Groves, 1981). This method is based on changes of electrical properties when a neuron gets active, like the change in membrane potential and the flow of ion currents. Functional imaging visualizes neuronal activity by measuring different cellular parameters. Largescale functional imaging techniques, like functional magnetic resonance imaging or positron emission tomography, rely on changes in blood flow or cell metabolism, respectively (Bailey et al., 2005; Huettel et al., 2009) . These techniques are widely used in human diagnosis as they are noninvasive and require a conscious but motionless subject. The most popular functional imaging technique in neuroscience is the detection of calcium traces within neurons, as calcium influx mainly occurs tightly correlated with changes in the excitation of a neuron. The detection of calcium concentration is based on indicators that change fluorescent properties depending on the calcium concentration within the cytosol (Grynkiewicz et al., 1985; Heim and Griesbeck, 2004; Miyawaki et al., 1997; Nakai et al., 2001; Romoser et al., 1997). Even though the temporal resolution is not as high as compared to electrophysiological recordings, functional imaging has the great advantage that it enables recordings of multiple neurons at the same time. In combination with the *in vivo* two-photon imaging technique it became possible to look at calcium traces of many neurons simultaneously at cellular resolution in awake animals (Grewe and Helmchen, 2009; Grienberger and Konnerth, 2012; Huber et al., 2012; Kampa et al., 2011; Katona et al., 2012).

To comprehensively study the function of a neuron or neuron type within a circuit, it is essential to get a clear picture of its properties. All the above mentioned techniques on their own only resolve a little piece of the big picture. Furthermore, the combination of techniques in a single individual is very limited. For example, electrophysiological recordings can be combined with subsequent filling of the neuron with a dye which allows correlating neuronal activity and morphology (Kitamura et al., 2008). However, to systematically characterize a given neuron or neuron type in a single animal is thus far not possible. Instead of applying several techniques within a single animal, it would be more practical to apply one technique per individual and combining the data across them. A fundamental prerequisite of this

approach is the reliable targeting of exactly the same neuron or neuron type in different individuals over and over again. This became possible with the development of genetic tools.

2.2.1 Impact of Genetic Tools to Target Specific Cell Types

Before highlighting the relevance of genetic tools to study specific cell types in the nervous system it is important to explain the term *cell type*. There is not a single decision criterion that ultimately defines the type of a cell. Neurons are classified into cell types using many different parameters including cell body position, morphology of dendritic arborization, axonal projection, gene expression, electrophysiological properties, neurotransmitter and receptor expression profile, and its functional role for an animal's behavior. As a consequence, two individual neurons can belong to the same or to a different cell type depending on which criteria are taken into account. Therefore, it is the combination of criteria that specifies a cell's identity. Interestingly, some of these criteria can even correlate with each other. In *Drosophila* for example, all olfactory receptor neurons expressing the same olfactory receptor project to the same glomerulus within the antennal lobe, showing a highly specific correlation between receptor expression and connectivity (Gao et al., 2000; Vosshall et al., 2000).

All cells of an animal contain exactly the same genome. However, each cell has a characteristic gene expression profile that could be completely different from another cell. Housekeeping genes are universally expressed in all the cells of an animal, as for example genes that encode for basic cytoskeletal components. In contrast, luxury genes are highly specific to a certain type of cells as for example the expression of choline acetyltransferase in cholinergic neurons. Moreover, a recent study analyzed the expression of different transcription factors in leg motoneurons of *Drosophila* melanogaster and identified one transcription factor that is only expressed in 3 neurons in the whole nervous system (Enriquez et al., 2015). This mosaicism of gene expression among neurons is the basis for the generation of transgenic tools to target defined sets of neurons.

Cis-regulatory elements, like enhancers and promoters, are regions of non-coding DNA that serve as transcriptional regulators to specify the expression of nearby genes. These elements can also be taken to drive the expression of a transgene (Figure 2A). The enhancer trap for example uses endogenous enhancers to drive the expression of a transgene (Bellen et al.,

1989; Bier et al., 1989; Brand and Perrimon, 1993; Hayashi et al., 2002; O'Kane and Gehring, 1987). An enhancer trap construct is randomly integrated into the genome and usually contains a transposable element, a minimal promoter, and a gene of interest. Nearby enhancer regions determine the expression of this construct which often mimics the expression pattern of the gene that is naturally regulated by this specific enhancer.

In contrast, a variety of approaches fuses endogenous enhancer/promoter regions to a transgene of interest and inserts this construct into the host genome (Figure 2B). Similar to the enhancer trap strategy, the expression of the transgene usually mimics the expression pattern of the endogenous gene regulated by this specific enhancer/promoter. One resulting advantage of these approaches is that the transgene is expressed more independently of its insertion site. Another big advantage is that the enhancer/promoter region can be cut in fragments often leading to sparse expression of the transgene in only small populations of cells (Pfeiffer et al., 2008). This restriction of expression is essential to study the structure and function of neuronal circuits at a single cell level (further introduced in chapter 2.3.1)

The fact that the constructs are inserted into the genome means that they can be inherited to the next generation opening the door to study the same set of neurons in different individuals over and over again. Due to the universal DNA code among species, the expressed transgene of interest can be any gene of any species. By expressing for example the gene that encodes the green fluorescent protein (GFP) from jellyfish enables the visualization of neuronal morphology. Up to now thousands of different transgenes can be expressed allowing not only visualization but also activation and inactivation of neurons, monitoring of neuronal activity, knockdown of proteins to manipulate cell signaling pathways, to mention some of the most important ones to pursue contemporary circuit neuroscience (Baines et al., 2001; Halfon et al., 2002; Kitamoto, 2001; Krashes et al., 2009; Nakai et al., 2001; Pfeiffer et al., 2010; Pielage et al., 2005; Yeh et al., 1995).

2.3 *Drosophila* as a Model System to Study Circuit Neuroscience

The fruit fly *Drosophila melanogaster* has a long and successful history in research due to many different advantages in comparison to vertebrates. Fruit flies are small, need little amount of space and food, and are cheap to maintain even if cultivated at large quantities. The

generation time is short and the fecundity high allowing the analysis of many individuals within a short time period.

The nervous system of a fruit fly contains about 100.000 neurons and thus about one thousand times less than a mouse and one million times less than a human being (Meinertzhagen, 2010). Nevertheless, the fruit fly has a rich repertoire of complex behaviors that can be studied. These include walking, flying, courtship and mating, grooming, feeding and drinking, aggression, the expression of a circadian rhythm, and learning and memory to adapt their behavior (Asahina et al., 2014; Davis, 2005; Dethier, 1976; Hall, 1994; Hampel et al., 2015; Mendes et al., 2013; Nitabach and Taghert, 2008; Sadaf et al., 2015; Wang and Anderson, 2010; Wang et al., 2008). Thus, the reduced numerical complexity of the nervous system while still able to allow the expression of a rich repertoire of complex behaviors is extremely beneficial to gain insights into how the activity of individual neurons functionally contribute to the expression of a specific behavior and how they must be connected within the circuitry.

Even though mammals and flies are phylogenetically different, their nervous systems share several similarities. In both systems, neurons communicate with each other at highly specialized sites called synapses which have a common protein composition (Bellen et al., 2010). In both cases, the change in membrane potential and the propagation of action potentials is mainly regulated by sodium, potassium and calcium channels. In addition, they have common neurotransmitters like glutamate, acetylcholine, and GABA. Besides the similarities in cell biological properties, flies and mammals express similar behaviors, as for example walking, feeding, and mating, which are essential for their survival and reproduction. This suggests that identifying the working principles of neuronal circuits underlying these specific behaviors in the fly, might also provide insights into mammalian circuit neuroscience. On top of that, and probably the most important reason why *Drosophila* has been used to study a huge variety of biological questions, is the abundance of powerful genetic tools that are extremely successfully applied in the fruit fly.

2.3.1 Manipulation and Characterization of Neuronal Circuits Using Genetic Tools

The genome of *Drosophila melanogaster* was the first genome of an insect and only the second one in the animal kingdom that has been fully sequenced (Adams et al., 2000).The fly has 4 chromosomes, 3 autosomes and 1 sex chromosome, and an estimated number of about

13.600 genes. Importantly, many genes of the fruit fly are conserved during evolution and have homologues in vertebrates (Zhao and Hortsch, 1998).

There are different ways to genetically target neurons, like for example the direct fusion of an enhancer/promoter to the desired gene as introduced above. In these approaches, cis-regulatory elements directly control the expression of a transgene. A more elegant way to express a gene of interest in genetically targeted cells is to use a binary expression system (Figure 2C). The development of the first binary expression system in the fly, the Gal4-UAS system, represents a major hallmark in *Drosophila* neurogenetics (Brand and Perrimon, 1993; Fischer et al., 1988). Gal4 is a yeast transcription factor which activates the expression of any gene that is placed downstream of a UAS (Upstream Activation Sequence) element. In this system, two different transgenes must be present in the genome of the same fly. The first construct contains the Gal4 sequence that is under the control of a cis-regulatory element which is either present endogenously (enhancer trap) or fused to the Gal4 sequence. This construct allows for the spatial control of Gal4 expression given by the enhancer/promoter that drives its expression. Transgenic fly lines expressing such a construct are usually called *driver lines*. The second construct consists of the UAS element upstream of a gene of interest which is consequently only expressed in cells where Gal4 is present and active. The gene of interest could be any gene, among the most popular ones are those that either encode a protein to visualize a neuron's morphology, or that enable manipulation or monitoring its activity. Transgenic fly lines containing such a construct are usually called *reporter lines*. In addition, other binary expression systems like the LexA-LexAop system (Lai and Lee, 2006) and the QF-QUAS system (Potter and Luo, 2011) have been developed that are very useful for intersectional genetic approaches.

2.3.1.1 Gal4 Driver Lines

Up to now, many thousands of Gal4 expressing transgenic fly lines exist which are used to reproducibly target a specific set of neurons. Earlier studies used the enhancer trap technique to generate driver lines (Figure 2A) (Bellen et al., 1989; Bier et al., 1989; Brand and Perrimon, 1993; Hayashi et al., 2002; O'Kane and Gehring, 1987). Even though very powerful, this technique also has limitations. As P-element insertion into the genome is random, the enhancer/promoter that drives Gal4 expression is unknown. This excludes the possibility to use the enhancer/promoter fragment to generate for example LexA or Gal80 driver lines with the same expression pattern (see below). On the other hand, enhancer trap

lines often recapitulate the full expression pattern of a particular gene. Therefore, the expression patterns of enhancer trap lines are usually too broad to study individual neurons.

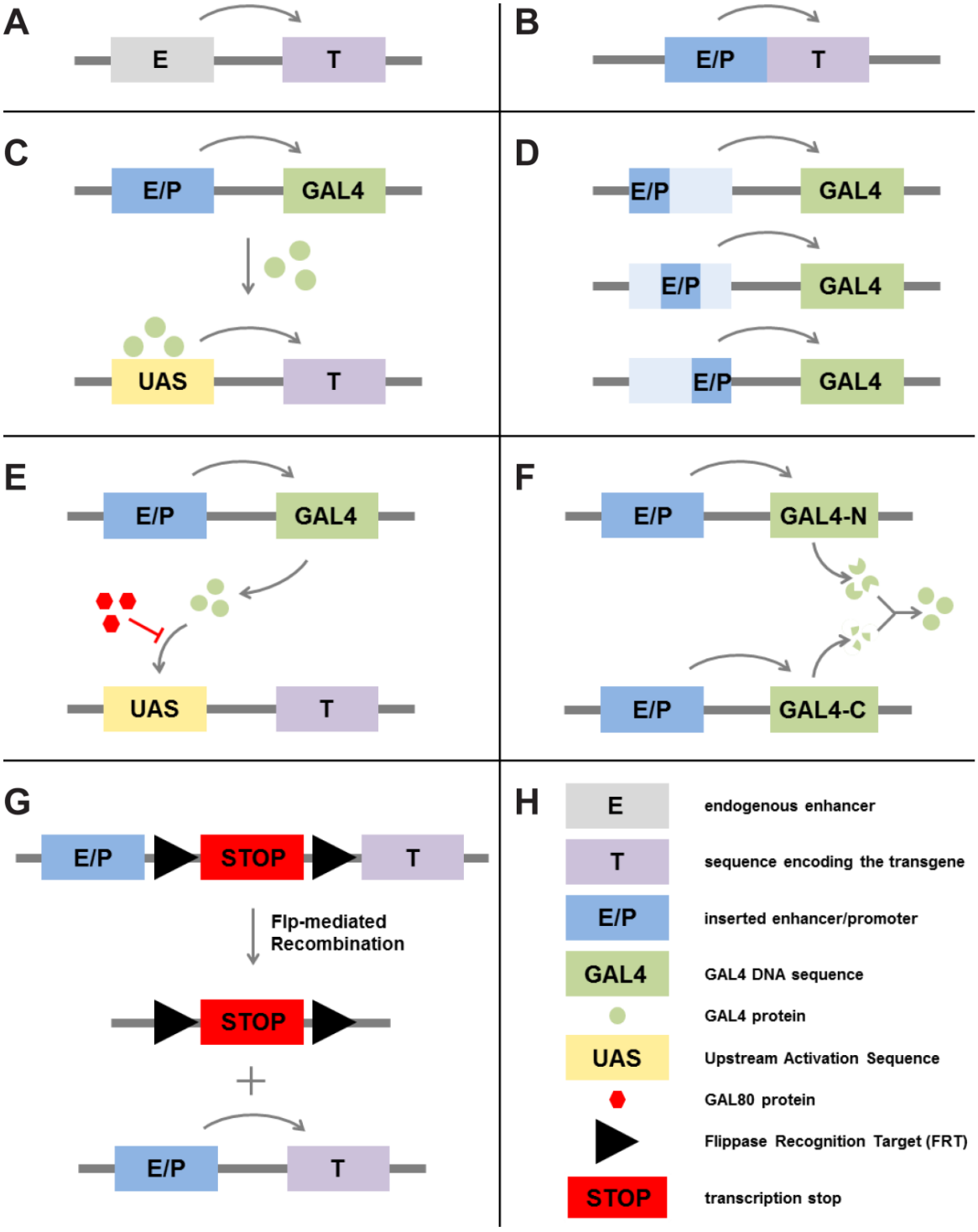

Figure 2. Schematic illustrations of genetic tools to target specific cell types
(A) Enhancer trap (B) Insertion of enhancer/promoter and transgene fusion-constructs (C) Gal4/UAS binary expression system (D) Enhancer-fragments driving Gal4 expression (E) GAL80 inhibits Gal4-activity (F) split-Gal4 strategy (G) Flippase-FRT system (H) Legend of the used symbols
(Modified from: Luo et al.; 2008; Venken et al., 2011)

The Rubin Collection

More recently, a huge collection of enhancer-Gal4 lines was generated to encompass these limitations (Jenett et al., 2012). For this purpose, almost a thousand genes from the fly genome were selected that are thought to be expressed in the nervous system as for example genes encoding neuropeptides, transcription factors, receptors, transporters, and ion channels (Pfeiffer et al., 2008). Corresponding upstream and downstream flanking transgenic regions as well as intronic regions were cut into fragments between 300 and 3.000 bases and therefore likely contain parts of enhancers or even complete enhancer regions (Figure 2D). These fragments were cloned into a vector together with a minimal promoter, the Gal4 sequence, and the *white* gene. These constructs were then inserted into the genome of the fly at a defined genomic location by site-specific recombination. Up to now, this collection contains about 7.000 transgenic fly lines. Enhancer-Gal4 lines from this collection, also called Rubin-Gal4 lines or GMR-Gal4 lines, have several advantages. First, the expression pattern is often very sparse compared to enhancer trap Gal4 lines. This is due to the fact that enhancer regions are cut into small fragments, also known as *enhancer bashing*. Second, the sequence of the genomic fragment driving Gal4 expression is known. This allows the generation of different kinds of driver lines (e.g. LexA instead of Gal4), that exactly recapitulate the same expression pattern as the original Gal4 driver line. This possibility is supported by the fact that site-specific integration into the same genomic location equalizes the effects of endogenously present cis-regulatory elements on construct expression among the lines (Bischof et al., 2007; Groth et al., 2004). Third, the expression patterns of all GMR-Gal4 lines are summed up in a database which is publically available (https://www.janelia.org/project-team/flylight). Similar to vertebrates, the brain of the fly consists of distinct areas, some of which are highly specific for a particular sense or to produce specific behaviors (Yarmolinsky et al., 2009). Thus, comparing the expression patterns provided by the database with the brain area of interest allows preselection of potentially interesting lines for a certain project. Forth, the number of enhancer-Gal4 lines is huge, each with its characteristic expression pattern. It is very likely, that all lines together cover the entire fly nervous system, which makes this collection an attractive tool for virtually all neuroscientific research areas in *Drosophila*.

Intersectional Strategies

Intersectional methods can be applied to further restrict Gal4 expression either spatially or temporally. The most common way to spatially restrict Gal4 expression is to co-express GAL80, an inhibitor of Gal4 (Lee and Luo, 1999) (Figure 2E). If for example Gal4 is

expressed in A and B, and GAL80 is only expressed in B, Gal4-activity will be restricted to subpopulation A.

Another intersectional strategy uses split-Gal4 to restrict Gal4 activity (Luan et al., 2006) (Figure 2F). Here, Gal4 is split into an N- and C-terminal half where each part is under the control of a different enhancer. The functional Gal4 protein can only be formed in neurons expressing both parts. If one part is expressed in A and B and the other part is expressed in B and C, Gal4 activity is only turned on in subpopulation B.

A different approach combines the Gal4-UAS binary expression system with the Flp/FRT recombination system (Golic and Lindquist, 1989). A genomic sequence that is flanked by FRT (Flippase Recognition Target) sites is cleaved out in cells that coexpress Flippase (Flp). Flanking a stop-cassette with FRT sites in front of a transgene will lead to transgene expression in neurons, where Flp is active (Struhl and Basler, 1993) (Figure 2G). Alternatively, flanking the Gal80 sequence itself with FRT-sites will lead to GAL80 expression in neurons, where Flp is not active, i.e. Gal4 is only active in neurons that co-express Flp (Gordon and Scott, 2009).

The most commonly used method to temporally regulate transgene expression is based on a temperature-sensitive mutation of Gal80, $Gal80^{ts}$ (McGuire et al., 2003). This is particularly important to avoid any unintentional side effects of transgene expression during development. At the permissive temperature, $GAL80^{ts}$ can fully deploy its function and inhibits Gal4-activity. At any given time, flies can be shifted to the restrictive temperature. Since flies are ectotherm, their body temperature quickly adapts to the outside temperature. Consequently, $GAL80^{ts}$ does not any longer inhibit Gal4-activity, thereby enabling Gal4-induced transgene expression.

2.3.1.2 Reporter Lines

The beauty of a binary expression system is that one can combine every single driver line with every available reporter line simply by crossing females and males with the right genotype. The offspring can be analyzed about 2 weeks later which is far less than generating a transgenic line for each desired combination which usually takes months to years. In addition, the nervous system of the fruit fly is highly stereotypic, meaning that one can, in theory, find the same neuron in every individual (Jefferis et al., 2002). Thus, combining a given Gal4 driver line with different UAS-reporter lines allows to “ask” the same set of neurons different questions: What is the morphology? Where do they receive input and where do they send their output? What neurons lie upstream and downstream? What

neurotransmitter do they express? What stimulus can excite these neurons? How do they contribute to a specific behavior? What happens upon artificial activation or inhibition on a behavioral level? All these questions and many more can be addressed enabled by the generation of diverse and powerful reporter lines.

Markers

Reporters expressing fluorescent proteins are the most commonly used reporters to study the morphology of a neuron (Halfon et al., 2002; Pfeiffer et al., 2010; Yeh et al., 1995). Membrane-tagged fluorescent proteins further improved visualization of fine neurite structures (Lee and Luo, 1999; Pfeiffer et al., 2010; Ritzenthaler et al., 2000). Other reporters even allow differentiating between dendritic and axonal arborization. These reporters express fluorescently tagged proteins that are specific for axons or dendrites, respectively (Nicolai et al., 2010; Zhang et al., 2002). This is particularly important in insects because the distinction between the axonal and the dendritic arborization just based on morphology is not as clear as in vertebrates. Active zones can be visualized by fusing a fluorescent protein to the presynaptic active zone marker Bruchpilot (Wagh et al., 2006). Additional markers are available to label organelles like for example the nucleus, mitochondria, the endoplasmatic reticulum, or the Golgi complex (LaJeunesse et al., 2004; Shiga et al., 1996; Yasunaga et al., 2006).

Manipulation of neuronal activity

As already described above, the fly is equipped with a rich repertoire of complex behaviors. Remote control of neuronal activity in freely behaving flies has an enormous potential to identify neurons that are necessary and sufficient to produce a certain behavior.

To test the requirement of a neuron for the production of a specific behavior, one has to subtract its function from the circuit. Elimination of a neuron can for example be achieved by expressing proapoptotic factors that trigger the endogenous cell death pathway (Wing et al., 1998; Zhou et al., 1997). Other approaches make use of the toxicity of certain proteins. Diphtheria toxin A induces cell death by inhibiting protein synthesis and tetanus toxin cleaves synaptobrevin and thereby blocks neurotransmitter exocytosis (Han et al., 2000; Sweeney et al., 1995). Neuronal activity can also be blocked by expressing the inward rectifying potassium channel Kir2.1 which hyperpolarizes the neuron and prevents membrane depolarization (Baines et al., 2001; Paradis et al., 2001). A more elegant way to inhibit neuronal activity is to express a dominant-negative, temperature-sensitive version of Dynamin

called Shibire^{ts} (Kitamoto, 2001). Flies can be raised and tested at the permissive temperature where the neurons function normally. This has the advantage to circumvent any developmental defects and to reduce the possibility for compensation by other neurons. Upon shifting the fly above the restrictive temperature the neurons become silent. Dynamin is a GTPase required for endocytosis and thus responsible for neurotransmitter recycling at presynaptic sites (Cremona and De Camilli, 1997; Poodry, 1990; van der Bliek and Meyerowitz, 1991). This means, that neuronal activity is only blocked as soon as the presynaptic vesicle pool is depleted.

On the other hand, artificial activation of neurons can be used to test for their sufficiency to elicit a specific behavior. The most common ways to increase neuronal activity is to express sodium channels that either open upon heat/cold or light stimulation (Bautista et al., 2007; Boyden et al., 2005; Peabody et al., 2009; Rosenzweig et al., 2005; Sineshchekov et al., 2002). Thermogenetic tools, like the heat-activated sodium channel TrpA1 (Hamada et al., 2008; Rosenzweig et al., 2005; Rosenzweig et al., 2008), have the advantage that heat fully penetrates the fly and also reaches neurons that are located deeply within the brain. In contrast, optogenetic tools have a great temporal resolution. Channelrhodopsin2 is a 470 nm light-gated cation channel that serves as a photoreceptor in algae to control phototaxis and can be used to artificially activate neurons (Boyden et al., 2005; Nagel et al., 2005; Sineshchekov et al., 2002). More sensitive, red-shifted versions of Channelrhodopsin2 can be even excited through the adult cuticle (Inagaki et al., 2014; Klapoetke et al., 2014; Zhang et al., 2008a). In addition, red-light is not part of the fly's visual spectrum which is beneficial for behavioral studies to avoid unnecessary artifacts.

Sensors

To test the necessity and sufficiency of a neuron or a set of neurons as described above is one way to correlate neuronal activity to behavior. Another way to understand how information is encoded by neuronal activity is to directly monitor neuronal activity in response to certain sensory stimuli or while performing a specific behavior. Functional live-imaging is widely used to record neuronal signals simultaneously in several neurons (Grewe and Helmchen, 2009; Grienberger and Konnerth, 2012; Huber et al., 2012; Kampa et al., 2011; Katona et al., 2012). Genetically encoded calcium indicators (GECIs) are fluorescent activity sensors that change fluorescent properties upon calcium influx into the neuron, a correlate of neuronal activity (Baird et al., 1999; Griesbeck, 2004; Nagai et al., 2001). The single-fluorophore sensor GCaMP (Nakai et al., 2001) has a high signal-to-noise ratio and has been extensively

used in *Drosophila* for example to reveal odor and taste representation in the brain (Harris et al., 2015; Wang et al., 2003; Wang et al., 2004). Other sensors report for example changes in voltage (Dimitrov et al., 2007; Sakai et al., 2001; Siegel and Isacoff, 1997) or changes in pH due to synaptic vesicle fusion (Miesenböck et al., 1998; Sankaranarayanan and Ryan, 2000).

Testing Connectivity

The connectivity between the neurons as well as the strength and type of these connections determine how information is relayed and processed within a circuitry. It is still a big challenge to show that two neurons are functionally connected to each other. One way to show that two neurons can in theory be connected to each other is simply by showing colocalization. Preferentially, the two neurons are genetically targeted by two different and sparse driver lines which allow high resolution imaging of individual projections and the application of two different kinds of binary expression systems. This has the advantage that the two lines can be labeled with two distinct cytosolic or membrane-tagged fluorescent proteins of different colors. Spots where the two markers come close to each other mark potential synapses. Another way to show potential synapses is to split GFP into two non-fluorescent parts, each separately expressed in one line (Feinberg et al., 2008). If a neuron from one line comes close to a neuron from the other line, the two complementary parts bind and reconstitute a fully functional GFP. This method is called GRASP (GFP Reconstitution Across Synaptic Partners) (Feinberg et al., 2008). Another approach uses photoactivatable fluorescent proteins that change fluorescent properties due to a light-induced chemical reaction (Ando et al., 2002). By shining a bright light spot onto a small region of interest, for example a neuron whose connectivity should be investigated, neurons with projections close enough to the spot can be identified.

Different trans-synaptic tracers have been successfully applied in vertebrates (Horowitz et al., 1999; Wickersham et al., 2007). However, so far no functional trans-neuronal labelling technique exists in the fly. All the above mentioned techniques to study circuit connectivity only allow conclusions about the proximity of two neurons but give no information about the presence of functional synapses. Other approaches focus on the functional connectivity of neurons within a circuit. It is for example possible to activate an upstream neuron by optogenetic means, and to perform calcium imaging or electrophysiological recording in a downstream neuron (Klapoetke et al., 2014). Even if activity can be measured in the downstream neuron it does not rule out the possibility of additional synapses in between the

two neurons. Up to now, the only way to visualize synapses is by electron microscopy which can also be done on genetically targeted neurons.

In summary, *Drosophila* represents an attractive model organism to study circuit neuroscience due to its easy handling, the rich repertoire of complex behaviors, the reduced numerical complexity and stereotypy of the nervous system, and the enormous power of the genetic. Reproducible genetic targeting of small sets of neurons in combination with labeling, activation, inactivation, and monitoring techniques opened the door to thoroughly study the structure, function, and connectivity of neurons within a circuitry.

2.3.2 The Adult Taste Circuitry of *Drosophila*

Sensory systems allow the perception of the world by translating physical and chemical inputs from the environment into neuronal activity and are thus essential for an animal's behavior. In particular, the sense of taste is crucial for the survival of nearly all animals as it enables the evaluation and discrimination of potential food sources and harmful chemicals prior to ingestion. While we have a good understanding about taste cue detection by sensory neurons (Hiroi et al., 2004; Thorne et al., 2005; Thorne et al., 2004), there is only little knowledge about the neuronal ensembles that build up the circuitry and how they process taste information.

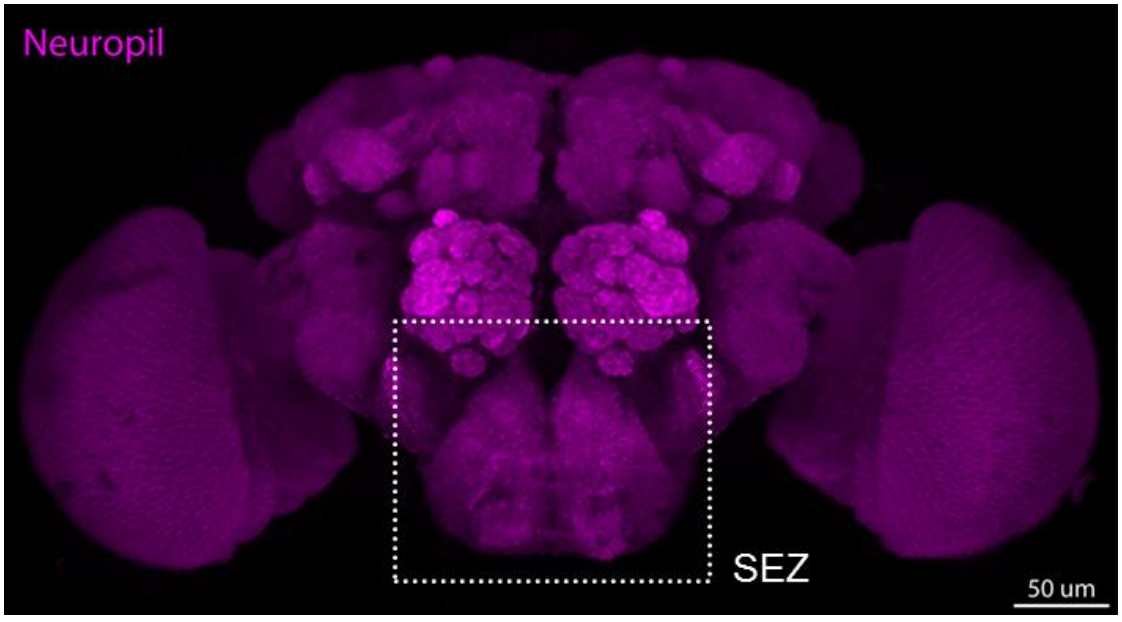

Figure 3. The adult *Drosophila* brain
The neuropil is visualized using the presynaptic active zone marker Bruchpilot (magenta). The white, dotted square indicates the location of the SEZ.

In the fly, attractive and aversive chemical substances are detected by gustatory sensory neurons (GSNs) that reside in sensilla or in internal mouthparts (Singh, 1997; Stocker, 1994). Taste sensilla are mainly present at the very tip of the proboscis, the feeding organ of a fly, as well as on the legs, wings, and the ovipositor (Clyne et al., 2000; Montell, 2009; Stocker, 1994; Thorne et al., 2004). Each sensillum contains 2-4 GSNs and a single mechanosensory neuron (Falk, 1976). Similar to the situation in mammals, gustation in flies is based on a very limited number of modalities that innately induce either acceptance (e.g. sweet) or rejection (e.g. bitter) behavior (Hiroi et al., 2004; Yarmolinsky et al., 2009).

GSNs express a combination of gustatory receptors (GRs) (Clyne et al., 2000; Dunipace et al., 2001; Scott et al., 2001) and send axons to the most ventral region within the fly brain (Figure 3), the subesophageal zone (SEZ, nomenclature according to Ito et al., 2014) (Dunipace et al., 2001; Stocker, 1994; Thorne et al., 2004; Wang et al., 2004). Interestingly, sweet GSNs, marked by the expression of Gr5a, also express receptors that are specific for compounds triggering acceptance behavior (i.e., sugar, low salt concentration) (Hiroi et al., 2004). In agreement, bitter GSNs, marked by the expression of Gr66a, coexpress receptors that are specific for compounds triggering rejection behavior (i.e., bitter, high salt concentration) (Hiroi et al., 2004).

Projections from sweet and bitter GSNs stay segregated within the SEZ (Figure 4) (Wang et al., 2004). Moreover, whole-brain calcium imaging showed that they activate different neuronal population within the SEZ and higher brain areas (Harris et al., 2015). The decision of a fly to eat or not to eat can be influenced by a variety of circumstances despite the chemical identity of the tastant, including starvation level, daytime, arousal, previous experience, and other internal and external states (Chatterjee and Hardin, 2010; Chatterjee et al., 2010; Dethier, 1976; Masek and Scott, 2010; Menda et al., 2011; Shiraiwa, 2008; Shiraiwa and Carlson, 2007). It was for example shown that starvation enhances dopamine release onto sugar-sensing GSNs resulting in an increase in sugar-evoked calcium influx, thereby increasing sugar sensitivity (Inagaki et al., 2012).

The question, how neuronal circuits encode the behavior of animals is probably best addressed by analyzing sensory-motor circuits, where input and output can be easily controlled and monitored. The taste sensory-motor system of the fruit fly fulfills these criteria and is very well suited to study circuit-related questions due to several reasons. First, the

sensory input into the system only consists of a few basic modalities and can be applied in a highly controllable, reproducible, and noninvasive manner simply by stimulating taste sensilla on the proboscis or on the legs with chosen tastants in living flies (Shiraiwa and Carlson, 2007).

Figure 4. Projections of sweet and bitter sensory neurons stay segregated within the SEZ.
Sensory neurons are marked by the expression of mCD8-GFP (green) and the neuropil is visualized using the presynaptic active zone marker Brp (magenta).

Second, the sensory input is relayed into a discrete brain region, the subesophageal SEZ (Dunipace et al., 2001; Stocker, 1994; Thorne et al., 2004; Wang et al., 2004), which only consists of a few thousands of neurons and also contains motoneuron cell bodies and arborization (Rajashekhar and Singh, 1994). Thus, the taste circuitry seems to be relatively simple and most of the information integration and processing from detection to behavior on a primary level likely occurs within the SEZ. Third, palatable tastants evoke an innate motor behavior, the extension of the proboscis towards the food source that is followed by ingestion. This behavior can be analyzed and quantified in a noninvasive manner to test the integrity of the circuit (Shiraiwa and Carlson, 2007). Forth, taste mainly acts in a single behavioral context, meaning that it mainly regulates feeding behavior. This restriction likely reduces overall circuit complexity. Fifth, the taste system is not a reflex circuitry. Its response to sensory stimuli can be modulated either by other external or internal stimuli or in response to

experience (Chatterjee and Hardin, 2010; Masek and Scott, 2010; Menda et al., 2011; Shiraiwa, 2008). This opens the door to study how neuromodulation is superimposed on the circuitry to influence its output and how and where learning is integrated into the circuitry.

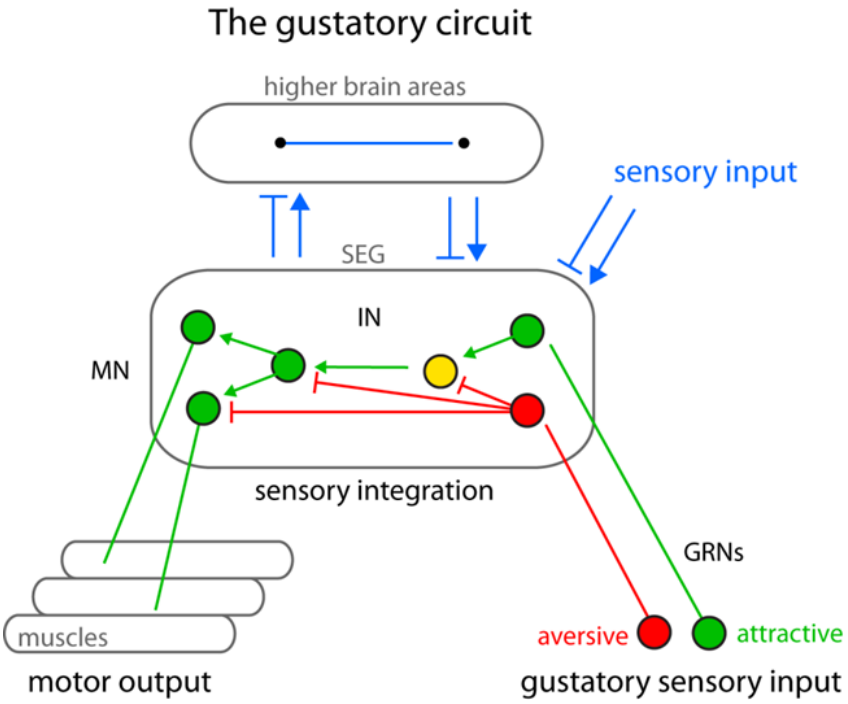

Figure 5. Schematic illustration of the *Drosophila* taste circuitry
Gustatory sensory neurons (GSN) of the proboscis and the legs of *Drosophila* project to the subesophageal zone (SEZ). They are connected through local interneurons (IN) to motoneurons (MN) that project to muscles controlling the extension, retraction, and pumping movements of the proboscis. In addition, the SEZ projects to and receives input from other brain areas for intermodal integration

2.4 Motor Control

It is a fundamental challenge of contemporary neuroscience to fully characterize a sensory-motor circuit from the sensory neurons in the periphery, via the interneurons that process and relay information, to the motoneurons that activate a specific set of muscles to execute an appropriate motor response. A sensory-motor circuitry can also be considered as a summation of the sensory circuit, different local circuits, and the motor circuit. Thus, analyzing different pieces separately will help to gain insights into the working principle of the entire sensory-motor circuitry that might also have the potential to be translated to other circuits among different species.

The coordinated movement of body parts requires the precise temporal activation of motoneurons innervating the corresponding musculature. In vertebrates as well as in invertebrates, several rhythmic and stereotypic movements such as swimming, walking,

feeding, and breathing are under the control of central pattern generators (CPGs), which generate rhythmic motor output through interactions among central neuronal elements even in the absence of any external input (Delcomyn, 1980; Gray, 1950; Marder and Bucher, 2001; Marder et al., 2005; Marder and Calabrese, 1996). Extensive work shed light on the cellular basis and the connectivity that build up such CPGs. In mammals for example, genetically different classes of spinal interneurons, V0, V1, V2, and V3, control different aspects of limbed locomotion such as rhythm generation, the speed of locomotion, left-right coordination, and flexor-extensor alternation (Crone et al., 2008; Gosgnach et al., 2006; Lanuza et al., 2004; Zhang et al., 2014; Zhang et al., 2008b). In invertebrates for example, the work on the stomatogastric CPG in crustaceans also revealed the impact of different neuromodulators and command-like interneurons on CPG activity to produce dynamic motor patterns (Marder et al., 2005; Marder and Thirumalai, 2002; Nusbaum and Beenhakker, 2002; Nusbaum et al., 2001).

On the other hand, much less is known about the neuronal control of sequential motor behaviors, such as grasping, grooming, retraction responses, or singing in songbirds. This type of sequential motor behaviors are not produced in a rhythmic manner but follow a fixed sequence of serial actions. Several different models evolved to account for the stereotypy of the temporal ordering of the motor output. For example the crayfish escape behavior occurs as a chained reflex in which each reflex action causes sensory feedback appropriate to elicit the next reflex (Reichert, 1981). On the other hand, the high temporal precision of song syllables in a zebra finch song motif is thought to arise from a synaptically connected chain of neurons in the premotor nucleus HVC (Long et al., 2010). In addition, a hierarchical suppression model can be applied to explain the sequential ordering of grooming movements in the fruit fly where motor programs that occur first suppress those that occur later in the sequence (Seeds et al., 2014).

2.4.1 The Proboscis Extension Response as a Model to Study Sequential Motor Behavior

The proboscis is a single appendage elongating from the head of different vertebrates and invertebrates. In the fly and other insects, the proboscis is the feeding organ and used to test the chemical composition of potential food sources (Dethier, 1976). Activation of an oscillatory pump situated within the proboscis leads to the ingestion of the food through the esophagus (Dethier, 1976; Miller, 1950). In addition, male flies also use the proboscis to taste

the pheromones and other carbohydrates on the cuticle of female flies prior to mating (Hall, 1994; Nichols et al., 2012). By default, the proboscis resides folded and retracted in a head cavity. The proboscis extension response (PER) elicited by a positive gustatory stimulus has widely been used as a measure for taste circuit integrity and sensitivity (Shiraiwa and Carlson, 2007). Additionally, the PER assay has been intensely and successfully used to study associative learning in honeybees and bumblebees (Hammer et al., 2009; Hori et al., 2007; Komischke et al., 2002; Riveros and Gronenberg, 2009). Movement of the proboscis and pumping of the food is executed by 13 bilateral muscles (Miller, 1950). Backfilling experiments of some of these muscles revealed that each muscle is innervated by one to three motoneurons and additionally gave insights into motoneuron cell body position, dendritic arborization, and nerve projection (Rajashekhar and Singh, 1994). More recently, Gal4 driver lines expressed in proboscis motoneurons allowed studying the functional contribution of muscle 9 for proboscis movement and muscle 11 and 12 for pumping (Gordon and Scott, 2009; Manzo et al., 2012; Tissot et al., 1998). However, the individual functions of the other muscles are unknown and difficult to predict simply based on the anatomy. In addition, genetic control and functional information of additional motoneurons innervating the proboscis musculature is still missing.

The extension of the proboscis is very well suited to study a neuronal circuitry underlying the production of a sequential motor behavior for many reasons. The PER is an innate motor behavior that can reliably be elicited and monitored in fully awake and intact flies (Shiraiwa and Carlson, 2007). The extension of the proboscis follows a highly stereotypic pattern that can be subdivided into a fixed sequence of events (Flood et al., 2013). These events can easily be distinguished from each other. Thus, individual muscles are activated at different time points within the sequence, implying a precise temporal and spatial orchestration of motoneuron activity innervating the proboscis musculature.

2.5 Aim of the Thesis

The aim of my thesis was to understand how neuronal circuits control the behavior of animals. Sensory-motor circuits allow an animal to perceive the world and to process and relay sensory information to the motor system to elicit an appropriate behavior. To gain insights into the principles of neuronal circuit formation and function it is crucial to identify

the participating neurons, to determine their connectivity within the circuit, and to analyze how the activity of these neurons controls a specific behavior.

In this study, I used the adult *Drosophila melanogaster* gustatory system as a model to study the principles underlying the connectivity and function of a simple circuit connecting sensory stimuli to a motor behavior.

First, I aimed to gain genetic control over individual neuronal elements of the taste circuitry in order to be able to exploit all the power of the genetic tools available in *Drosophila*. With a combined behavioral and morphological screen of preselected Gal4 lines, I aimed to identify these genetic control elements, allowing the selective manipulation and characterization of a defined set of genetically targeted neurons.

In addition, the proboscis extension response, representing the motor output of the taste circuitry, represents an ideal behavioral model to study the neuronal control underlying the generation of a stereotypic, sequential movement in a behaving animal. Thus, I particularly focused on identifying motoneurons innervating the proboscis musculature and premotor interneurons that control motoneuron activity with the goal to identify how the precise temporal orchestration of motoneuron activation is achieved.

3. Results

3.1 Behavioral Screen to Identify Neuronal Taste Circuit Elements

3.1.1 Introduction

To study how the nervous system controls taste behavior in *Drosophila* it is crucial to first genetically target individual gustatory circuit elements. The full potency of genetic tools available in *Drosophila* can only be revealed by using the Gal4-UAS binary expression system. The two big enhancer Gal-4 collections, the Rubin collection (Jenett et al., 2012) and the VT collection from the VDRC (Dickson and Stark), showing random but mostly sparse expression patterns are ideally well suited to identify driver-lines expressed in neurons belonging to the taste circuitry.

Since it is known, that the SEZ is the primary gustatory center in the fly (Dunipace et al., 2001; Stocker, 1994; Thorne et al., 2004; Wang et al., 2004), it is very likely that the cell bodies and neurite arborizations of the majority of neurons controlling taste behavior are located within this discrete brain region. Searching through these collections with the focus on sparse, SEZ-expressing Gal4 lines allows a reasonable preselection of potentially interesting driver-lines. We decided to initially perform a behavioral activation screen, using the heat-activated sodium channel TrpA1 (Hamada et al., 2008; Rosenzweig et al., 2005; Rosenzweig et al., 2008), to identify neurons whose activity is sufficient to elicit a full or partial proboscis extension response.

This decision was based on several reasons. First, the rational to perform a behavioral screen and not a morphological screen was to avoid spending time on characterizing neurons with no or no identifiable influence on gustatory behavior and because we already have an approximation of the expression pattern based on the publically available collection database (https://www.janelia.org/project-team/flylight). Second, a behavioral activation screen is very efficient and has a high throughput. In contrast, an artificial silencing screen would be more laborious because reducing neuronal activity in a certain population of neurons most likely has no effect on a fly's behavior *per se*. In such an experimental setup, one would present a sensory stimulus to the fly and then look for phenotypic changes in behavior, requiring time-intense experiments. Furthermore, potential redundancy in the nervous system can prevent

any change in behavior and if Gal4 levels are low, partial inhibition of neurons may have no effect on their efficacy to transmit signals. Thus, the potential to observe a phenotypic behavior is much higher in an artificial activation than a silencing screen. Third, since flies are ectotherm, the temperature increase that is applied to activate TrpA1 expressing neurons reaches the deepest tissue within a fly's body. At the time when we started the screen, the sensitivity of the available optogenetic tools was not high enough to reliably activate neurons located within the brain which is surrounded by the head cuticle (Schroll et al., 2006; Zhang et al., 2006).

It is important to note, that a behavioral activation screen also has its limitations. This experimental design does not allow the identification of neurons that are not sufficient but required to produce a certain behavior or of neurons that process and relay aversive taste information or otherwise inhibit the execution of the proboscis extension response. However, the use of TrpA1 to remotely increase neuronal activity within intact, behaving flies bears an enormous potential to identify lines expressed in essential elements of the taste circuitry. The wide spectrum of the genetic toolbox available in *Drosophila* offers the possibility to further determine morphological and structural characteristics, the requirement for a specific behavior, as well as the connectivity between specific neuronal elements of the gustatory circuitry, with a special focus on motoneurons and premotor interneurons.

3.1.2 Results

3.1.2.1 The Wildtype Proboscis Extension Response

In the initial behavioral activation screen we searched for Gal4 lines expressed in neurons that are sufficient to elicit the entire proboscis extension response or specific parts of it. Thus, it is important to know in detail how a wildtype PER in response to a positive gustatory stimulus looks like. Only then it will be possible to classify different phenotypic behaviors. For this purpose, flies were immobilized either in a pipette tip or by gluing their wings onto a glass coverslip. To robustly induce PER we starved flies to increase their demand for high caloric, i.e. sweet substances. Stimulation of GSNs on the proboscis or on the anterior legs with a sucrose soaked tissue elicits a highly stereotypic PER that can be subdivided into a fixed sequence of events. It starts by lifting the rostrum and the extension of the haustellum. Subsequently, the labellum extends and opens. This enables the ingestion of the food by the

rhythmic activation of the pump. As soon as ingestion is terminated the proboscis retracts to its original resting position (Figure 6; Movie 1).

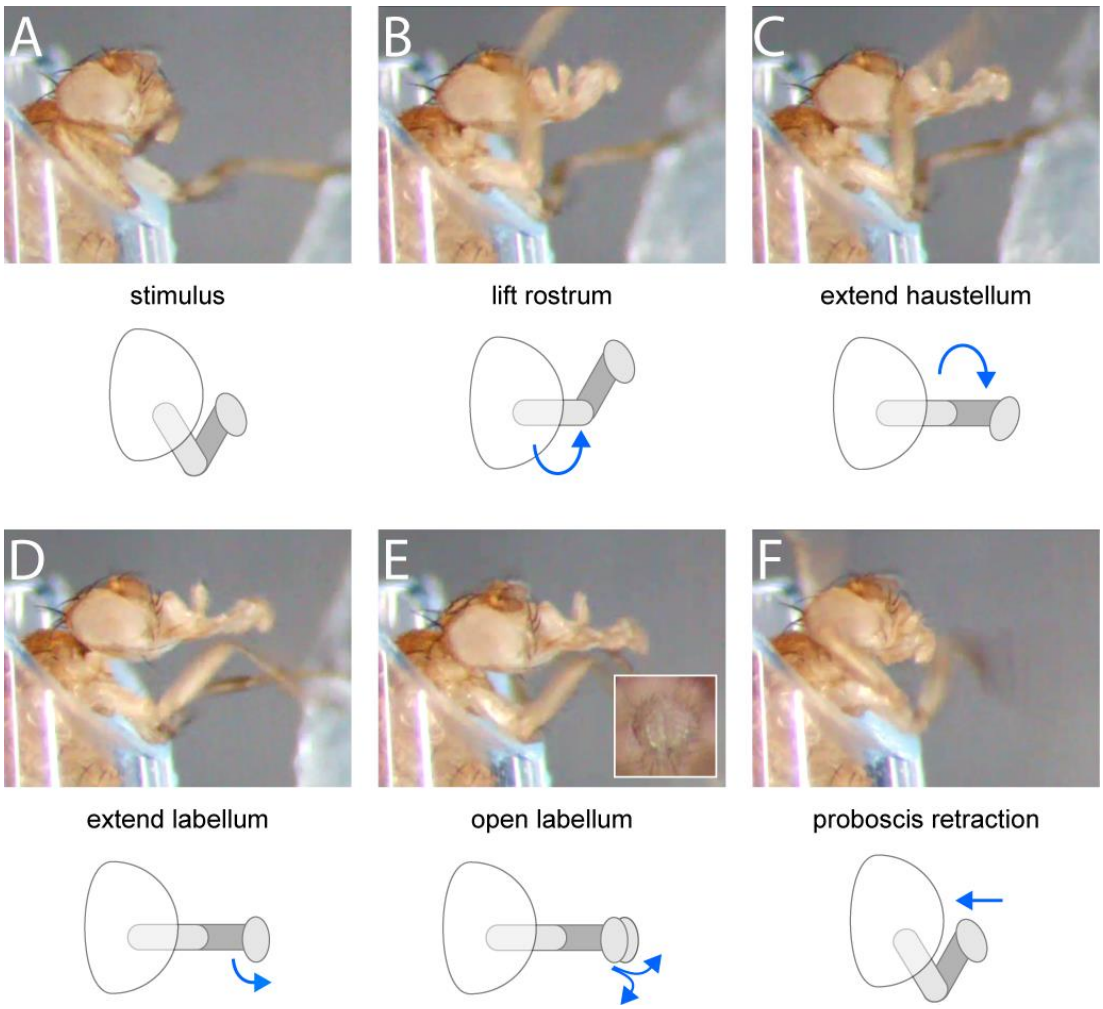

Figure 6. The *Drosophila* proboscis extension response follows a fixed motor sequence
The wildtype PER can be devided into stereotypic order. After GSNs on the anterior legs are positively stimulated with 200 mM sucrose (A), the rostrum lifts (B) and the haustellum extends (C). This is followed by the extension (D) and opening (E) of the labellum. After ingesting the food, the proboscis retracts to its original position (F).

3.1.2.2 Establishment of the PER Assay

The PER assay has been widely used to analyze different aspects of the taste system, including food preference and discrimination as well as to test for the integrity and sensitivity of the circuit (Dethier, 1976; Masek and Scott, 2010; Shiraiwa and Carlson, 2007; Wang et al., 2004). In many studies, the extension probability of fly populations was quantified simply by scoring if a gustatory stimulation was followed by a PER or not. However, we observed that the strength of the PER also has intermediate stages and were not satisfied with a *yes or no* scoring system. To refine the PER assay quantification, we developed a PER score system

from 0 to 4, where 0 reflects no response, 1 reflects twitching of the proboscis, 2 reflects a partial extension, 3 reflects at least one full extension, and 4 reflects 3 or more full extensions including labellum opening (Movie 2). We verified this newly introduced scoring system by generating a dose-response curve in 18 hrs starved flies by applying increasing sugar concentrations. Indeed, we observe a progressive dose-dependent increase in PER strength and moreover, if we define scores of 0 and 1 as no extension and 2 to 4 as extension, we can exactly reproduce previously published data (Wang et al., 2004) (Figure 7).

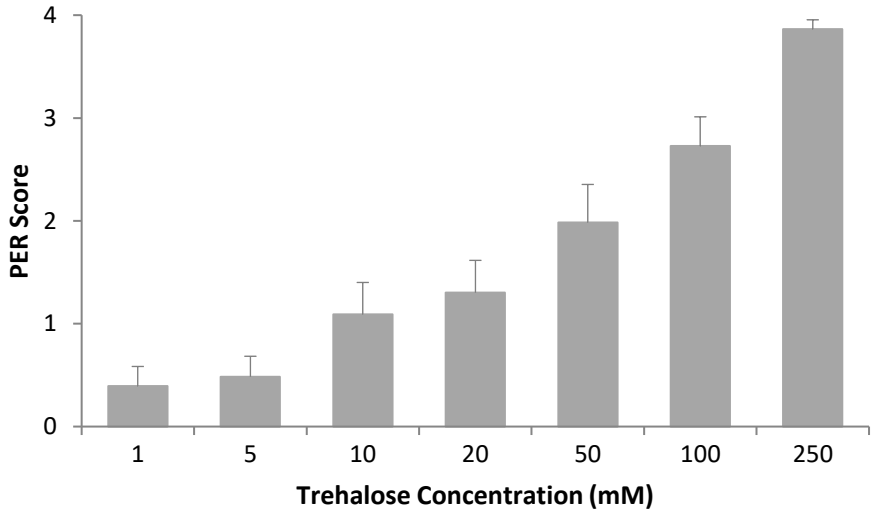

Figure 7. Dose-response curve to trehalose by applying the PER-score system
Increasing concentrations of Trehalose were presented to 18 hrs starved wildtype flies. The behavior of every single stimulation was quantified by applying the newly introduced PER-score system that ranges from 0 to 4.

3.1.2.3 Behavioral Activation Screen

Preselection of GMR-Gal4 lines for expression in the SEZ was kindly performed by the group of Prof. Dr. Heinrich Reichert. Flies of each Gal4 line were crossed to UAS-TrpA1 flies and the offspring containing both transgenic constructs was analyzed. Xinyu Liu, another PhD student in our lab, and I screened 164 lines. To reduce spontaneous activity, fed flies were immobilized in a pipette tip and at least six flies from each line were analyzed at control temperature (22°C), where TrpA1 is in a closed conformation, and at the activation temperature (>27C°), where opening of the heat-sensitive sodium-channel leads to artificial activation of the genetically targeted neurons. At the activation temperature, we observed many different aspects of the PER and these behaviors were assigned to different categories (Figure 8; Supplementary Table 1). Two main categories were those, where we observed either constant (n=73) or repetitive (n=59) extensions. Both categories can be further split into complete or partial extensions. Other behavioral phenotypes included twitching of the

proboscis (n=66), the development of a labellar drop (n=18), pumping (n=16), and labellum opening (n=5). In some cases, more than one phenotype was observed for one line or even a single fly. In addition, some lines showed no reaction upon temperature increase (n=39).

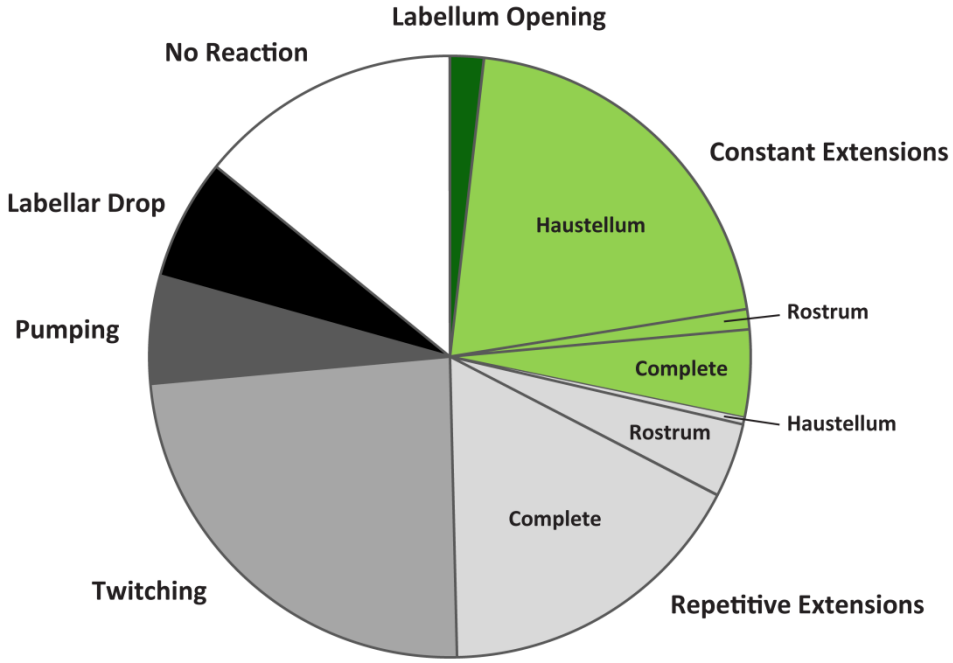

Figure 8. Summary of the behavioral activation screen
The different behaviors that appeared in the screen were put into categories and are summarized in this illustration. The size of each area corresponds to the frequency of lines displaying this particular behavior. The categories, that we suggest to contain lines expressing in motoneurons, are marked in green.

3.1.2.4 Identification of Motoneurons

We hypothesized that artificial activation of a motoneuron leads to the constant contraction of the corresponding muscle which in turn evokes a constant behavioral phenotype. Thus, to find GMR-lines expressed in motoneurons innervating the proboscis musculature, I focused on the categories *labellum spreading* and *constant extensions*. Candidate GMR-Gal4 lines were crossed to UAS-mCD8-GFP flies to visualize the neurons that elicited the specific behavior. To analyze if indeed motoneurons were involved, I developed a whole-head dissection method that enables visualization and immunostaining of neurons and muscles within a completely intact *Drosophila* head (See Chapter 5: *Materials and Methods*). Thereby it was possible to identify 5 GMR-Gal4 lines that are expressed in proboscis motoneurons. One line, GMR81B12, is only expressed in one bilateral pair of motoneurons within the entire nervous system.

3.2 Characterization of Proboscis Motoneurons

Manuscript

Motor control of Drosophila feeding behavior

Olivia Schwarz[1,2,3], Ali Asgar Bohra[4], Xinyu Liu[1,2], Heinrich Reichert[2], Krishnaswamy VijayRaghavan[4], and Jan Pielage[1,2,3#]

[1] Friedrich Miescher Institute for Biomedical Research,
Maulbeerstrasse 66,
4058 Basel,
Switzerland

[2] Biozentrum
University of Basel
Klingelbergstrasse 50,
4056 Basel,
Switzerland

[3]Technical University Kaiserslautern
Division of Zoology and Neurobiology
Erwin-Schroedinger-Strasse 13,
67663 Kaiserslautern,
Germany

[4]National Centre for Biological Sciences,
Tata Institute for Fundamental Research,
Bangalore, India

to whom correspondence should be addressed:
Email: pielage@bio.uni-kl.de
Phone: +49 631 205-2426

Abstract

The precise coordination of body parts is essential for survival and behavior of higher organisms. While progress has been made towards the identification of central mechanisms coordinating limb movement, only limited knowledge exists regarding the generation and execution of sequential motor action patterns at the level of individual motoneurons. Here we use Drosophila proboscis extension as a model system for a reaching-like behavior. We first provide a neuroanatomical description of the motoneurons and muscles contributing to proboscis motion. Using genetic targeting in combination with artificial activation and silencing assays we identify the individual motoneurons controlling the five major sequential steps of proboscis extension and retraction. Activity-manipulations during naturally evoked proboscis extension show that orchestration of serial motoneuron activation does not rely on feed-forward mechanisms. Our data support a model in which central command circuits recruit individual motoneurons to generate task-specific proboscis extension sequences.

Introduction

Locomotion and behavioral motor sequences are generated by a precise movement of selected body parts. These movements include both the coordination of individual elements of an appendage or limb to generate stereotyped serial motor patterns and bilateral interlimb coordination. In the last years, significant progress has been made towards the identification of central neuronal circuitries mediating and controlling the alternation of limb movement necessary for walking or swimming in both invertebrate and vertebrate model systems (Berkowitz et al., 2010; Guertin, 2009; Marder et al., 2005; Talpalar et al., 2013). These studies demonstrated that in many cases local central pattern generators (CPGs) and reciprocal inhibitory interneuron networks coordinate the alternating activation of limb motor units (Berkowitz et al., 2010; Borgmann and Buschges, 2015; Buschges et al., 2011; Crone et al., 2008; Guertin, 2009; Lanuza et al., 2004; Marder et al., 2005; Talpalar et al., 2013). Similarly, CPGs are involved in the generation and coordination of stereotyped motion patterns of limb or appendage segments depending on alternating extensor-flexor muscle activation (Grillner, 2003; Talpalar et al., 2011; Tripodi et al., 2011; Zhang et al., 2014). Intra-limb coordination of body parts has been mainly explored using vertebrate limb movement, turtle scratch behavior and directed locomotion of locust legs (Berkowitz and Laurent, 1996; Calas-List et al., 2014; Durr and Matheson, 2003; Guzulaitis et al., 2014; Machado et al., 2015; Snyder and Rubin, 2015; Stein, 2010). In addition, analysis of Drosophila larval locomotion recently provided insights into the generation of temporally delayed but overlapping muscle activation patterns (Zwart et al., 2016). This study demonstrated similar segregation of premotor excitatory input as observed in vertebrates (Bikoff et al., 2016; Goetz et al., 2015; Tripodi et al., 2011) and showed that inhibitory interneuron input mediates phase delay of intrasegmental motoneuron (MN) activation (Zwart et al., 2016). Despite these advances, for complex reaching-like behaviors we currently have only a limited understanding regarding the circuit architecture that controls individual MN activation to elicit and coordinate these precise temporal and spatial motion patterns.

Here, we use the stereotypic motor response of *Drosophila melanogaster* proboscis extension to address in vivo the cellular and circuit mechanisms underlying the serial activation pattern of muscle groups necessary to coordinate a reaching-like behavior. The proboscis extension response (PER) is part of the sensory-motor taste circuitry of adult Drosophila (McKellar, 2016). The proboscis is the feeding organ of flies and is used for both taste cue detection and food ingestion (Dethier, 1976; Masek and Scott, 2010; Shiraiwa and Carlson, 2007; Wang et al., 2004). Comparable to mammals, gustation in flies is based on a limited number of modalities

which are perceived by gustatory receptor neurons (GRNs) present in taste sensilla on the proboscis, legs, wings, and ovipositor. Stimulation with an attractive stimulus (sweet) will trigger the extension of the proboscis towards the food source while aversive stimuli (bitter) will prevent the PER (Clyne et al., 2000; Dunipace et al., 2001; Falk, 1976; Hiroi et al., 2004; Montell, 2009; Scott et al., 2001; Singh, 1997; Stocker, 1994; Thorne et al., 2004; Yarmolinsky et al., 2009).

For a number of reasons Drosophila proboscis extension represents an ideal model system to unravel the structural and functional basis of a serial motor action. First, the PER represents an innate, sequential behavior that can be subdivided into a discrete number of movement steps (Flood et al., 2013). This motor sequence likely requires activation of different muscle groups at distinct time points within the PER sequence, implying a precise temporal orchestration of upstream MN activity. Second, the PER can reliably and noninvasively be elicited in living flies simply by applying a positive gustatory stimulus to GRNs (Shiraiwa and Carlson, 2007). Third, the MNs innervating the proboscis reside in a specific, highly regionalized brain region, the subesophageal zone (SEZ, nomenclature according to Ito et al., 2014) (Hampel et al., 2011; Rajashekhar and Singh, 1994). It is thought that the relay of gustatory sensory information from GRNs to MNs occurs mainly within the SEZ (Altman and Kien, 1987; Dunipace et al., 2001; Stocker, 1994; Thorne et al., 2004; Wang et al., 2004).

Importantly, stereotypic proboscis extension is also part of additional innate behavioral programs. The proboscis is partially extended both during fly grooming to enable cleaning of the proboscis (Hampel et al., 2015; Seeds et al., 2014) and during the male courtship to enable contact to the female fly (courtship licking) (Hall, 1994; Nichols et al., 2012). As these movements differ significantly from each other at least three independent motor programs controlling proboscis extension must exist.

The current description of the Drosophila proboscis motor system largely relies on comparative anatomical studies of the proboscis musculature based on cross-sections of the adult head in different fly species (Graham-Smith, 1930; Miller, 1950). First insights regarding the anatomy of MNs were obtained using backfilling studies (Rajashekhar and Singh, 1994) and by selective expression of marker genes in MNs innervating the musculature of the pharyngeal pump (Tissot et al., 1998). More recently, by gaining genetic access to individual MNs a functional analysis enabled the characterization of the role of a single MN during feeding induced proboscis

extension (Gordon and Scott, 2009) and of MNs contributing to food intake by controlling pharyngeal contractions (Manzo et al., 2012; Tissot et al., 1998). However, to gain insights into the principles underlying the motor program controlling proboscis movement a comprehensive neuroanatomical and functional characterization of proboscis muscles and MNs is essential.

Here, we first analyze the sequential features of the motion pattern underlying the PER and provide a comprehensive morphological description of proboscis MNs and muscles. Using a MARCM (Mosaic Analysis with a Repressible Cell Marker) approach (Lee and Luo, 1999) we identify and characterize cell body position, dendritic arborization, nerve projections, and muscle innervation patterns of all proboscis MNs at the single cell level. Using a functional behavioral screen, we then identify essential MNs controlling the serial motor sequence of the PER. Light and temperature-mediated activation and silencing of genetically identified MNs in vivo enables us to assign individual MNs to all major steps of the motor sequence controlling proboscis extension and retraction. Finally, by using targeted neuronal activity manipulations during natural, stimulus-evoked PER we demonstrate that the motor sequence units act independently from each other. Our study indicates that the serial PER action sequence is centrally programmed and does not represent a chain reflex sequence.

Results

Characterization of the PER motor sequence

First, we aimed to determine the precise motion pattern underlying the PER motor program. Therefore, we monitored and quantified proboscis movements in 14 starved and immobilized wild type (w^{1118}) flies in response to sucrose stimulations of the anterior legs. Our analysis revealed that the PER program consists of four major extension steps prior to food ingestion. Upon sucrose stimulation flies (1) lift the rostrum, (2) extend the haustellum, (3) extend the labella and (4) spread the labella to prepare for food intake (Figure 1A-F, Video 1 – see slow motion). This sequence is consistent with the reported sequences both during natural feeding and sucrose stimulation (Dethier, 1976; Flood et al., 2013; Gordon and Scott, 2009) with the exception of the labella extension step that has not been described before. Importantly, this sequence was highly stereotypic both within individual flies and across multiple flies (Figure 1G). We observed a deviation from this sequence only in 4 out of 93 stimulations (n = 14 flies) in which labella extensions preceded haustellum extensions. Between individual flies small alterations in the temporal profiles of individual movement steps could be observed (Figure 1G). These alterations are likely not a consequence of the feeding status of the flies as we did not observe significant deviations of the temporal sequence in fed flies compared to starved flies (Figure 1G).

Identification of proboscis musculature

We next aimed to unambiguously identify all muscle groups potentially contributing to proboscis movement and food ingestion. We used a muscle specific reporter (MHC-GFP; Chen and Olson, 2001) to visualize the position and organization of all muscles within an intact head capsule and proboscis (Figure 2A,B). Our whole-head preparation allowed us to visualize all muscles in their natural position and enabled identification of muscle groups that were not recognized as distinct groups in prior studies (Miller, 1950; Rajashekhar and Singh, 1994). For nomenclature, we follow the numbered system introduced by Miller et al., 1950. The analysis of muscle organization at different focal positions within the head capsule resulted in a number of novel findings. Muscle 1 represents the largest muscle group extending through the entire head capsule (Figure 2A,B). Analysis of the flanking muscles revealed that muscle 2 is comprised of two independent muscles with unique attachment sites and different expression levels of the MHC-GFP reporter (Figure 2B). Similarly, the *in situ* visualization of muscle groups surrounding the

pharynx revealed novel aspects of muscle group organization (Figure 2b', displayed at higher exposure levels). As previously described, muscle group 12 is composed of two different muscles, 12-1 and 12-2 (Flood et al., 2013; Figure 2b'). In addition, our data shows that the large muscle group 11 can be subdivided into three distinct muscle sets (11-1, 11-2, and 11-3) that attach to the upper sclerotized plate of the pharyngeal pump at unique angles (Figure 2b´). Within the haustellum muscles 6 and 7 share posterior attachment positions but connect to the dorsal and ventral part at the anterior end of the haustellum, respectively (Figure 2b''). Muscle 8 forms a connection between the dorsal and ventral parts of the labella, orthogonal to muscles 6 and 7 (Figure 2b''). Based on these data, the proboscis musculature consists of 17 individual muscles forming 13 major muscle groups.

Proboscis motoneurons are located in the subesophageal zone

To characterize the MNs innervating these muscle groups we first visualized MN cell bodies by backfilling the proboscis nerves (labial and pharyngeal nerve) with rhodamine-labeled dextran dye. These experiments, recapturing an original analysis of Rajashekhar and Singh, 1994, revealed 20 pairs of bilaterally symmetric MNs, with MN somata arranged in two bilaterally symmetric clusters in the SEZ (Figure 2D). Consistent with prior reports we observe that all dendritic MN arborizations are confined to the SEZ. Thus, at least 20 distinct MNs in each brain hemisphere control the activation of the 13 muscle groups contributing to either proboscis movement or pharynx-mediated food uptake.

Developmental origin and neuroanatomy of proboscis MNs

To characterize the neuroanatomical features of all MNs in detail and to gain insights into their developmental origin we used the MARCM technique that allows genetic labeling of individual MNs at the time of their birth (Lee and Luo, 1999). Proboscis MNs can be visualized using the Gal4 driver line OK371 that labels all glutamatergic neurons (Daniels et al., 2008). Interestingly, we only recovered MN clones when heat-shock mediated flippase activation was induced during early embryogenesis (0-12h after egg-laying (AEL)) but not when the activation was performed during late embryogenesis or during larval stages. Furthermore, we never recovered multiple MNs within a brain hemisphere (Figures 3 and 4). This is in contrast to the development of leg MNs that occurs throughout larval development and is coupled to the development of the adult leg with individual neuroblasts giving rise to a large number of MNs (Baek and Mann, 2009; Brierley et al., 2012). We analyzed the dendritic arborization, axon projection and muscle

innervation pattern of 96 proboscis MN clones (Figure 2E, 3, 4) and defined MN types as MNs innervating the same muscle group. A minimum of two independent single cell clones was obtained for each MN type (Figures 3, 4 and data not shown) with the exception of MNs innervating muscle 13 (no clones recovered). Based on their innervation patterns, the twelve analyzed MN types can be subdivided into two major groups. Eight MN types innervate target muscles only on the ipsilateral side of the proboscis (with respect to the soma); these MNs innervate muscles that are involved in the extension, retraction, and positioning of the proboscis and mouthparts (this paper; Figures 2E, 3, and below). Strikingly, the axons of the remaining four MN types bifurcate and simultaneously innervate bilateral symmetric target muscles associated with the pharyngeal pump (Figure 4). These muscle groups are thought to mainly control food ingestion and pumping (Manzo et al., 2012; Tissot et al., 1998).

MNs innervating muscles controlling proboscis movement

The eight muscle groups innervated by ipsilateral MN types have been previously categorized based on anatomical criteria in Drosophila by Miller, 1950 and in the blowfly by Graham-Smith, 1930. Functional data thus far only exists for muscle 9 that has been demonstrated to control rostrum lifting (Gordon and Scott, 2009). Representative single cell clones of MN types that innervate seven of these muscles are shown in Figure 2E and Figure 3. As the precise role of these muscles for proboscis movement has not yet been established through functional analysis we utilize the target muscle number and not the anatomically based role for MN classification throughout this manuscript. The MN innervating muscle 1 (= MN1) has both ipsilateral and contralateral dendritic arborizations and innervates the ipsilateral muscle through the labial nerve (Figure 2E). Based on the co-staining with the postsynaptic muscle marker Discslarge (Dlg) it is evident that at least one additional MN innervates muscle 1. In general, MNs controlling proboscis movement differ significantly in the localization and complexity of dendritic arborization. MNs 3 and 4 display almost exclusively ipsilateral dendritic arborization (Figures 3A,B), while MNs 9 and 8 have predominantly ipsilateral arborization with minor extensions to the contralateral side (Figures 3C,F). In contrast, MN7 has similar dendritic arborizations on both sides (Figure 3E) while MN6 displays predominant contralateral arborization with only minor extensions to the ipsilateral side (Figure 3D). Thus, while all these MNs strictly innervate ipsilateral located muscles they receive presynaptic input either predominantly ipsilateral, equal from both sides or predominantly from the contralateral side.

Proboscis motoneurons innervating pharyngeal muscles

Some of the muscle groups innervated by the bifurcating MNs (5, 10, 11, and 12, Figure 4A) have been previously associated with food ingestion and pumping (Flood et al., 2013; Graham-Smith, 1930; Manzo et al., 2012; Miller, 1950; Tissot et al., 1998). The general anatomy of these four MN types is highly stereotypic. All MN axons project through the pharyngeal nerve, bifurcate into two bilateral axon branches and innervate homologous muscles on both sides of the midline. These MNs display similar dendritic arborizations in both brain hemispheres and the innervation pattern on the two homologous bilateral muscles is almost identical (Figure 4B-F). Interestingly, prior analysis of the MNs innervating muscle groups 11 and 12 using specific Gal4 lines demonstrated that they have contralateral homologs (Manzo et al., 2012; Tissot et al., 1998). Indeed, in our MARCM analysis we identified single MNs innervating muscle group 11 bilaterally with the cell body present in either the left or right brain hemisphere (data not shown). Thus, pharyngeal muscles on both sides are innervated by two bilateral homologous MNs with highly overlapping dendritic arborizations.

Gal4-mediated genetic control of proboscis MNs

Next we aimed to assign functional roles to the MNs innervating proboscis musculature. Thus far, only the role of the MN innervating muscle 9 has been adequately studied by selective activation and silencing using a specific Gal4-driver line (Gordon and Scott, 2009). To identify the functional role of the MNs and their target muscles and to investigate the circuit mechanisms controlling proboscis extension and retraction we aimed to genetically control individual MNs. We performed a functional screen using the Gal4-UAS binary expression system (Brand and Perrimon, 1993) to identify Gal4-driver lines selectively expressing in different proboscis MNs. We used two publically available enhancer-Gal4 line collections (GMR-Gal4 lines, Bloomington Drosophila Stock Center, Jenett et al., 2012; VT-Gal4 lines, Vienna Drosophila RNAi Center, Kvon et al., 2014) which express the yeast transcription activator protein Gal4 in a random but fixed subset of neurons (Pfeiffer et al., 2008; Pfeiffer et al., 2010). Gal4-lines were prescreened for expression within the SEZ and then crossed to UAS-effector lines enabling either neuronal activation or silencing (Hamada et al., 2008; Kitamoto, 2001; Klapoetke et al., 2014). Artificial activation of Gr5a-Gal4 sweet sensory neurons by expressing either the heat-activatable Na^+-channel TrpA1 (Hamada et al., 2008) or the red-shifted Channelrhodopsin2 Chrimson (Klapoetke et al., 2014) resulted in repetitive complete extensions of the proboscis mimicking natural activation by sucrose (Video 2). In contrast, it has been reported that constant activation

of MN9 caused a constant displacement of the proboscis consistent with the contraction of muscle 9 (Gordon and Scott, 2009). Based on these results, we hypothesized that constant activation of MNs should elicit a constant change of proboscis posture at the activation temperature (TrpA1) or upon red light stimulation (Chrimson).

MNs controlling rostrum lifting and labella spreading

Artificial activation of flies expressing TrpA1 using GMR18B07-Gal4 resulted in a constant lifting of the rostrum identical to the behavioral pattern previously described for MN9 activation (E49-Gal4; Gordon and Scott, 2009) (Figure 5A,H and Video 3). In addition to rostrum lifting the flies also spread their labella at the activation temperature (29°C) (Figure 5A, inset) but not at control temperature (22°C). To confirm these results, we next used Chrimson as an alternative activation method. Upon red light stimulation, the rostrum was lifted and the labella were spread. Importantly, Chrimson-mediated activation allowed precise temporal control of the behavior as rostrum lifting correlated perfectly with red light exposure (Figure 5B,H and Video 4). To investigate whether the neurons expressing Gal4 are not only sufficient but also necessary for rostrum lifting and labella spreading we next silenced these neurons using the temperature-sensitive version of Dynamin, shibire^{ts} (Kitamoto, 2001). At the permissive temperature (22°C) the flies were able to fully extend the proboscis towards a positive stimulus (tissue soaked in 200 mM sucrose solution). In contrast, at the restrictive temperature (29°C, please see methods for details) the flies were no longer able to lift the rostrum upon sucrose stimulation (Figure 5C middle panel, 5H and Video 5; GMR18B07, repo-Gal80 > shi^{ts} animals, see below). Importantly, this behavior was completely reversible as shifting to the permissive temperature restored full proboscis extension upon sucrose stimulation (Figure 5C right panel and Video 5). Thus, the failure to lift the rostrum was indeed due to the acute inhibition of GMR18B07 neurons and not due to habituation or proboscis damage. In contrast to the efficient inhibition of rostrum lifting we did not observe a significant failure to spread the labella in these flies. Together, these results demonstrate that GMR18B07 neurons are both sufficient and required for rostrum lifting and at least partially involved in the control of labella spreading.

We next analyzed the expression pattern of the GMR18B07-Gal4 line using membrane-tagged GFP (UAS-mCD8-GFP) as a reporter. This analysis revealed a broad expression in glia cells throughout the brain preventing characterization of SEZ neurons (Figure 5D). To restrict Gal4-expression to neurons we co-expressed the Gal4 inhibitor Gal80 in all glial cells (repo-Gal80; Awasaki et al., 2008). Absence of glial expression revealed 4 pairs of bilaterally symmetric

neurons within the SEZ (Figure 5E). To identify potential MNs we used the whole head preparation method that enables simultaneous analysis of the SEZ and all proboscis muscles (Figure 5F, see methods). Analysis of GMR18B07, repoGal80>mCD8-GFP flies revealed one MN pair innervating muscle 9, and another MN pair innervating muscle 8 (Figure 5F,G). To validate our behavior results we repeated all behavior experiments in the presence of repo-Gal80. We observed identical results in these animals (Figure 5A-C,H and Video 3-5). These results confirm the previously described role of MN9 and muscle 9 for rostrum lifting (Gordon and Scott, 2009) and identify MN8 and muscle 8 as potential regulators of labella spreading.

MNs controlling haustellum extension

During sucrose-mediated activation of proboscis extension the lifting of the rostrum is followed by haustellum extension (folding down of the haustellum). In our functional screen using TrpA1 mediated activation we identified the line GMR26A01 as sufficient to induce a constant extension of the haustellum (Figure 6A,G and Video 6). Light-induced activation using Chrimson confirmed these results with the extension of the haustellum precisely correlating with the on and off-times of the red light stimulus (Figure 6G and Video 7). Consistent with these neurons controlling haustellum extension acute inhibition (GMR26A01>shibire^{ts}) prevented extension of the haustellum at the restrictive temperature in response to sucrose stimulation (Figure 6B middle panel,G and Video 8). However, these flies were still able to lift their rostrum and to extend and spread their labella (Figure 6B). The failure to extend the haustellum was fully reversible as flies completely extended their proboscis after reversal to the permissive temperature (Figure 6B and Video 8). Analysis of the expression pattern of GMR26A01-Gal4 revealed expression in 8-10 SEZ neurons (Figure 6C). While MNs in Drosophila are mainly glutamatergic the majority of excitatory neurons in the brain are cholinergic. To restrict expression to MNs we performed an intersectional genetic approach and co-expressed Gal80 selectively in all cholinergic neurons (cha-Gal80; Kitamoto, 2002) (GMR26A01, chaGal80>mCD8-GFP). These experiments restricted mCD8-GFP expression to a single pair of bilateral MNs with axons extending to the proboscis musculature (Figure 6D,E). The whole head preparation revealed that the MNs innervate muscle 2-1 (Figure 6E,F). Likely due to leakiness of the cha-Gal80 line, expression levels in MN 2-1 were strongly reduced (data not shown); however, in a small number of cases artificial activation using Chrimson (GMR26A01, chaGal80>Chrimson) was still sufficient to induce haustellum extension (Figure 6G and Video 9). Interestingly, in two flies we observed extension of the haustellum to either the left or the right side (Figure 6-figure supplement 1A,B and Video 10). Analysis of the Chrimson expression

pattern revealed a unilateral expression in the ipsilateral MN2 correlating with the direction of the haustellum extension (Figure 6-figure supplement 1C). Together these data indicate that MN2 controls the extension of the haustellum via activation of muscle 2-1.

MNs controlling labella extension

Prior analysis of the proboscis extension sequence indicated that rostrum lifting and haustellum extension is followed by the spreading of the labella to enable food ingestion. Here, we identify extension of the labella as an additional step in the motor sequence that precedes labella spreading. Artificial activation of GMR81B12 expressing neurons (GMR81B12>TrpA1) resulted in a constant extension of the labella at the activation but not at the control temperature (Figure 7A,G and Video 11). Forward movement of the labella was particularly evident when using light-induced activation (GMR81B12>Chrimson; Video 12; Figure 7G). Acute silencing of GMR81B12 neurons (GMR81B12>shibire^{ts}) during sucrose-mediated activation of the PER demonstrated that these neurons are not only sufficient but also required for labella extension (Figure 7B,G and Video 13). Analysis of the expression pattern revealed that GMR81B12-Gal4 is expressed within a single neuron in each brain-hemisphere (Figure 7C). This neuron innervates muscle 6 that is attached to the base of the labella (Figure 7E,F). The Gal4-expression within a single MN pair enabled us to determine the extent of dendritic versus axonal neurite arborization within the SEZ. To mark the dendritic compartment, we co-expressed the mCherry-tagged dendritic marker DenMark (Nicolai et al., 2010) with the general membrane marker mCD8-GFP. Within the SEZ DenMark completely co-localized with mCD8-GFP indicating that the entire SEZ arborization is of dendritic nature (Figure 7D). The MN axons projecting through the labial nerve lacked any DenMark expression demonstrating the specificity of the marker. These results demonstrate that MN6 controls extension of the labella via activation of muscle 6.

MNs controlling labella spreading

The analysis of GMR18B07-Gal4 revealed that artificial activation of muscle 8 via MN8 is sufficient to induce spreading of the labella (Figure 5). We identified two additional lines, GMR58H01 and VT020958, that induced spreading of the labella upon artificial activation with either TrpA1 or Chrimson (Figure 8A,C,G and Video 14 and 15; Figure 8-figure supplement 1A,F). While both lines are expressed in multiple MNs (Figure 8D-F, Figure 8-figure supplement 1C-E) the only common MN between the three lines is MN8 suggesting that activation of muscle 8 controls labella spreading. However, silencing of these neurons was not

sufficient to prevent labella spreading upon sucrose stimulation (Supplementary File 1). This failure to impair labella spreading is likely due to insufficient inhibition of the MN. Together, these results suggest that MN8 controls labella spreading but we cannot formally rule out the contribution of additional MNs. Consistent with the expression of line VT020958 in labella muscles 6 and 8 artificial activation induced not only labella spreading but also labella extension verifying the role of MN6 (Figure 8-figure supplement 1B-E). Artificial activation did not reveal a role for MN7 that is also targeted by line GMR58H01 (Figure 8, Figure 8-figure supplement1).

MNs controlling proboscis retraction

Artificial activation of neurons of line GMR58H01 did not only resulted in labella spreading but at the same time caused a retraction of the proboscis into the head capsule (Figure 8B,C, Video 14,16). To directly test a potential contribution of GMR58H01 MNs to proboscis retraction we combined Chrimson-mediated activation with sucrose induced proboscis extension. Under control conditions (blue light) sucrose stimulation of fly legs induced complete proboscis extension (Figure 8C, Video 16). In contrast, under activation conditions (red light) these flies failed to extend their proboscis in response to sucrose stimulation (Figure 8C, Video 16; note also MN8 dependent labella spreading). Analysis of the expression pattern of GMR58H01 revealed selective expression in 4 MNs, MN1, MN4, MN7 and MN8 (Figure 8D-F). Based on morphology and cross-comparison to the other MN lines we can exclude MN4, 7 and 8 indicating that MN1 likely mediates active retraction of the proboscis into the head capsule. Indeed, such a function has been previously suggested for MN1 in blowflies (van der Starre and Ruigrok, 1980). Silencing of GMR58H01 neurons including MN1 did not significantly impair retraction of the proboscis after sucrose stimulation. In contrast to muscle 8 that is innervated by a single MN our MARCM data revealed that muscle 1 is innervated by multiple MNs (Figure 2E) and inhibition of a single MN is likely not sufficient to prevent muscle contraction. Alternatively, additional muscles may participate in proboscis retraction.

Step-wise control of proboscis extension and retraction

The identification and genetic control of the MNs controlling five major steps of proboscis extension and retraction, lifting of the rostrum (MN9), extension of the haustellum (MN2), extension of the labella (MN6), spreading of the labella (MN8) and proboscis retraction (MN1) enabled us to next address the neuronal circuit architecture controlling the motor pattern. In general, two alternative principles could generate the observed fixed sequence of events. In a

first model, the PER is based on a chain reflex sequence in which the initiation of each step depends on the successful execution of the preceding step of the motor sequence. Alternatively, all steps are independently initiated and coordinated at the level of pre-motor interneurons. To address these alternative hypotheses, we first analyzed the proboscis extension sequence of flies in which single MNs were silenced while applying positive taste stimuli. In a second step, we performed corresponding experiments in which we artificially activated MNs while applying positive taste stimuli. Single image analysis of the recorded sequences of our silencing experiments demonstrated that subsequent steps of the motor sequence could be efficiently executed despite the failure to perform a central step of the serial sequence (Figures 5, 6, 7, 8, Figure 5-figure supplement 1 and Figure 8-figure supplement 1). For example, despite complete inhibition of rostrum lifting (MN9 silencing) flies were still able to extend the haustellum and labella (Figure 5B and Video 5). Similarly, blocking haustellum extension did not prevent extension or spreading of labella (Figures 6B and Video 8). The only exception from this rule was observed in flies where we blocked labella extension. Here, sucrose stimulation of legs was no longer sufficient to induce labella spreading (Video 13 and Figure 5-figure supplement 1). However, direct sucrose stimulation of gustatory sensory sensilla present on the labella reliably elicited labella spreading in these flies. Thus, despite inappropriate positioning of individual proboscis elements the consecutive steps of the motor sequence were efficiently executed. In contrast, analysis of the temporal profiles of individual sequence steps revealed significant alterations in these flies. In control flies sucrose stimulation induces a rapid progression through the PER sequence (Figure 1G, Figure 5-figure supplement 1A). Inhibition of rostrum lifting significantly prolonged the time from stimulus to haustellum extension but accelerated progression from labella extension to labella spreading (Figure 5-figure supplement 1B). Inhibition of haustellum extension significantly reduced the time from rostrum lifting to labella extension and from labella extension to labella spreading (Figure 5-figure supplement 1C). Inhibition of labella extension not only perturbed progression to labella spreading but also increased the time duration from stimulus to rostrum lifting. These data indicate that serial execution of the individual movements is necessary to achieve the temporal precision observed in wild type flies. A potential explanation for the majority of the observed alterations may be anatomical constrains of the movement, however we cannot rule out that sensory feedback mechanisms contribute to the robustness of the motion sequence.

We next analyzed whether artificial activation of individual MNs would impair the normal extension response elicited by positive (sweet) stimulation of the gustatory sensory neurons on

the forelegs. As a readout, we measured the maximum proboscis extension distance in response to sucrose stimulation in control flies and in flies with artificially activated MNs (Figure 9, see methods). We first applied this method to line GMR58H01 (MN1, 4, 7, 8) to quantify the consequences of activation of the retractor MN1. Artificial activation (via TrpA1 or Chrimson) of MN1 almost completely prevented proboscis extension in response to the sweet sensory stimulus despite normal displacement at the permissive temperature and under blue light exposure (Figure 9A). Indeed, just activation of line GMR58H01 induced a retraction of the proboscis into the head capsule resulting in a small but significant negative extension value (Figure 9A). In contrast, activation of MN6 (line GMR81B12, labella extension) did not significantly alter sucrose evoked proboscis extension distance (Figure 9B,F). However, artificial activation of both line VT020958 (MN2, 6, 7, 8; labella extension and spreading) and of line GMR18B07 (MN9, 8; activation of rostrum lifting and labella spreading) significantly reduced the maximum proboscis extension distance (Figure 9C,D,F). These experiments demonstrate that full extension of the proboscis is not achieved by additive complete contractions of participating muscle groups but requires a precise temporal coordination of activation intensities.

MN based control of the proboscis extension response

Based on these results we propose that 5 MNs control the major steps of proboscis extension and retraction (Figure 10). Upon a positive gustatory stimulus flies first lift the rostrum (MN9), extend the haustellum (MN2), extend the labella (MN6), spread the labella for food ingestion (MN8) and finally retract the proboscis (MN1) (Figure 10). Analysis of the dendritic arborizations of these MNs revealed a stereotypic organization within the SEZ with all MN dendrites sharing a common space that mainly occupies the anteroventral regions of the SEZ with two spared “ball like-structures” on both sides of the midline (Figure 10B-F, right panels; Figure 10-figure supplement 1A-C). It has been previously reported that MN9 is not directly connected to gustatory sensory neurons (Gordon and Scott, 2009) that innervate posterior-dorsal regions of the SEZ (Figure 10-figure supplement 1D). To determine whether this observation holds true for all MNs we investigated potential connectivity of our MN lines to Gr5a-expressing sweet gustatory sensory neurons using the same GRASP approach (Feinberg et al., 2008). In these experiments, we did not observe significant GRASP signals (Figure 10-figure supplement 2). As a positive control, we observed strong GRASP signals between Gr5a-positive sensory neurons and inhibitory interneurons (*gad1*-Gal4; Sakai et al., 2009). Thus, control of the proboscis motor sequence is likely mediated via a dedicated set of interneurons downstream of gustatory sensory neurons.

Finally, we performed MN co-labelling experiments to investigate the spatial relationship of MN dendrites within the SEZ. We utilized a LexA-version of our MN6-Gal4 line (GMR81B12-LexA = MN6-LexA) that shows co-labelling of the soma and dendrites with the MN6-Gal4 line (Figure 11A). Simultaneous labelling of MN2 (GMR26A01-Gal4, cha-Gal80) and MN6 revealed largely overlapping dendritic arborization patterns with more extensive arborization of MN6 at the midline region (Figure 11B). The high regional overlap of dendrites of distinct identity was particularly evident when the dendritic arborization of MN6 was analyzed together with MNs 1,4,7 and 8 (GMR58H01-Gal4) (Figure 11C). In single sections a close but non-overlapping association of MN dendrites can be observed (Figure 11B, C lower panels).

Discussion

In this study, we provide a comprehensive developmental, neuroanatomical and functional characterization of the MNs controlling proboscis extension and retraction. We demonstrate that four MN types control the four major steps of proboscis extension while one MN likely contributes to the active retraction of the proboscis. These temporally ordered steps are independently controlled in a one-to-one manner with the majority of MNs both sufficient and required for the execution of one individual step of the forward reaching behavior. Our data demonstrate that MN-based feed-forward activation does not contribute to the precise temporal control of proboscis motion. Coupling of individual motor steps likely occurs at the level of premotor interneurons that provide the basis for selective execution of different motor subprograms of proboscis motion required during innate behaviors including courtship and gustatory behavior.

Organization and origin of proboscis motoneurons

Our MARCM-based single cell clonal analysis shows that the different types of proboscis MNs can be divided into two major groups that differ in terms of cell body position, dendritic arborization, axonal projection and muscle innervation pattern. The first group comprises seven MN types innervating muscles 1, 2, 3, 4, 6, 7, and 8. These MNs are bilaterally symmetric and their entire dendritic arborization is restricted to the anteroventral SEZ. Within each hemi-ganglion the MN cell bodies are clustered together, axons project through the labial nerve and they innervate ipsilateral muscle groups with respect to their cell body position. The second group comprises four MN types innervating muscle groups 5, 10, 11 and 12 via the pharyngeal nerve. Strikingly, in contrast to the first group the axons of these MNs bifurcate and simultaneously innervate homologous muscles on both the ipsi- and contralateral side. The only exception to these rules is MN9 that based on its ipsilateral innervation of muscle 9 belongs to group 1, however its cell body clusters with group 2 MNs and it projects via the pharyngeal nerve to the proboscis.

The neuroanatomical features of the two MN groups directly reflect their unique and different functional roles. Group 2 MNs control muscle groups (5, 10, 11, and 12) that elicit the rhythmic and bilaterally symmetric activity of the pharyngeal pump required for food ingestion (Dethier, 1976; Miller, 1950). Our data now demonstrate that the axons of these MNs bifurcate and provide equal input to target muscles on the ipsi- and contralateral site. As, in addition, the

dendritic arborizations are equally distributed within both hemispheres any stimulatory input (frontal, left or right) will be translated into a symmetric activation of pharyngeal pump muscles to ensure appropriate food uptake.

In contrast, group 1 MNs control muscle groups that mediate the extension, retraction and positioning of the proboscis (muscle groups 1, 2, 3, 4, 6, 7, 8 and 9). Our analysis demonstrates that all these MNs innervate ipsilateral located muscles but differ in their dendritic arborization patterns within the SEZ. Some MNs have predominantly ipsilateral while others have predominantly contralateral dendritic arborizations. All group 1 MN dendrites are restricted to the anteroventral SEZ region with dendrites of different MNs often present in close proximity to each other (Figure 11). This highly elaborate dendritic organization likely enables a direct translation of side-specific stimulation into directed movement. Indeed, similar to prior observations in the blowfly (Yetman and Pollack, 1987) sucrose stimulations of one leg induce proboscis extension towards the stimulus direction (Video 17). Furthermore, selective activation of an individual MN2 induced the extension of the haustellum towards the activation side (Figure 6-figure supplement 1). Together, our analysis revealed a remarkable level of hard-wired organization to accommodate the specific tasks of direction-selective and direction-independent MNs.

The fly proboscis is an appendage of the head composed of highly reduced and bilaterally fused mouthparts that represents a serial homolog of other segmental appendages such as the thoracic legs. It is thus interesting to consider possible homologies between proboscis and thoracic leg MNs. The MNs innervating the prothoracic leg have been well characterized and comprise 53 MNs that derive from 11 independent neuroblasts, with two lineages giving rise to 35 of the 53 MNs (Baek and Mann, 2009; Brierley et al., 2012). Most of these MNs are generated postembryonically during larval development and match the development of the leg (Estella and Mann, 2008; Estella et al., 2008; McKay et al., 2009; Morata, 2001; Soler et al., 2004). In contrast, a hemi-proboscis is only innervated by approximately 20 MNs, and our MARCM labeling demonstrated that all MNs are born during embryogenesis (0-12h AEL). In contrast to the leg MNs, individual labeled clones never included more than one type of proboscis MN suggesting that each of the thirteen different MN types are generated by different neuroblasts. The fact that proboscis MNs are generated during embryogenesis indicates that these MNs also have potential roles during larval stages. Indeed, it has been reported that MNs innervating the adult muscle 11 are also required for feeding in larvae (Tissot et al., 1998). Thus, proboscis MNs

may provide analogous functions during larval food ingestion despite different functional requirements and body organization. It will be of great interest to determine the precise use of these MNs during larval development and to address the potential developmental mechanism underlying the morphological and functional reorganizations necessary to accommodate the different functional requirements.

Motor control of the serial proboscis extension response

The detailed anatomical analysis of proboscis muscles and MNs together with the genetic manipulation of individual MNs enabled us to demonstrate that five MNs are sufficient to control the major steps of proboscis extension behavior. We show that gustatory stimulation elicits five consecutive, partially overlapping movements: rostrum lifting, haustellum extension, labella extension, labella spreading and proboscis retraction. Each of the steps is controlled by one bilateral pair of muscles that are innervated by one or multiple pairs of MNs. In all cases, artificial MN activation was sufficient to elicit a single step of the serial proboscis motion. In contrast, inhibition of MN activity did not always prevent execution of the specific movement. Three reasons can account for this observation: First, some muscles are innervated by multiple MNs and inhibition of a single MN is not sufficient to prevent muscle contraction as observed for muscle1. Second, the expression levels of the inhibitory construct may not always be sufficient to shut down MN activity. And third, we cannot exclude the possibility that additional muscles contribute to individual steps of the PER that would act at least partially redundant. Despite these limitations regarding the requirements of individual muscle groups our combined data clearly demonstrate that all steps of the motor sequence are individually controlled. Importantly not only proboscis extension but also proboscis retraction is potentially controlled by active mechanisms. Active termination of the PER likely contributes both to the repetitive PER behavior observed in vivo (Itskov et al., 2014, see below) and to aversive responses to bitter substances (active retraction of the proboscis, data not shown).

In addition, we provide evidence that initiation of individual movements does not depend on the execution of earlier steps of the motor sequence. However, the selective block of individual MNs resulted in perturbations of the stereotypic temporal profile of the PER motion. These alterations are likely due to anatomic constraints of proboscis displacement but could also point to a potential role for sensory feedback as observed in the leg motor system (Mendes et al., 2013).
Using activation experiments we demonstrated that the execution of one movement does not automatically trigger the initiation of the subsequent movement. In contrast to a reflex chain as

observed for crayfish escape behavior (Reichert et al., 1981) the movement of the proboscis elements is likely controlled in a one-to-one manner by individual MNs. Thus, our data indicates that the generation of the temporal proboscis motion sequence is programmed upstream of the MNs in the central brain.

This central coordination of MN activity is consistent with the observation that different stereotypic proboscis movements are part of at least two additional innate behavior programs. During male courtship behavior the proboscis displays an upward motion that includes rostrum lifting, labella extension and labella spreading (courtship licking) (Hall, 1994; Nichols et al., 2012) while the proboscis is placed outwards of the head capsule during proboscis cleaning (Hampel et al., 2015; Seeds et al., 2014). It is thus likely, that these three innate proboscis motions, feeding, licking and grooming, are independently controlled by central circuits inducing context-specific motor unit recruitment profiles. This is supported by the observation that activation of an individual command interneuron is sufficient to induce the entire proboscis feeding motion (Flood et al., 2013). As this command neuron is not directly connected to MNs (Flood et al., 2013) the selective and sequential activation of the individual MNs requires at least an additional layer of interneurons. For peristaltic larval locomotion it has recently been demonstrated that the sequential and partially overlapping activation of intrasegmental MNs is controlled by both excitatory and inhibitory interneurons (Zwart et al., 2016). The MNs controlling distinct muscle groups are innervated by largely non-overlapping excitatory interneurons similar to observations in vertebrates (Bikoff et al., 2016; Goetz et al., 2015; Tripodi et al., 2011). Interestingly, however, the phasic motoneuron activation delay is mainly generated by selective inhibitory MN innervation (Zwart et al., 2016).

While we currently lack any information regarding the upstream interneurons controlling proboscis motion our data is consistent with either selective inhibition or excitation generating unique proboscis extension motions. For example, in contrast to the feeding motion the proboscis extension sequence during courtship licking lacks the haustellum extension step. Finally, analysis of natural feeding behavior demonstrated that flies display rhythmic patterns of proboscis extension and retraction when feeding on gelatinous food but not when drinking liquids. Thus, depending on the food quality a CPG contributes to the control of repetitive proboscis extension (Itskov et al., 2014). The genetic control and simplicity of the underlying motor system will greatly facilitate the identification and characterization of cellular and circuit principles controlling this reaching-like motor sequence.

Materials and Methods

Fly Stocks

Fly stocks were maintained on standard fly food at 25°C. Crosses for immunohistochemistry were kept at 25°C, while crosses for neuronal activation and silencing experiments were kept at 22°C. Enhancer-Gal4 and -LexA lines were obtained from the Bloomington Drosophila Stock Center (Jenett et al., 2012) and the Vienna Drosophila RNAi Center (Kvon et al., 2014). The following fly strains were used in this study: w^{1118}, GMR18B07-*Gal4* (RRID:BDSC_47476), GMR26A01-*Gal4* (RRID:BDSC_49148), GMR81B12-*Gal4* (RRID:BDSC 40107*)*, GMR58H01-*Gal4* (RRID:BDSC_39197), VT020958-*Gal4* (RRID:FlyBase_FBst0485173), GMR81B12-*LexA* (RRID:BDSC_54389) OK371-*Gal4* (RRID:BDSC_26160), *FRT19A/FM7c*, *FRT19A,hsFLP,*Tubulin-*Gal80; OK371-Gal4,*UAS-*mCD8-GFP/CyO,* Gr5a-*LexA*;UAS-*tdTomato::LexAop2-CD4-spGFP11*;*UAS-CD4-spGFP1-10* (Feinberg et al., 2008; Gordon and Scott, 2009), Gad1-*Gal4* (RRID:BDSC_51630; Sakai et al., 2009), MHC-GFP (RRID:BDSC_38462; Chen and Olson, 2001), 5xUAS-*mCD8-GFP* (RRID:BDSC_32192), 10xUAS-*mCD8-GFP* (RRID:BDSC_32186), UAS-*CD4-tdTomato* (RRID:BDSC_35841), 13xLexAop2-*mCD8-GFP* (RRID:BDSC_32203), UAS-*DenMark* (RRID:BDSC_33061; Nicolai et al., 2010), UAS-*TrpA1* (RRID:BDSC_26263; Hamada et al., 2008), UAS-*Chrimson* (RRID:BDSC_55135; Klapoetke et al., 2014), UAS-*shibire*^{ts} (Kitamoto, 2001), cha-*Gal80* (Kitamoto, 2002), repo-*Gal80* (Awasaki et al., 2008).

Backfilling of motoneuron nerves

To label all the MNs innervating the proboscis, flies with the genotype *OK371-Gal4,*UAS-*mCD8GFP* were used. The proboscis was cut from the tip of the head and a crystal of rhodamine-labelled dextran dye was placed on cut nerves. The dye was left to diffuse for 4 hrs at 4°C. The brain was then dissected, fixed, washed and mounted as described below.

MARCM analysis

To label individual MNs, single cell MARCM clones were induced during embryonic or post embryonic neurogenesis. For these experiments, females of the genotype *FRT19A/FM7c* were crossed with males of the genotype *FRT19A,hsFLP,*Tubulin-*Gal80; OK371-Gal4,*UAS-*mCD8-GFP/CyO*. For clone induction during embryogenesis, embryos were collected for 4 hrs at 25°C and heat shocks were applied for 1 h at 37°C at different time points. Similarly, for post

embryonic clone induction larvae were collected at different time intervals from 24 hrs after larval hatching (ALH) to 96 hrs ALH and heat shocks were applied after different time points.

Immunohistochemistry of MARCM samples

Dissections of adult brains with the proboscis were carried out in 1x phosphate-buffered saline (PBS) and fixed in 4% freshly prepared PFA (in 1x PBS) for 30 min at RT. After removal of the fixative the preparations were washed for 6x 15 min with 0.3% PTX (0.3% Triton X-100 in 1× PBS) at RT. Blocking of samples was performed for 15 min at RT in 0.1% PBTX (0.1% BSA in 0.3% PTX). Primary antibody was diluted in 0.1% PBTX and samples were incubated at 4°C for 12 hrs on a shaker. The following primary antibodies were used: chicken anti-GFP (1:500; Abcam, Cambridge, UK) and mouse anti-neurotactin (Nrt, BP106, 1:10; DSHB; RRID:AB_528404). Samples were washed in 0.3% PTX for 1 h and Alexa-488, 568, and 647 conjugated secondary antibodies were applied in 0.1% PBTX for 2 hrs. Rhodamine-conjugated phalloidin (1:200 Sigma) was used to visualize muscles. Preparations were mounted in Vectashield mounting media (Vector Laboratories) and imaged on an Olympus FV 1000 confocal point scanning microscope. ImageJ, Adobe Photoshop and Amira 5.4.3 software (Visage Imaging, Berlin, Germany) was used for image processing and 3D reconstructions.

Immunohistochemistry of enhancer-Gal4 lines

2-10 days old male and female flies were incubated in fixative (4% PFA in PBS, 0.2% Triton-X 100) for 3 hrs at 4°C and washed with PBST (0.2% Triton-X 100) 3x 30 min. Brain, proboscis, and head dissections were performed in PBST. Brains were dissected and transferred to a tube with ice cold PBST. Primary antibodies were incubated for 3 days at 4°C and secondary antibodies for 2 days at 4°C.

For proboscis and head dissections flies were decapitated with a razor blade. For the proboscis dissection the part of interest was isolated. For complete head dissection only a few holes were pierced into the cuticle on the ventral side of the proboscis (26-gauge needle) to allow antibody penetration. Primary antibodies were incubated for 5 days at RT and secondary antibodies for 3 days at RT.

Antibodies were diluted in PBST and used at the following concentrations: mouse anti-Bruchpilot (nc82; RRID:AB_2314868) 1:200, mouse anti-Synapsin (3c11; RRID:AB_528479) 1:100 (both obtained from Developmental Studies Hybridoma Bank, IA), rabbit anti-Discs-large (Pielage et al., 2011) 1:1,000, rabbit anti-GFP (A6455, Life technologies) 1:1,000, mouse anti-

mCherry (632543, Clontech) 1:1,000, phalloidin Alexa 647 (Life technologies) 1:1,000. Alexa 488, 555, and 647-coupled secondary antibodies (Life technologies) were used at 1:1,000.
Brains, proboscises, and heads were mounted in Vectashield and images were acquired with a Zeiss LSM 700/710 laser scanning confocal microscope with a 10x (NA 0.3) objective, a 20x (NA 0.7) oil immersion objective, or a 40x (NA 1.25-0.75) oil immersion objective. Images were processed using Imaris (Bitplane) and Adobe Photoshop software.

GFP Reconstitution Across Synaptic Partners (GRASP)

Enhancer-*Gal4* lines were crossed to *Gr5a-LexA;* UAS-*tdTomato::LexAop2-CD4-spGFP11;* UAS-*CD4-spGFP1-10* and offspring with the genotype *Gr5a-Lexa*/+; UAS-*tdTomato::LexAop-CD4-spGFP11/+;* UAS-*CD4-spGFP1-10/*enhancer-*Gal4* was dissected in ice cold PBST. Brains were incubated in fixative for 20 min at 4°C and washed with PBST 3x 30 min. Primary and secondary antibodies were incubated overnight at 4°C.

Analysis of fly behavior

For all behavior experiments 2-10 days old male and female flies were used. Fed or starved (24 hrs) flies were mounted on a glass coverslip 30 min prior to testing. The PER was analyzed using a custom-made, temperature-controlled chamber and recorded with a Canon EOS 60D camera at 25 or 50 frames/s.

Analysis of the PER motion pattern

PER was elicited by application of 200 mM sucrose to the anterior legs. Videos were analyzed using *Adobe Premiere Pro CC* and the initiation time point of each movement (i.e. rostrum lifting, haustellum extension, labella extension, and labella spreading) as well as the time point of sucrose stimulation was measured.

Artificial activation using TrpA1

Enhancer-Gal4 lines were crossed to UAS-TrpA1 at 22°C. The behavior was analyzed in a custom-made heating chamber and monitored at control (22°C) and activation (28°C - 32°C) temperature. Numbers of analyzed animals are indicated in Supplementary File 1 as responding animals/total animals.

Artificial activation using Chrimson

Enhancer-Gal4 lines were crossed to UAS-Chrimson at 25°C and kept in the dark. Crosses were raised on standard food mixed with 200 uM all-trans retinal. The behavior, with and without gustatory stimulation, was analyzed and monitored under control (475nm) and activation wavelength (633nm) in a dark room.

Artificial silencing using shibire^{ts}

Enhancer-Gal4 lines were crossed to UAS-shibire^{ts} at 22°C. To elicit PER a positive stimulus (200 mM Sucrose) was applied to the anterior legs. First, PER was observed at 22°C. Flies that showed no or only incomplete PER were excluded. Second, after the chamber was heated to 29°C flies were repeatedly stimulated to deplete the synaptic vesicle pool and PER was analyzed at the restrictive temperature. Third, after the chamber was cooled to 22°C responsiveness was tested again. All flies that showed no or only incomplete PER at this stage were excluded from the analysis.

Quantification of proboscis displacement

Enhancer-Gal4 lines were crossed to UAS-Chrimson at 25°C and kept in the dark. Crosses were raised on standard food mixed with 200 uM all-trans retinal. The behavior was analyzed and monitored in a dark room. The maximum proboscis extension (MPE) is defined as the distance between the most anterior part of the eye and the tip of the labella when the proboscis is maximally extended. One dataset consists of four MPE data points: Two at blue light with (blue$^+$) and without (blue$^-$) sucrose stimulation and two at red light with (red$^+$) and without stimulation (red$^-$). The data points at blue light and red light for one dataset are from two consecutive stimulations. In all quantifications for Figure 9A-E values are normalized to (blue$^+$-blue$^-$) which represents 100% proboscis extension distance. The values for Figure 9A-E are calculated the following: $\frac{\text{blue+ (−) blue−}}{\text{blue+ (−) blue−}} * 100\%$ for grey bars, $\frac{\text{red− (−) blue−}}{\text{blue+ (−) blue−}} * 100\%$ for green bars and $\frac{\text{red+ (−) blue−}}{\text{blue+ (−) blue−}} * 100\%$ for green+blue bars. Data are presented as mean ± SEM. For Figure 9F the values are normalized to [(blue$^+$-blue$^-$) – (red$^-$-blue$^-$)] to neglect the distance that is reached due to red light alone thereby focusing on the distance that is added upon sucrose stimulation. These values are calculated the following: $\frac{(\text{red+ (−) blue−}) - (\text{red− (−) blue−})}{(\text{blue+ (−) blue−}) - (\text{red− (−) blue−})} * 100\%$.

Ten stimulations on >5 different flies were used for quantifications (except for control flies: 8 stimulations on 3 different flies). Data are presented as mean ± SEM.

Statistical analysis

We used d'Agostino-Pearson omnibus normality test to test for Gaussian distributions.

Figure 1. Quantification of the initiation time points of individual steps during PER: Individual flies (flies A, B, and C) were compared to each other using the Mann-Whitney U test.

Figure 5-figure supplement 1. Quantification of the initiation time points of individual steps during PER: w^{1118} flies were compared to GMR-Gal4>shibire^{ts} flies using the Mann-Whitney U test.

Supplementary File 1 – for Figures 5,6,7,8 and Figure 8-figure supplement 1. Quantification of animals showing behavioral phenotypes: Experimental flies (Gal4/UAS) were compared to control flies (w^{1118}; Gal4/+; UAS/+) using the Wilcoxon signed-rank test.

Figure 9. Proboscis displacements of the same set of flies under different conditions were compared using a paired, parametric t-test

For all statistical tests asterisks indicate: * = $p < 0.05$; ** = $p < 0.01$; *** = $p < 0.001$

Acknowledgements

We thank Yunpo Zhao and Dominique Siegenthaler for help during initial phases of the project and for input to the manuscript. We thank all members of the Reichert, VijayRaghavan and Pielage lab for critical discussions throughout the project.

Funding

This study was funded by Swiss National Science Foundation (SNF) Sinergia grants to H.R. and J.P, an NCBS-TIFR grant to A.A.B and K.V., and a JC Bose Fellowship of the Department of Science and Technology and CEFIPRA to K.V.

Competing interests

Authors declare no financial or non-financial competing interests.

References

Altman, J.S., and J. Kien. 1987. Functional organization of the subesophageal ganglion in arthropods. *Arthropod Brain: Its Evolution, Development, Structure , and Functions. New York: Wiley*:265-301.

Awasaki, T., S.L. Lai, K. Ito, and T. Lee. 2008. Organization and postembryonic development of glial cells in the adult central brain of Drosophila. *J Neurosci*. 28:13742-13753.

Baek, M., and R.S. Mann. 2009. Lineage and birth date specify motor neuron targeting and dendritic architecture in adult Drosophila. *J Neurosci*. 29:6904-6916.

Berkowitz, A., and G. Laurent. 1996. Local control of leg movements and motor patterns during grooming in locusts. *J Neurosci*. 16:8067-8078.

Berkowitz, A., A. Roberts, and S.R. Soffe. 2010. Roles for multifunctional and specialized spinal interneurons during motor pattern generation in tadpoles, zebrafish larvae, and turtles. *Front Behav Neurosci*. 4:36.

Bikoff, J.B., M.I. Gabitto, A.F. Rivard, E. Drobac, T.A. Machado, A. Miri, S. Brenner-Morton, E. Famojure, C. Diaz, F.J. Alvarez, G.Z. Mentis, and T.M. Jessell. 2016. Spinal Inhibitory Interneuron Diversity Delineates Variant Motor Microcircuits. *Cell*. 165:207-219.

Borgmann, A., and A. Buschges. 2015. Insect motor control: methodological advances, descending control and inter-leg coordination on the move. *Curr Opin Neurobiol*. 33:8-15.

Brand, A.H., and N. Perrimon. 1993. Targeted gene expression as a means of altering cell fates and generating dominant phenotypes. *Development*. 118:401-415.

Brierley, D.J., K. Rathore, K. VijayRaghavan, and D.W. Williams. 2012. Developmental origins and architecture of Drosophila leg motoneurons. *J Comp Neurol*. 520:1629-1649.

Buschges, A., H. Scholz, and A. El Manira. 2011. New moves in motor control. *Curr Biol*. 21:R513-524.

Calas-List, D., A.J. Clare, A. Komissarova, T.A. Nielsen, and T. Matheson. 2014. Motor inhibition affects the speed but not accuracy of aimed limb movements in an insect. *J Neurosci*. 34:7509-7521.

Chen, E.H., and E.N. Olson. 2001. Antisocial, an intracellular adaptor protein, is required for myoblast fusion in Drosophila. *Dev Cell*. 1:705-715.

Clyne, P.J., C.G. Warr, and J.R. Carlson. 2000. Candidate taste receptors in Drosophila. *Science*. 287:1830-1834.

Crone, S.A., K.A. Quinlan, L. Zagoraiou, S. Droho, C.E. Restrepo, L. Lundfald, T. Endo, J. Setlak, T.M. Jessell, O. Kiehn, and K. Sharma. 2008. Genetic ablation of V2a ipsilateral interneurons disrupts left-right locomotor coordination in mammalian spinal cord. *Neuron*. 60:70-83.

Daniels, R.W., M.V. Gelfand, C.A. Collins, and A. DiAntonio. 2008. Visualizing glutamatergic cell bodies and synapses in Drosophila larval and adult CNS. *J Comp Neurol*. 508:131-152.

Dethier, V.G. 1976. The Hungry Fly: A Physiological Study of the Behavior Associated with Feeding.

Dunipace, L., S. Meister, C. McNealy, and H. Amrein. 2001. Spatially restricted expression of candidate taste receptors in the Drosophila gustatory system. *Curr Biol*. 11:822-835.

Durr, V., and T. Matheson. 2003. Graded limb targeting in an insect is caused by the shift of a single movement pattern. *J Neurophysiol*. 90:1754-1765.

Estella, C., and R.S. Mann. 2008. Logic of Wg and Dpp induction of distal and medial fates in the Drosophila leg. *Development*. 135:627-636.

Estella, C., D.J. McKay, and R.S. Mann. 2008. Molecular integration of wingless, decapentaplegic, and autoregulatory inputs into Distalless during Drosophila leg development. *Dev Cell*. 14:86-96.

Falk, R.B.-A., N.; Atidia, J. 1976. Labellar taste organs of Drosophila melanogaster. *Journal of Morphology*. 150:327-341.

Feinberg, E.H., M.K. Vanhoven, A. Bendesky, G. Wang, R.D. Fetter, K. Shen, and C.I. Bargmann. 2008. GFP Reconstitution Across Synaptic Partners (GRASP) defines cell contacts and synapses in living nervous systems. *Neuron*. 57:353-363.

Flood, T.F., S. Iguchi, M. Gorczyca, B. White, K. Ito, and M. Yoshihara. 2013. A single pair of interneurons commands the Drosophila feeding motor program. *Nature*. 499:83-87.

Goetz, C., C. Pivetta, and S. Arber. 2015. Distinct limb and trunk premotor circuits establish laterality in the spinal cord. *Neuron*. 85:131-144.

Gordon, M.D., and K. Scott. 2009. Motor control in a Drosophila taste circuit. *Neuron*. 61:373-384.

Graham-Smith, G.S. 1930. Further Observations on the Anatomy and Function of the Proboscis of the Blow-fly, Calliphora erythrocephala L. *Parasitology*. 22:47-115.

Grillner, S. 2003. The motor infrastructure: from ion channels to neuronal networks. *Nat Rev Neurosci*. 4:573-586.

Guertin, P.A. 2009. The mammalian central pattern generator for locomotion. *Brain Res Rev*. 62:45-56.

Guzulaitis, R., A. Alaburda, and J. Hounsgaard. 2014. Dense distributed processing in a hindlimb scratch motor network. *J Neurosci*. 34:10756-10764.

Hall, J.C. 1994. The mating of a fly. *Science*. 264:1702-1714.

Hamada, F.N., M. Rosenzweig, K. Kang, S.R. Pulver, A. Ghezzi, T.J. Jegla, and P.A. Garrity. 2008. An internal thermal sensor controlling temperature preference in Drosophila. *Nature*. 454:217-220.

Hampel, S., P. Chung, C.E. McKellar, D. Hall, L.L. Looger, and J.H. Simpson. 2011. Drosophila Brainbow: a recombinase-based fluorescence labeling technique to subdivide neural expression patterns. *Nat Methods*. 8:253-259.

Hampel, S., R. Franconville, J.H. Simpson, and A.M. Seeds. 2015. A neural command circuit for grooming movement control. *Elife*. 4.

Hiroi, M., N. Meunier, F. Marion-Poll, and T. Tanimura. 2004. Two antagonistic gustatory receptor neurons responding to sweet-salty and bitter taste in Drosophila. *J Neurobiol*. 61:333-342.

Ito, K., K. Shinomiya, M. Ito, J.D. Armstrong, G. Boyan, V. Hartenstein, S. Harzsch, M. Heisenberg, U. Homberg, A. Jenett, H. Keshishian, L.L. Restifo, W. Rossler, J.H. Simpson, N.J. Strausfeld, R. Strauss, L.B. Vosshall, and G. Insect Brain Name Working. 2014. A systematic nomenclature for the insect brain. *Neuron*. 81:755-765.

Itskov, P.M., J.M. Moreira, E. Vinnik, G. Lopes, S. Safarik, M.H. Dickinson, and C. Ribeiro. 2014. Automated monitoring and quantitative analysis of feeding behaviour in Drosophila. *Nat Commun*. 5:4560.

Jenett, A., G.M. Rubin, T.T. Ngo, D. Shepherd, C. Murphy, H. Dionne, B.D. Pfeiffer, A. Cavallaro, D. Hall, J. Jeter, N. Iyer, D. Fetter, J.H. Hausenfluck, H. Peng, E.T. Trautman, R.R. Svirskas, E.W. Myers, Z.R. Iwinski, Y. Aso, G.M. DePasquale, A. Enos, P. Hulamm, S.C. Lam, H.H. Li, T.R. Laverty, F. Long, L. Qu, S.D. Murphy, K. Rokicki, T. Safford, K. Shaw, J.H. Simpson, A. Sowell, S. Tae, Y. Yu, and C.T. Zugates. 2012. A GAL4-driver line resource for Drosophila neurobiology. *Cell Rep*. 2:991-1001.

Kitamoto, T. 2001. Conditional modification of behavior in Drosophila by targeted expression of a temperature-sensitive shibire allele in defined neurons. *J Neurobiol*. 47:81-92.

Kitamoto, T. 2002. Conditional disruption of synaptic transmission induces male-male courtship behavior in Drosophila. *Proc Natl Acad Sci U S A*. 99:13232-13237.

Klapoetke, N.C., Y. Murata, S.S. Kim, S.R. Pulver, A. Birdsey-Benson, Y.K. Cho, T.K. Morimoto, A.S. Chuong, E.J. Carpenter, Z. Tian, J. Wang, Y. Xie, Z. Yan, Y. Zhang, B.Y. Chow, B. Surek, M. Melkonian, V. Jayaraman, M. Constantine-Paton, G.K. Wong, and E.S. Boyden. 2014. Independent optical excitation of distinct neural populations. *Nat Methods*. 11:338-346.

Kvon, E.Z., T. Kazmar, G. Stampfel, J.O. Yanez-Cuna, M. Pagani, K. Schernhuber, B.J. Dickson, and A. Stark. 2014. Genome-scale functional characterization of Drosophila developmental enhancers in vivo. *Nature*. 512:91-95.

Lanuza, G.M., S. Gosgnach, A. Pierani, T.M. Jessell, and M. Goulding. 2004. Genetic identification of spinal interneurons that coordinate left-right locomotor activity necessary for walking movements. *Neuron*. 42:375-386.

Lee, T., and L. Luo. 1999. Mosaic analysis with a repressible cell marker for studies of gene function in neuronal morphogenesis. *Neuron*. 22:451-461.

Machado, T.A., E. Pnevmatikakis, L. Paninski, T.M. Jessell, and A. Miri. 2015. Primacy of Flexor Locomotor Pattern Revealed by Ancestral Reversion of Motor Neuron Identity. *Cell*. 162:338-350.

Manzo, A., M. Silies, D.M. Gohl, and K. Scott. 2012. Motor neurons controlling fluid ingestion in Drosophila. *Proc Natl Acad Sci U S A*. 109:6307-6312.

Marder, E., D. Bucher, D.J. Schulz, and A.L. Taylor. 2005. Invertebrate central pattern generation moves along. *Curr Biol*. 15:R685-699.

Masek, P., and K. Scott. 2010. Limited taste discrimination in Drosophila. *Proc Natl Acad Sci U S A*. 107:14833-14838.

McKay, D.J., C. Estella, and R.S. Mann. 2009. The origins of the Drosophila leg revealed by the cis-regulatory architecture of the Distalless gene. *Development*. 136:61-71.

McKellar, C.E. 2016. Motor control of fly feeding. *J Neurogenet*. 30:101-111.

Mendes, C.S., I. Bartos, T. Akay, S. Marka, and R.S. Mann. 2013. Quantification of gait parameters in freely walking wild type and sensory deprived Drosophila melanogaster. *Elife*. 2:e00231.

Miller, A. 1950. The internal anatomy and histology of the imago of Drosophila melanogaster. In "Biology of Drosophila" (M. Demerec, ed.). *John Wiley & Sons, New York*:420-534.

Montell, C. 2009. A taste of the Drosophila gustatory receptors. *Curr Opin Neurobiol*. 19:345-353.

Morata, G. 2001. How Drosophila appendages develop. *Nat Rev Mol Cell Biol*. 2:89-97.

Nichols, C.D., J. Becnel, and U.B. Pandey. 2012. Methods to Assay Drosophila Behavior.e3795.

Nicolai, L.J., A. Ramaekers, T. Raemaekers, A. Drozdzecki, A.S. Mauss, J. Yan, M. Landgraf, W. Annaert, and B.A. Hassan. 2010. Genetically encoded dendritic marker sheds light on neuronal connectivity in Drosophila. *Proc Natl Acad Sci U S A*. 107:20553-20558.

Pfeiffer, B.D., A. Jenett, A.S. Hammonds, T.T. Ngo, S. Misra, C. Murphy, A. Scully, J.W. Carlson, K.H. Wan, T.R. Laverty, C. Mungall, R. Svirskas, J.T. Kadonaga, C.Q. Doe, M.B. Eisen, S.E. Celniker, and G.M. Rubin. 2008. Tools for neuroanatomy and neurogenetics in Drosophila. *Proc Natl Acad Sci U S A*. 105:9715-9720.

Pfeiffer, B.D., T.T. Ngo, K.L. Hibbard, C. Murphy, A. Jenett, J.W. Truman, and G.M. Rubin. 2010. Refinement of tools for targeted gene expression in Drosophila. *Genetics*. 186:735-755.

Rajashekhar, K.P., and R.N. Singh. 1994. Organization of Motor-Neurons Innervating the Proboscis Musculature in Drosophila-Melanogaster Meigen (Diptera, Drosophilidae). *Int J Insect Morphol*. 23:225-242.

Reichert, H., J.J. Wine, and G. Hagiwara. 1981. Crayfish Escape Behavior: Neurobehavioral Analysis of Phasic Extension reveals Dual Systems for Motor Control. *Journal of Comparative Physiology*. 142:687-717.

Sakai, T., J. Kasuya, T. Kitamoto, and T. Aigaki. 2009. The Drosophila TRPA channel, Painless, regulates sexual receptivity in virgin females. *Genes Brain Behav*. 8:546-557.

Scott, K., R. Brady, Jr., A. Cravchik, P. Morozov, A. Rzhetsky, C. Zuker, and R. Axel. 2001. A chemosensory gene family encoding candidate gustatory and olfactory receptors in Drosophila. *Cell*. 104:661-673.

Seeds, A.M., P. Ravbar, P. Chung, S. Hampel, F.M. Midgley, Jr., B.D. Mensh, and J.H. Simpson. 2014. A suppression hierarchy among competing motor programs drives sequential grooming in Drosophila. *Elife*. 3:e02951.

Shiraiwa, T., and J.R. Carlson. 2007. Proboscis extension response (PER) assay in Drosophila. *J Vis Exp*:193.

Singh, R.N. 1997. Neurobiology of the gustatory systems of Drosophila and some terrestrial insects. *Microsc Res Tech*. 39:547-563.

Snyder, A.C., and J.E. Rubin. 2015. Conditions for Multi-functionality in a Rhythm Generating Network Inspired by Turtle Scratching. *J Math Neurosci*. 5:26.

Soler, C., M. Daczewska, J.P. Da Ponte, B. Dastugue, and K. Jagla. 2004. Coordinated development of muscles and tendons of the Drosophila leg. *Development*. 131:6041-6051.

Stein, P.S. 2010. Alternation of agonists and antagonists during turtle hindlimb motor rhythms. *Ann N Y Acad Sci*. 1198:105-118.

Stocker, R.F. 1994. The organization of the chemosensory system in Drosophila melanogaster: a review. *Cell Tissue Res*. 275:3-26.

Talpalar, A.E., J. Bouvier, L. Borgius, G. Fortin, A. Pierani, and O. Kiehn. 2013. Dual-mode operation of neuronal networks involved in left-right alternation. *Nature*. 500:85-88.

Talpalar, A.E., T. Endo, P. Low, L. Borgius, M. Hagglund, K.J. Dougherty, J. Ryge, T.S. Hnasko, and O. Kiehn. 2011. Identification of minimal neuronal networks involved in flexor-extensor alternation in the mammalian spinal cord. *Neuron*. 71:1071-1084.

Thorne, N., C. Chromey, S. Bray, and H. Amrein. 2004. Taste perception and coding in Drosophila. *Curr Biol*. 14:1065-1079.

Tissot, M., N. Gendre, and R.F. Stocker. 1998. Drosophila P[Gal4] lines reveal that motor neurons involved in feeding persist through metamorphosis. *J Neurobiol*. 37:237-250.

Tripodi, M., A.E. Stepien, and S. Arber. 2011. Motor antagonism exposed by spatial segregation and timing of neurogenesis. *Nature*. 479:61-66.

van der Starre, H., and T. Ruigrok. 1980. Proboscis extension and retraction in the blowfly, *Calliphora Vicina*. *Physiological Entomology*. 5:87-92.

Wang, Z., A. Singhvi, P. Kong, and K. Scott. 2004. Taste representations in the Drosophila brain. *Cell*. 117:981-991.

Yarmolinsky, D.A., C.S. Zuker, and N.J. Ryba. 2009. Common sense about taste: from mammals to insects. *Cell*. 139:234-244.

Yetman, S., and G.S. Pollack. 1987. Proboscis extension in the blowfly: directional responses to stimulation of identified chemosensitive hairs. *Journal of Comparative Physiology*. 160:367-374.

Zhang, J., G.M. Lanuza, O. Britz, Z. Wang, V.C. Siembab, Y. Zhang, T. Velasquez, F.J. Alvarez, E. Frank, and M. Goulding. 2014. V1 and v2b interneurons secure the alternating flexor-extensor motor activity mice require for limbed locomotion. *Neuron*. 82:138-150.

Zwart, M.F., S.R. Pulver, J.W. Truman, A. Fushiki, R.D. Fetter, A. Cardona, and M. Landgraf. 2016. Selective Inhibition Mediates the Sequential Recruitment of Motor Pools. *Neuron*. 91:615-628.

Figures Legends

Figure 1. The motor sequence of the proboscis extension response

(A-E) In response to sucrose stimulation to the leg the proboscis is extended in a stereotypic motion pattern: (A) fly before stimulus, (B) sucrose stimulation, (C) rostrum lifting, (D) haustellum extension, (E) labella extension, (F) labella spreading.

(G) Temporal quantification of proboscis extensions. The initiation time point of each step was determined in the video sequence and plotted with rostrum lifting set to zero. Data are shown for: single fly (magenta), multiple stimulations of three individual flies (A n = 13, B n = 10, C n = 13 stimulations), fed flies (red, n = 4 animals, 7 stimulations), mean ± SEM of the second stimulation of 12 individual flies (black). The following data points are not displayed on the graph: FlyA, stimulus (-28), labella spreading (+35); flyB, stimulus (-31, -54); flyC: labella spreading (32, 46).

Statistical comparison of flies A-C (Mann-Whitney U test) revealed small significant differences for the following data points: A vs C, labella extension – labella spreading, $p = 0.0006$; B vs C, stimulus – rostrum lifting, $p = 0.0304$). No significant differences were detected when comparing fed flies to individual flies or to the 12 control flies. However, these flies failed to spread the labella in response to leg stimulation but not when stimulated at the labella.

See also Video 1.

Figure 2. Muscles and motoneurons of the Drosophila proboscis

(A) Whole mount preparation of a Drosophila head. Muscle-specific expression of GFP (MHC-GFP) reveals the position of all proboscis muscles (red) in the head (bright field image).

(B) Same head as in (A) with muscles displayed in black (inverted). Pharynx and haustellum muscles are shown with adjusted settings and individually in b’ and b’’. Blue numbers indicate individual muscle groups. Scale bars, 50 μm.

(C) Schematic drawing of head muscles.

(D) Proboscis MNs. Upper panel, backfilling of all MN axons innervating the proboscis musculature reveals MN cell bodies within the SEZ. Two clusters of MN cell bodies (DMA, dorsal medial anterior; VLP, ventral lateral posterior) are present on both sides of the midline. Lower panel, enlargements of the DMA (I) and VLP (II) clusters. Scale bars, 20 μm.

(E) Single cell MARCM clone of a proboscis MN innervating muscle 1. Left, overview showing MN cell body and dendritic arborization in the brain that is connected by a single axon (arrow) to the NMJ on muscle 1. The asterisk indicates the pharyngeal plate. Right, enlargements of the

SEZ (top) and NMJ (bottom). In all panels, the MN is marked by the expression of mCD8-GFP (green) and postsynaptic sites are labeled using anti-Discs large (Dlg, red). Scale bars, 20 μm.

Figure 3. Morphology of MNs contributing to proboscis motion

Single cell MARCM clones of MNs innervating muscle 3 (A), muscle 4 (B), muscle 9 (C), muscle 6 (D), muscle 7 (E), and muscle 8 (F) are shown. For each MN type, brain localization (middle panels) and muscle innervation (lower panels) are shown. In all panels, MNs are marked by the expression of mCD8-GFP (green), the neuropil is visualized using an anti-Neurotactin antibody (Nrt, red, middle panels), and muscles are labeled using rhodamine-conjugated phalloidin (red, bottom row). A digital reconstruction of each MN is shown (top panel, dotted line indicates midline). Cell bodies are artificially colored in green and neurites in magenta. Scale bars, 20 μm.

Figure 4. Morphology of MNs contributing to food ingestion

(A) Schematic drawing of the muscles in the fly head. Muscles implicated in food ingestion are marked in blue. Single cell MARCM clones of MNs innervating muscle 5 (B), muscle 10 (C), muscle 11 (D), muscle 12 (E), and muscle 12-2 (F) are shown. For each MN type (B-F), brain localization (middle panels) and muscle innervation (bottom panels) are shown. In all panels, MNs are marked by the expression of mCD8-GFP (green), the neuropil is visualized using Nrt (red, middle row), and muscles are labeled using rhodamine-conjugated phalloidin (red, bottom row). A digital reconstruction of each MN is shown (top panel, dotted line indicates midline). Cell bodies are artificially colored in green and neurites in magenta. Scale bars, 20 μm.

Figure 5. GMR18B07 neurons control rostrum lifting and labella spreading

(A) Artificial activation of GMR18B07, repoGal80 neurons using TrpA1. Heat induced activation elicits rostrum lifting (middle panel, arrow) and labella spreading (double arrow). The inset shows a top view of the spread labella. At the control temperature before (left panel) and after (right panel) activation the proboscis is retracted.

(B) Artificial activation of GMR18B07, repoGal80 neurons using Chrimson. Red light induced activation (middle panel) elicits rostrum lifting (arrow) and labella spreading. At blue light before (left panel) and after (right panel) activation the proboscis is retracted.

(C) Heat induced silencing of GMR18B07, repoGal80 neurons using shibire^{ts}. Flies at the permissive temperature show full PER upon 200 mM sucrose stimulation (left and right panel).

At the restrictive temperature, these flies fail to lift the rostrum (middle panel, arrow) upon 200 mM sucrose stimulation (asterisk) but still extend the haustellum.

(D) Expression pattern of GMR18B07 in the adult central brain. Cells are marked by the expression of mCD8-GFP (green) and the neuropil is visualized using the presynaptic active zone marker Bruchpilot (Brp, magenta).

(E) Suppression of glia cell expression using repo-Gal80 reveals four pairs of bilateral neurons in the SEZ.

(F) Whole head preparation of GMR18B07, repoGal80 > mCD8-GFP animals (left panel) reveals expression in two bilateral pairs of MNs (green) with one pair innervating muscle 9 (axon marked by arrowhead) and one muscle 8 (axon marked by arrow). Side view of the proboscis (right panels) shows innervation of muscle 8 (asterisks). Muscles are marked by phalloidin (blue).

(G) Schematic drawing of the head muscles with innervated muscles highlighted in blue. Scale bars, 50 μm.

(H) Quantification of the behavioral phenotypes in control and experimental animals. Numbers and significances are listed in Supplementary File 1.

See also Figure 5-figure supplement 1 and Videos 3, 4, 5.

Figure 6. GMR26A01 neurons are sufficient and required for haustellum extension

(A) Artificial activation of GMR26A01 neurons using TrpA1. Heat induced activation elicits haustellum extension (middle panel, arrow). At the control temperature before (left panel) and after (right panel) activation the proboscis is retracted.

(B) Heat induced silencing of GMR26A01 neurons using shibire^{ts}. Flies at the permissive temperature show full PER upon 200 mM sucrose stimulation (left and right panel). At the restrictive temperature, these flies fail to extend the haustellum (middle panel, arrow).

(C) Expression pattern of GMR26A01 (mCD8-GFP, green) in the adult central brain (Brp, magenta).

(D) Suppression of cholinergic expression using cha-Gal80. This intersectional strategy restricts expression to a single bilateral pair of MNs (arrow points to the axon)

(E) Whole head preparation of GMR26A01, chaGal80 > mCD8-GFP demonstrates innervation of muscle 2 (asterisk). The boxed region is magnified in the right panels. Muscles are visualized by the F-actin marker phalloidin (blue).

(F) Schematic drawing of the head muscles with innervated muscles highlighted in blue. Scale bars, 50 μm.

(G) Quantification of the behavioral phenotypes in control and experimental animals. Numbers and significances are listed in Supplementary File 1.

See also Figure 5-figure supplement 1, Figure 6-figure supplement 1 and Videos 6, 7, 8, 9 and 10.

Figure 7. GMR81B12 neurons are sufficient and required for labella extension

(A) Artificial activation of GMR81B12 neurons using TrpA1. Heat induced activation elicits labella extension (middle panel, arrow). At the control temperature before (left panel) and after (right panel) activation the proboscis is retracted.

(B) Heat induced silencing of GMR81B12 neurons using shibire^{ts}. Flies at the permissive temperature show full PER upon 200 mM sucrose stimulation (left and right panel). At the restrictive temperature, these flies fail to extend the labella (middle panel, arrow). Insets show magnifications of the labella.

(C) Expression of GMR81B12 (mCD8-GFP, green) in the adult central brain reveals a single MN in each brain hemisphere.

(D) Analysis of dendritic versus axonal arborization. The mCherry-tagged dendritic marker DenMark (red, left panel; white, right panel) co-localizes with the general membrane marker mCD8-GFP (green) in the SEZ but not in the MN-axons projecting out of the brain (arrow). The neuropil is marked by Dlg (blue).

(E) Whole head and proboscis preparation of GMR81B12 > mCD8-GFP flies reveals that the MNs (green, arrow indicates MN cell body) innervate muscle 6. Muscles are visualized by the F-actin marker phalloidin (blue) and NMJs are labeled using the presynaptic vesicle marker Synapsin (red).

(F) Schematic drawing of the head muscles with innervated muscles highlighted in blue. Scale bars, 50 μm.

(G) Quantification of the behavioral phenotypes in control and experimental animals. Numbers and significances are listed in Supplementary File 1.

See also Figure 5-figure supplement 1 and Videos 11, 12 and 13

Figure 8. GMR58H01 neurons elicit labella spreading and proboscis retraction

(A,B) Artificial activation of GMR58H01 neurons using TrpA1. Heat induced activation elicits labella spreading (middle panel (A)) and leads to the retraction of the proboscis (middle panel (B), arrow). At the control temperature before (left panels) and after (right panels) activation the

proboscis is retracted. Insets in (A) show magnifications of the labella and the double arrow indicates the spreading of the labella. See also Figure 7-figure supplement 1 and Video 12.

(C) Artificially activation of GMR58H01 neurons using Chrimson while evoking sucrose induced proboscis extension. At blue light (control), flies show full PER upon 200 mM sucrose stimulation (left panel). Red light activation results in labella spreading and proboscis extension (middle panel). Red light activation during 200 mM sucrose stimulation prevents proboscis extension (right panel).

(D) Expression pattern of GMR58H01 in the adult central brain. Arrow points to the axons that are leaving the brain.

(E) Whole head preparation of GMR58H01>mCD8-GFP flies (left panel) reveals that the identified MNs (green) innervate muscle 1, 4, and haustellum muscles (asterisk). The side view of the proboscis (right panels) shows innervation of muscles 7 and 8 in the haustellum. Muscles are visualized by the F-actin marker phalloidin (blue).

(F) Schematic drawing of the head muscles with innervated muscles highlighted in blue. Scale bars, 50 μm.

(G) Quantification of the behavioral phenotypes in control and experimental animals. Numbers and significances are listed in Supplementary File 1.

See also Figure 8-figure supplement 1, Videos 14, 15 and 16.

Figure 9. The PER motor program relies on the precise coordination of motoneuron activity

(A-D) MN-Gal4>TrpA1 and MN-Gal4>Chrimson animals were used to display (TrpA1) and quantify (Chrimson) the effects of constant MN activation during sucrose evoked proboscis extension. Animals were stimulated with 200 mM sucrose and snapshots of the maximum proboscis displacement at control (panel 1) and activation temperature (panel 3) are shown. Proboscis displacement in response to heat induced activation is shown in panel 2. Graphs: Maximum proboscis displacement was measured at blue light (control) upon 200 mM sucrose stimulation (grey bar), at red light (activation) without sucrose stimulation (green bar), and at red light upon 200 mM sucrose stimulation (green + blue bar). The zero point is defined by the position of the proboscis at blue light without sucrose stimulation and 100% proboscis extension represents the maximum proboscis displacement at blue light upon 200 mM sucrose stimulation. Data are presented as mean ± SEM.

(E) Same quantification as in (A-D) for control (w^{1118}>Chrimson) animals.

(F) Quantification of percentage of expected proboscis distance. The zero point is defined by the proboscis displacement at red light without sucrose stimulation while 100% proboscis extension represents maximum proboscis displacement at blue light upon 200 mM sucrose stimulation. Data are presented as mean ± SEM. Statistical analysis: see Material and Methods.

Figure 10. Motoneurons and muscles controlling the major steps of the PER motor program

The extension of the proboscis in response to an attractive stimulus (200 mM sucrose, A-E) follows a stereotypic pattern that can be subdivided into a sequence of events. Snapshots of the motion pattern of a control fly (w^{1118}) executing a continuous proboscis extension (left panels) and in the schematic drawings illustrating the direction of the movements (blue arrows) are shown. Muscles and MNs controlling the individual steps are indicated in the schematics (blue numbers) and in brains (right panels, inverted fluorescence images from Figures 5-8). MNs display a striking overlap in dendritic organization. Scale bar, 20 μm.

See also Figure 10-figure supplement 1 and 2.

Figure 11. Analysis of dendritic arborizations of proboscis MNs

(A-C) Coexpression of mCD8-GFP and tdTomato/mCherry in MN-expressing lines using two binary expression systems (Gal4 and LexA). Maximum intensity projections (upper panel) and single z-stack sections (lower panel) are displayed. Spatial relationship between GMR81B12-LexA targeted MN6 (green) and one of the following MN-lines are shown: GMR81B12-Gal4 targeted MN6 (A, magenta), GMR26A01-Gal4, cha-Gal80 targeted MN2 (B, magenta), and GMR81B12-Gal4 targeted MNs1, 4, 7, 8 (C, magenta). Single sections in B, C show close, but non-overlapping association of MN dendrites of different MN populations. Scale bar, 20 μm (overview), 10 μm (single sections).

Video Legends

Video 1. Proboscis extension sequence in wild type flies (related to Figure 1)

This video shows a side view sequence of a sucrose-evoked proboscis extension of a wildtype (w^{1118}) fly first in real time followed by slow motion (0.1 x speed).

Video 2. Activation of Gr5a-expressing sweet sensory neurons using Chrimson

This video shows a continuous sequence of a Gr5a-Gal4>Chrimson fly at the control wavelength (475nm), at the activation wavelength (633nm), and at the control wavelength. First in real time followed by slow motion (0.4 x speed).

Video 3. Activation of GMR18B07, repoGal80 neurons using TrpA1 (related to Figure 5)

This video shows a GMR18B07, repoGal80 > TrpA1 fly at control and activation temperatures. Order of sequence: Side view at 22°C, side view at 29°C, top view at 29°C, and side view at 22°C.

Video 4. Activation of GMR18B07, repoGal80 neurons using Chrimson (related to Figure 5)

This video shows a continuous sequence of a GMR18B07, repoGal80 > Chrimson fly at the control wavelength (475nm), then at the activation wavelength (633nm), and at the control wavelength.

Video 5. Silencing of GMR18B07, repoGal80 neurons using shi^{ts} (related to Figure 5)

This video shows sucrose stimulations of a GMR18B07, repoGal80 > shi^{ts} fly at 22°C, at 29°C, and at 22°C, displayed at a 0.5 x speed.

Video 6. Activation of GMR26A01 neurons using TrpA1 (related to Figure 6)

This video shows side view sequences of a GMR26A01 > TrpA1 fly at 22°C, at 29°C, and at 22°C.

Video 7. Activation of GMR26A01 neurons using Chrimson (related to Figure 6)

This video shows a side view sequence of a GMR26A01 > Chrimson fly at the control wavelength (475nm), then at the activation wavelength (633nm), and at the control wavelength.

Video 8. Silencing of GMR26A01 neurons using shi^{ts} (related to Figure 6)

This video shows sucrose stimulations of a GMR26A01 > shi^{ts} fly first at 22°C, at 29°C, and at 22°C, displayed at 0.5 x speed.

Video 9. Activation of GMR26A01, chaGal80 neurons using Chrimson (related to Figure 6)
This video shows a side view sequence of a GMR26A01, chaGal80 > Chrimson fly at the control wavelength (475nm), then at the activation wavelength (633nm), and at the control wavelength.

Video 10. Activation of a unilateral GMR26A01, chaGal80 neuron using Chrimson (related to Figure 6-figure supplement 1)
This video shows a side view and front view sequence of a GMR26A01, chaGal80 > Chrimson fly at the control wavelength (475nm), at the activation wavelength (633nm), and at the control wavelength.

Video 11. Activation of GMR81B12 neurons using TrpA1 (related to Figure 7)
This video shows side view sequences of a GMR81B12 > TrpA1 fly at 22°C, at 29°C, and at 22°C.

Video 12. Activation of GMR81B12 neurons using Chrimson (related to Figure 7)
This video shows a side view sequence of a GMR81B12 > Chrimson fly at the control wavelength (475nm), then at the activation wavelength (633nm), and at the control wavelength.

Video 13. Silencing of GMR81B12 neurons using shi^{ts} (related to Figure 8)
This video shows sucrose stimulations of a GMR81B12 > shi^{ts} fly at 22°C, at 29°C, and at 22°C, displayed at 0.5 x or 0.125 x speed.

Video 14. Activation of GMR58H01 neurons using TrpA1 (related to Figure 8)
This video shows front view sequences of a GMR58H01 > TrpA1 fly at 22°C, at 29°C, and at 22°C.

Video 15. Activation of VT020958 Neurons Using TrpA1 (related to Figure 8–figure supplement 1)
This video shows sequences of a VT020958 > TrpA1 at control and activation temperatures. Order of video sequences: Front view at 22°C, front view at the transition to 29°C, front view at 22°C, side view at 22°C, side view at 29°C, and a side view at 22°C.

Video 16. Activation of GMR58H01 neurons using Chrimson (related to Figure 8)

This video shows sucrose stimulations of a GMR58H01 > Chrimson fly at the control wavelength (475) and then at the activation wavelength (633nm).

Video 17. Proboscis extension response after unilateral leg stimulation

This video shows a top view sequence of a unilateral sucrose stimulation to the right front leg first in real time followed by slow motion (0.32 x speed).

Supplementary Figure Legends

Figure 5-figure supplement 1. Analysis of the PER sequence during MN silencing

(A-D) Analysis of the temporal profile of the PER sequence in (A) wildtype (w^{1118}) flies, and in comparison to flies in which selective MNs were silenced by inducing $shibire^{ts}$ expression and a temperature shift to 29°C.

The first three proboscis extensions were used for the quantifications. (A) w^{1118}: 36 stimulations, 12 flies; (B-D) w^{1118}: 38 stimulations, 14 flies; (B) GMR18B07, repoGal80 > $shibire^{ts}$ MN9: 14 stimulations, 5 flies; (C) GMR26A01 > $shibire^{ts}$ MN2: 32 stimulations, 13 flies; GMR81B12 > $shibire^{ts}$ MN6: 12 stimulations, 5 flies. Data are presented as mean ± SEM. For statistical analysis: See Materials and Methods

Figure 6-figure supplement 1. Unilateral proboscis MN activation induces asymmetric proboscis movement

Artificial activation of a GMR26A01, chaGal80 > Chrimson fly using red light (633nm) induces an asymmetric extension of the haustellum to the left side. (A) side view, (B) top view.

(C) Dissection of the brain of the stimulated fly reveals Chrimson-mVenus (GFP, green) expression almost exclusively in the MN2 located on the left side of the SEZ. Brain structure visualized using Brp (magenta).

See also Video 10

Figure 8–figure supplement 1. VT020958 neurons elicit labella spreading

(A,B) Artificial activation of VT020958 neurons using TrpA1. Heat induced activation elicits labella spreading (middle panel (A)) and leads to the extension of the labella (middle panel (B), arrow). At the control temperature before (left panels) and after (right panels) activation the proboscis is retracted. Insets in (A) show magnifications of the labella and the double arrow indicates the spreading of the labella.

(C) Expression pattern of VT020958 in the adult central brain. Cells are marked by the expression of mCD8-GFP (green) and the neuropil is visualized using the presynaptic active zone marker Bruchpilot (Brp, magenta).

(D) Whole head preparation of VT020958>mCD8-GFP flies (left panel) reveals that the identified MNs (green) innervate muscle 2 and haustellum muscles (asterisk). The side view of the proboscis (right panels) reveals innervation of muscles 6, 7, and 8. Muscles are visualized by the F-actin marker phalloidin (blue).

(E) Schematic drawing of the head muscles with innervated muscles highlighted in blue. Scale bars, 50 μm.

(F) Quantification of the behavioral phenotypes in control and experimental animals. Numbers and significances are listed in Supplementary File 1.

See also Video 15.

Figure 10-figure supplement 1. Spatial organization of MN dendrites in the SEZ

(A-D) The expression pattern (mCD8-GFP, green) of three identified MN-Gal4-lines GMR26A01, chaGal80 MN2 (A), GMR81B12 MN6 (B), and GMR58H01 MN1,4,7,8 (C) is shown in comparison to the axonal projections of Gr5a-expressing sweet sensory neurons (D) in the adult central brain (Brp, magenta). For each genotype a front view (left panel), angled top view (middle panel), and a side view is shown.

Scale bar, 50 μm

Figure 10–figure supplement 2. Gr5a sensory neurons do not form synaptic connections with proboscis MNs

Analysis of endogenous GRASP signal (green, top panels; white, bottom panels) between GMR26A01-Gal4 (A), GMR26A01-Gal4, chaGal80 (B), GMR58H01-Gal4 (C), VT020958-Gal4 (D), GMR81B12 (E), Gad1-Gal4 (F) and Gr5a-LexA. The neuropil is visualized using the presynaptic active zone marker Brp (blue, top row). Weak GRASP-signals are present in the combination GMR26A01-Gal4 to Gr5a-LexA (A). These signals are likely due to interneurons marked in the Gal4-line as no signal can be detected when expression is restricted to MN2 by using cha-Gal80 (B). Similarly, we did not detect significant GRASP signals in all other MN-Gr5 combinations but strong signals were present in the positive control gad1-Gal4 to Gr5a-LexA. Scale bar, 20 μm.

Supplementary File 1. Quantification and statistical analysis of behavioral phenotypes

Numbers are shown as flies displaying phenotype/total flies analyzed.

Experimental flies (Gal4/UAS) were compared to control flies (w^{1118}; Gal4/+; UAS/+) using a Wilcoxon signed-rank test.

* GMR26A01, chaGal80>Chrimson flies were starved for 24 hrs prior to testing.

Schwarz et al. Figure 1

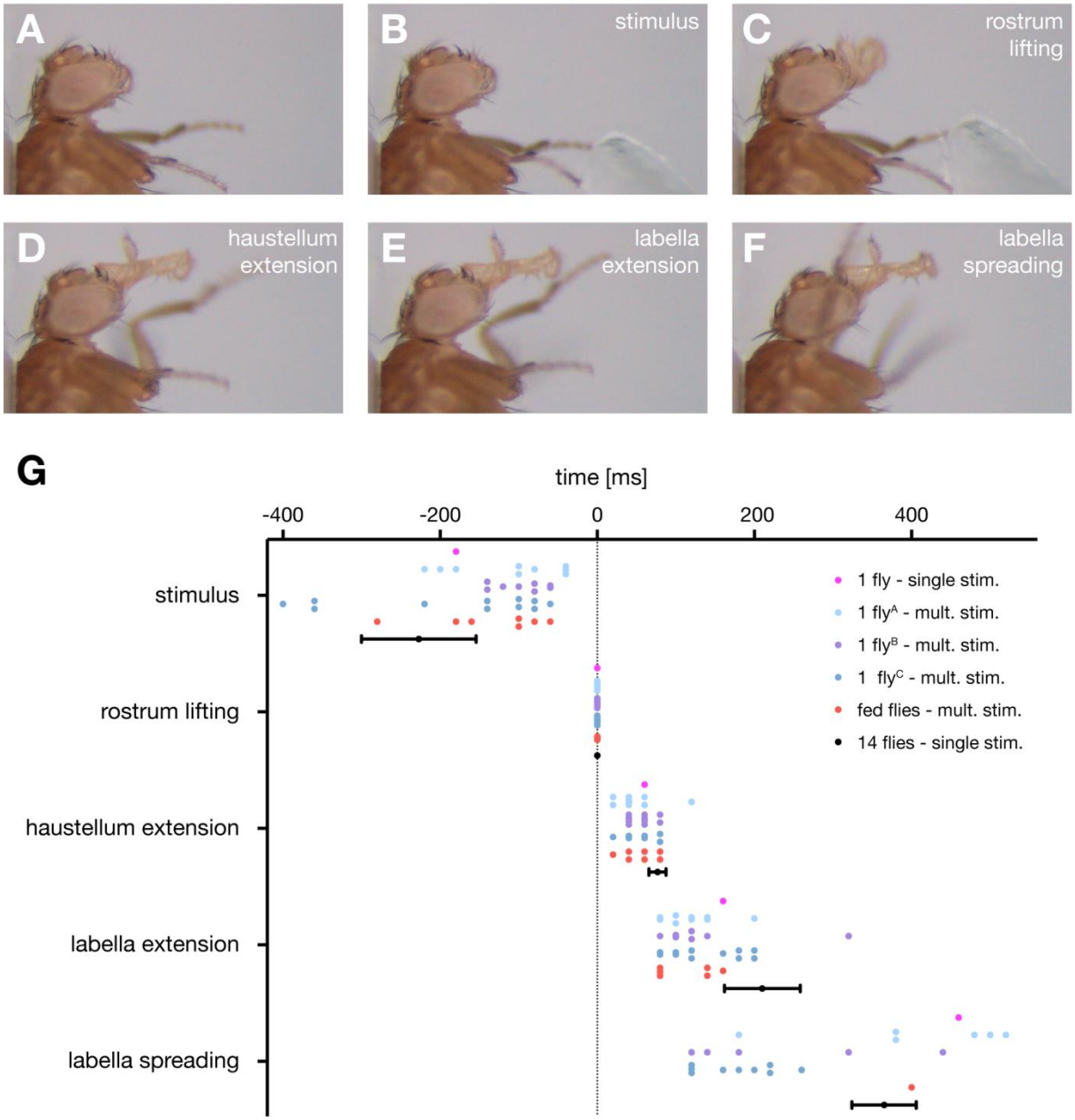

Schwarz et al. Figure 2

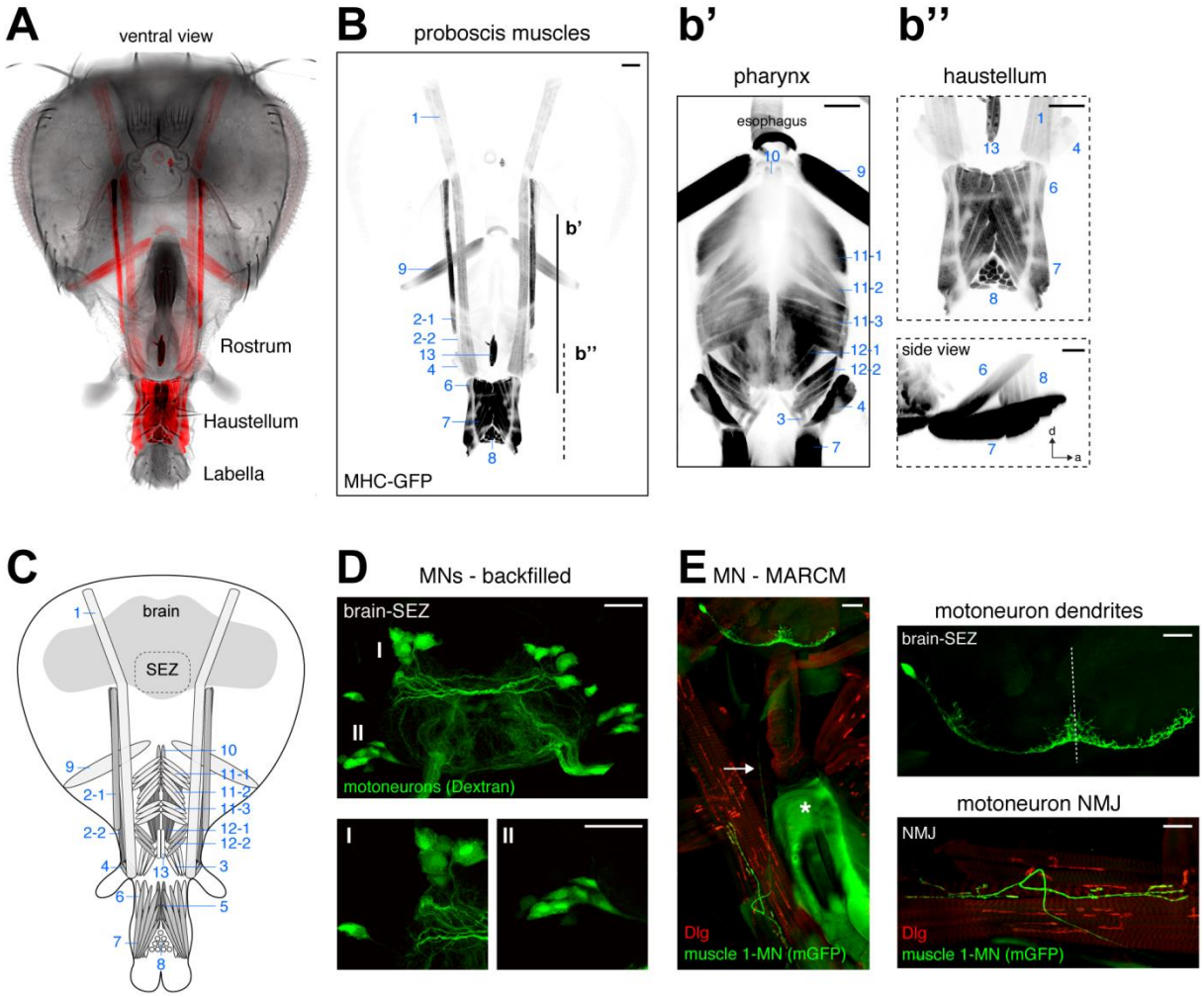

Schwarz et al. Figure 3

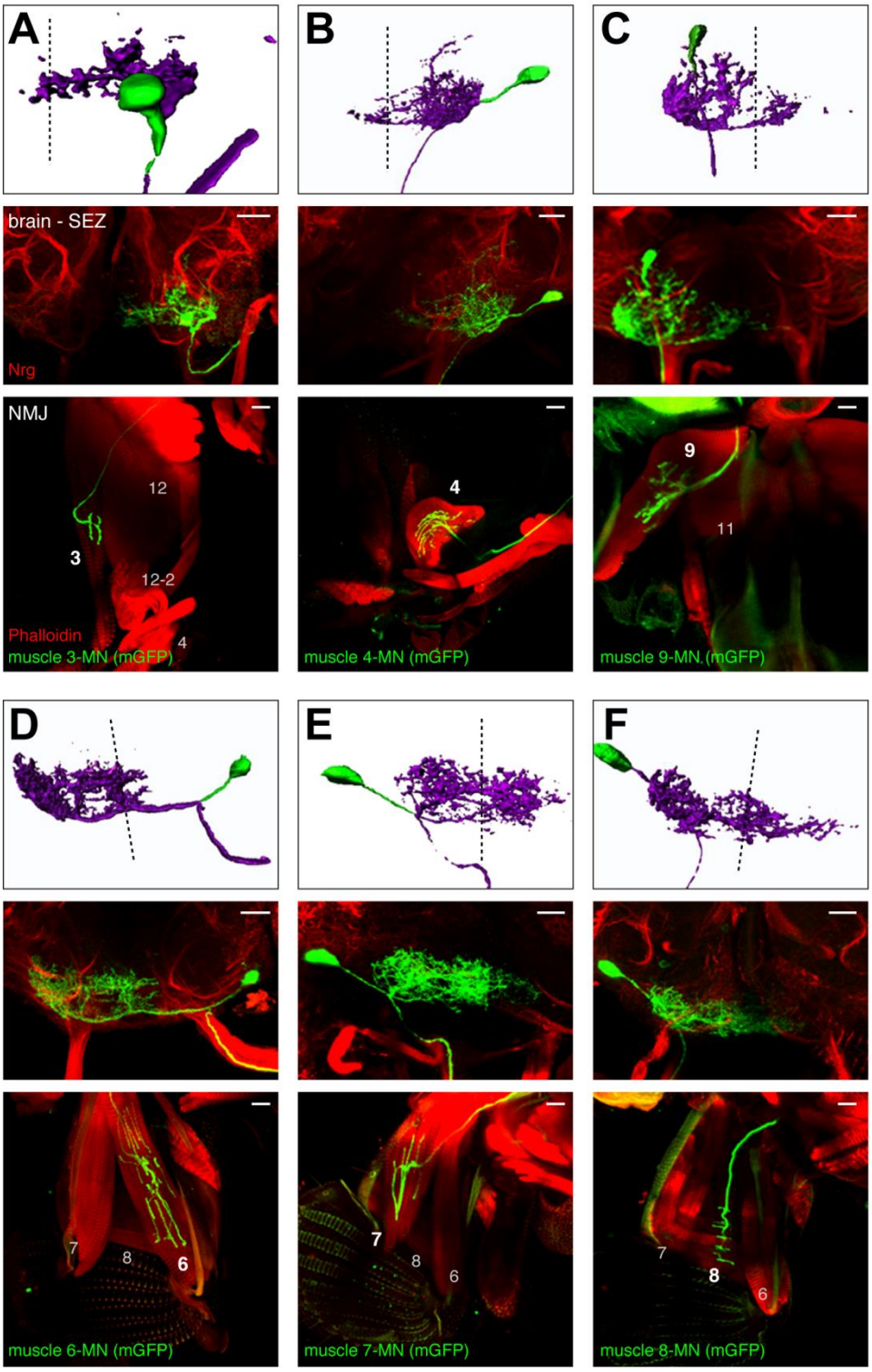

Schwarz et al. Figure 4

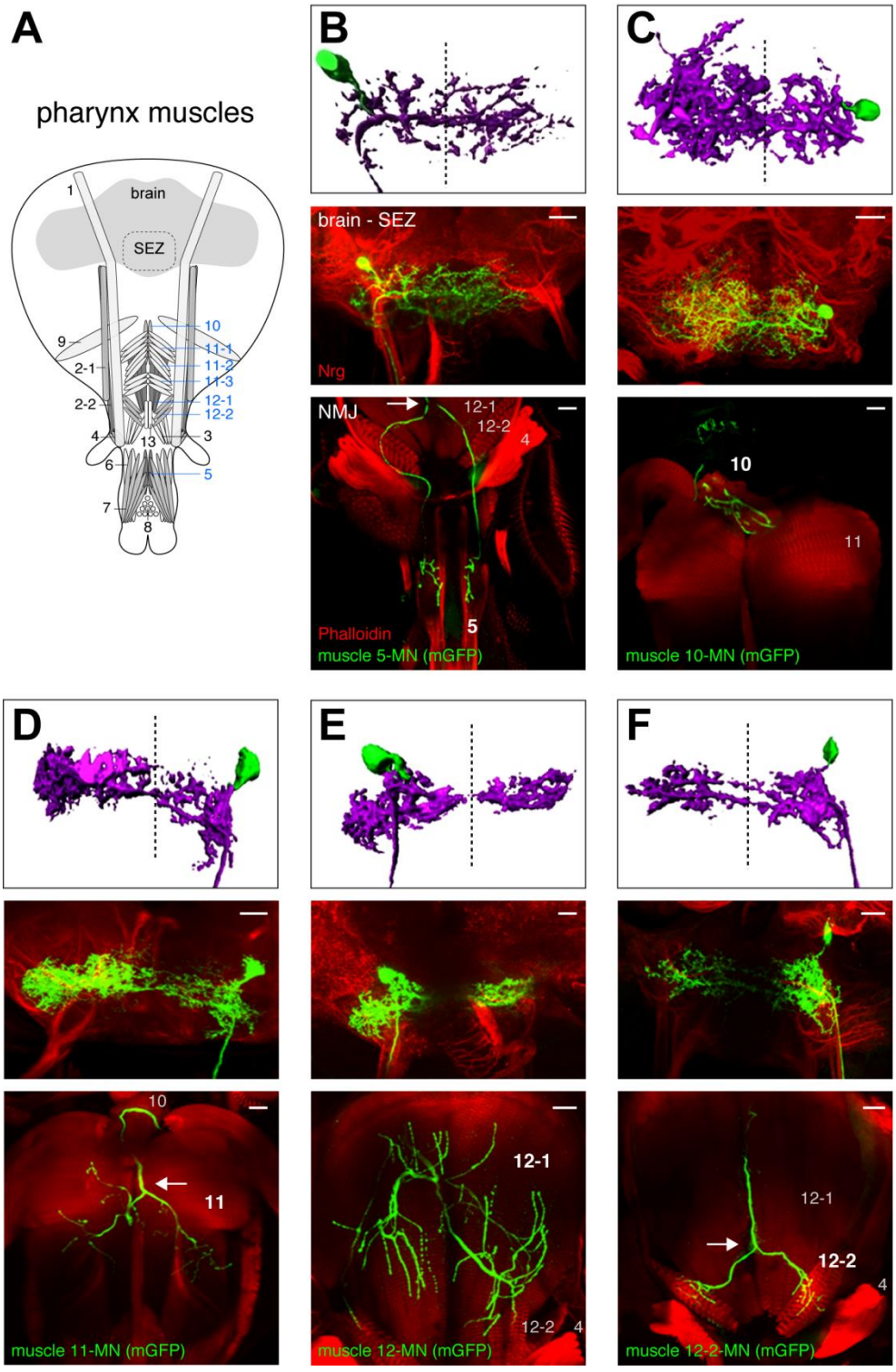

Schwarz et al. Figure 5

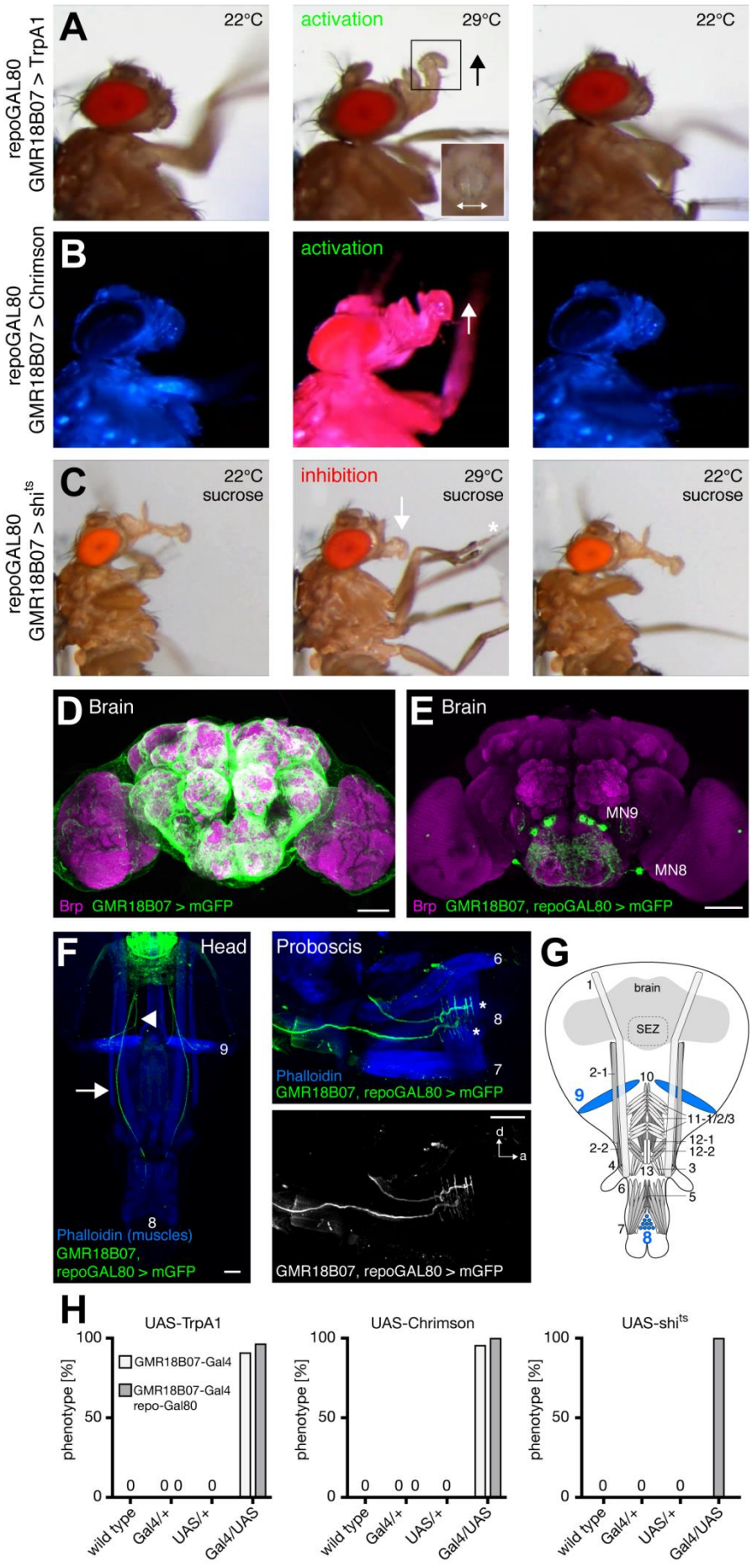

Schwarz et al. Figure 6

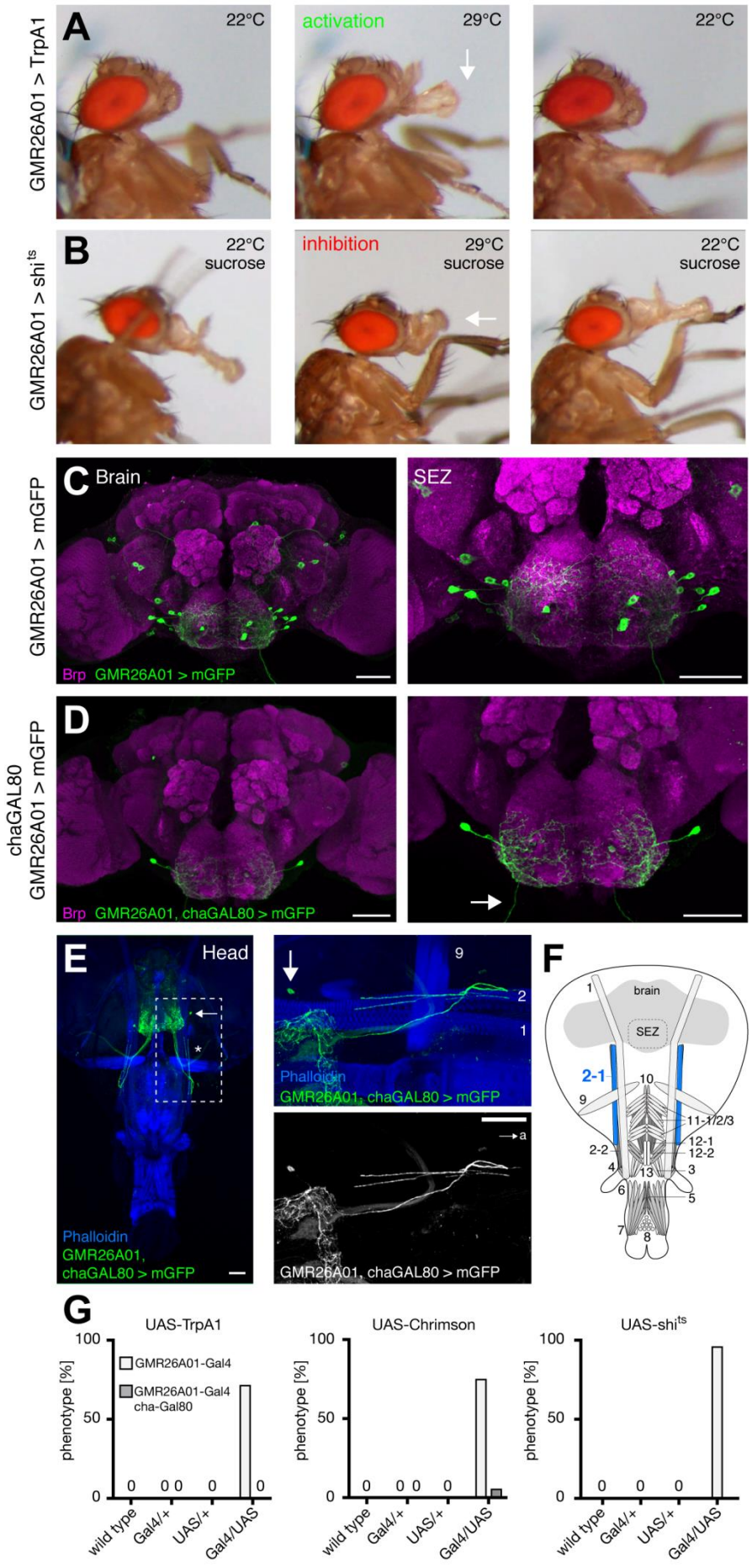

Schwarz et al. Figure 7

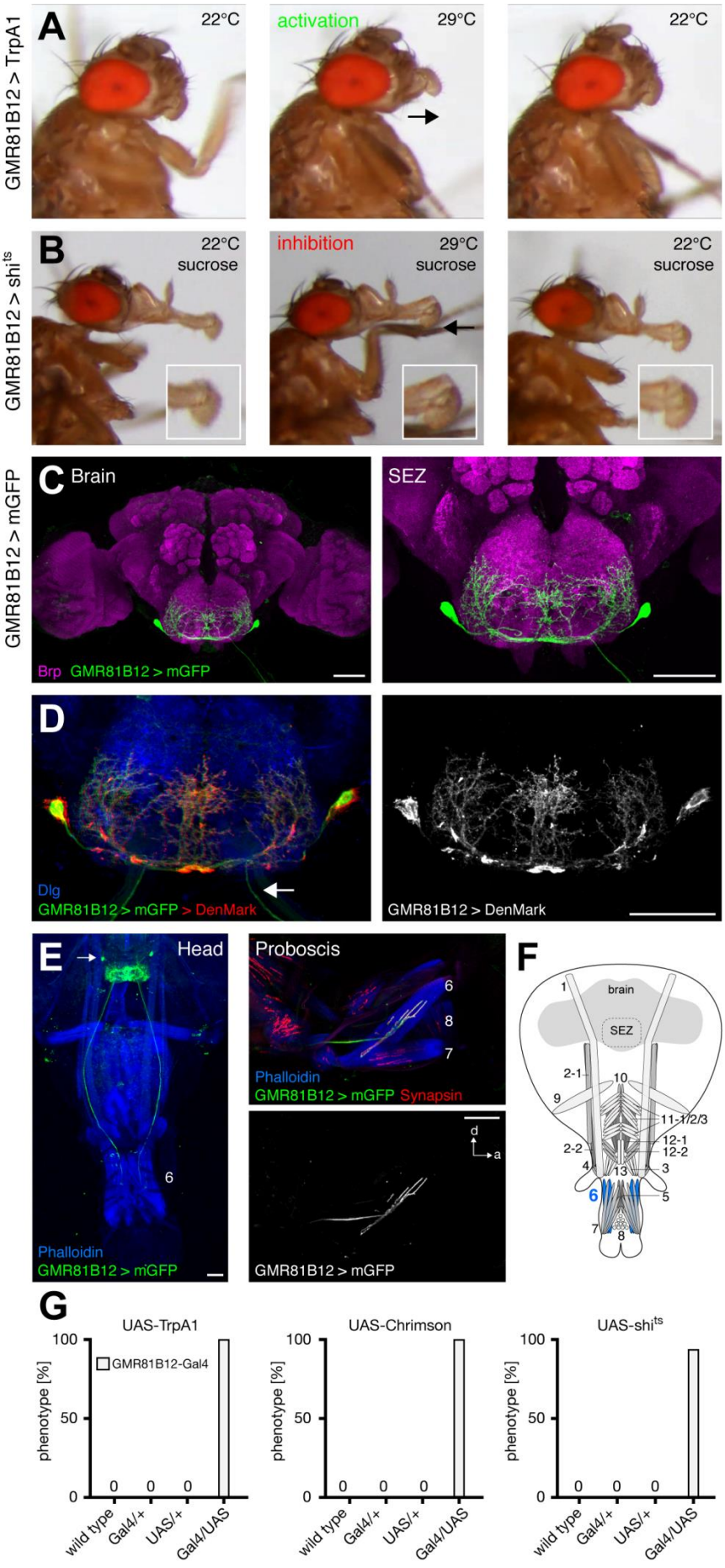

Schwarz et al. Figure 8

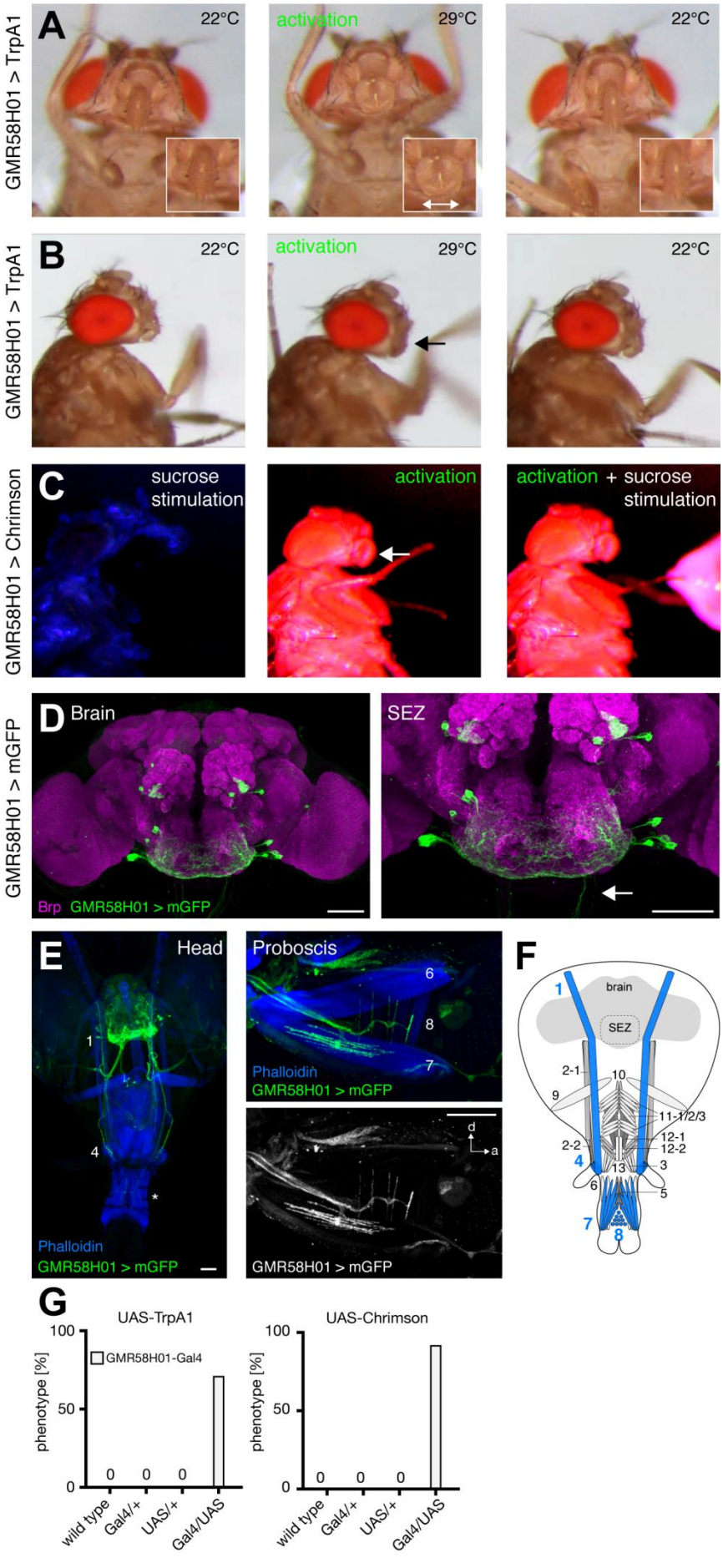

Schwarz et al. Figure 9

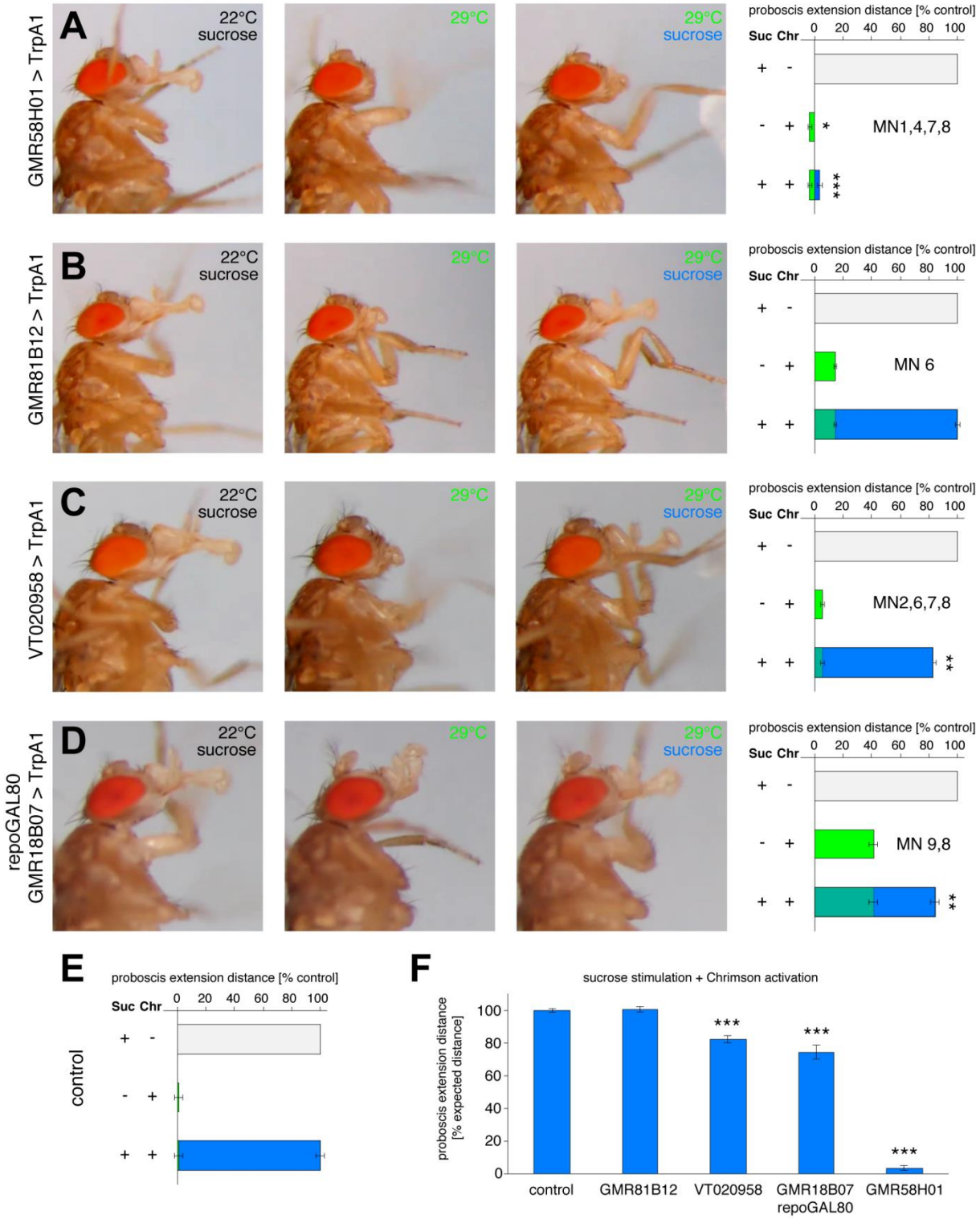

Schwarz et al. Figure 10

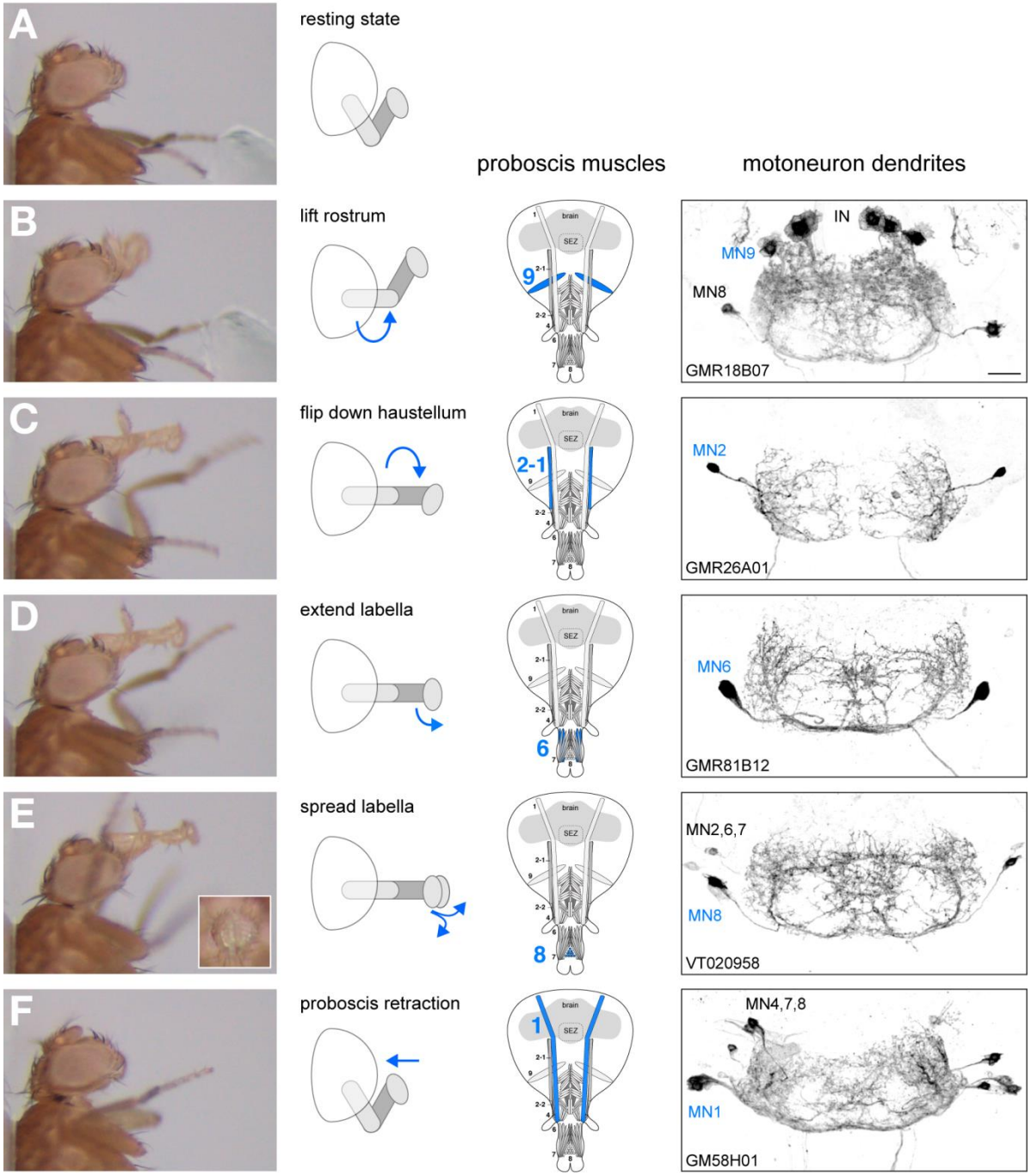

Schwarz et al. Figure 11

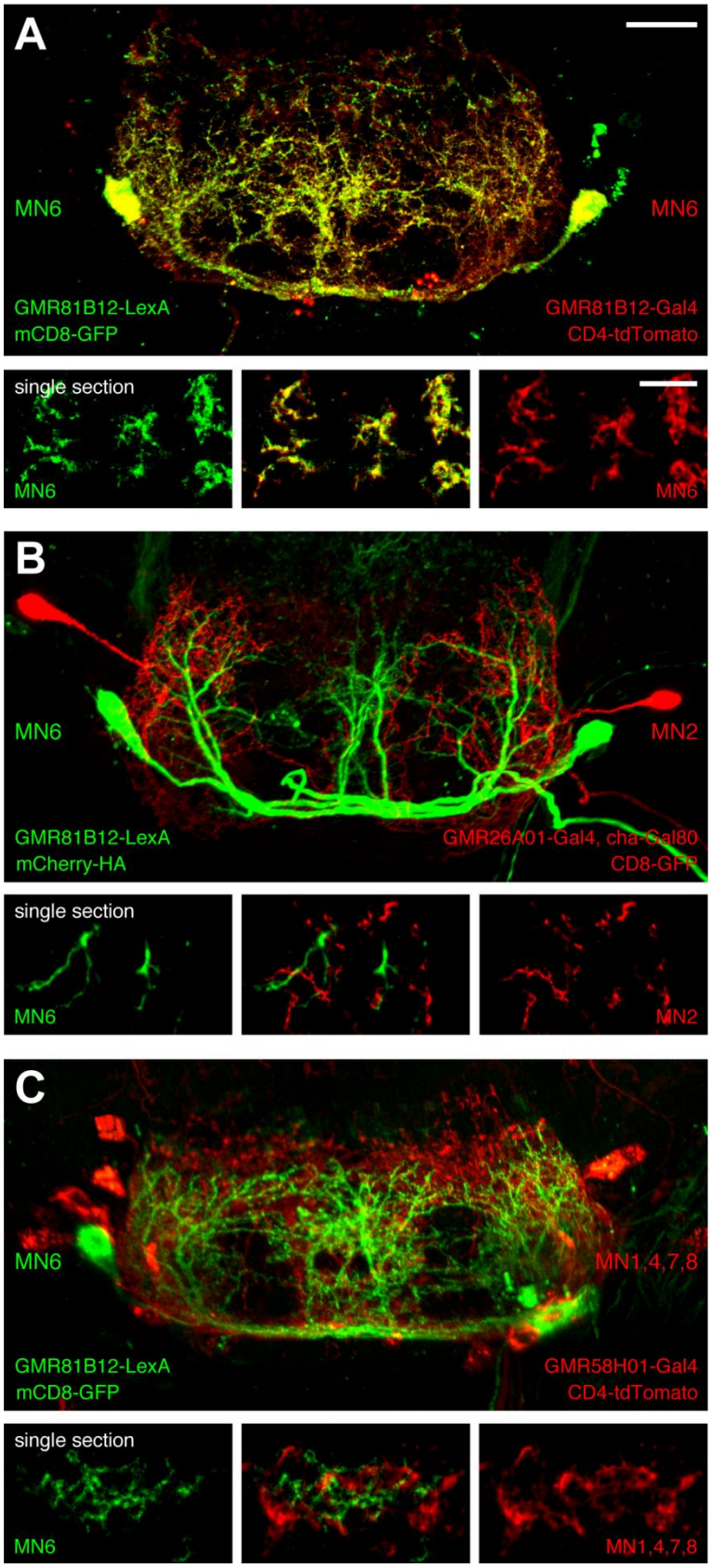

Schwarz et al. Figure 5-figure supplement 1

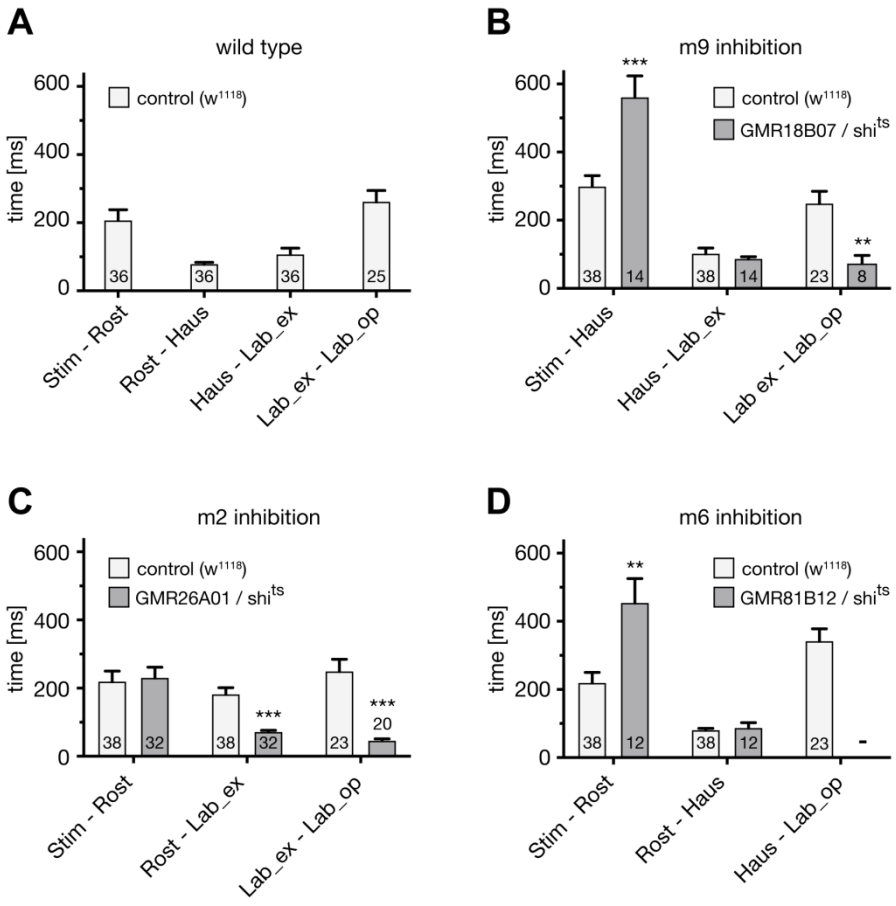

Schwarz et al. Figure 6-figure supplement 1

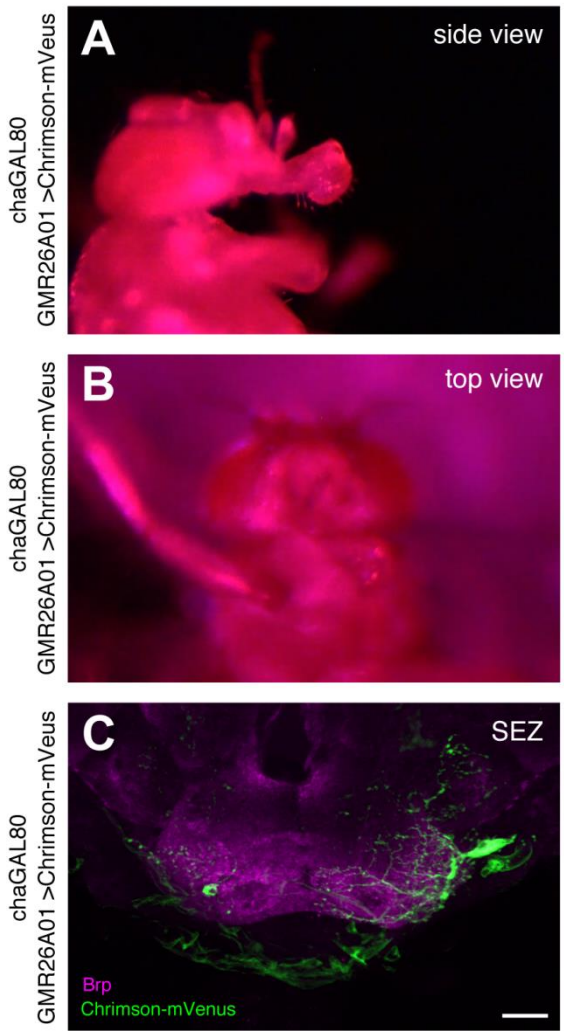

Schwarz et al. Figure 8-figure supplement 1

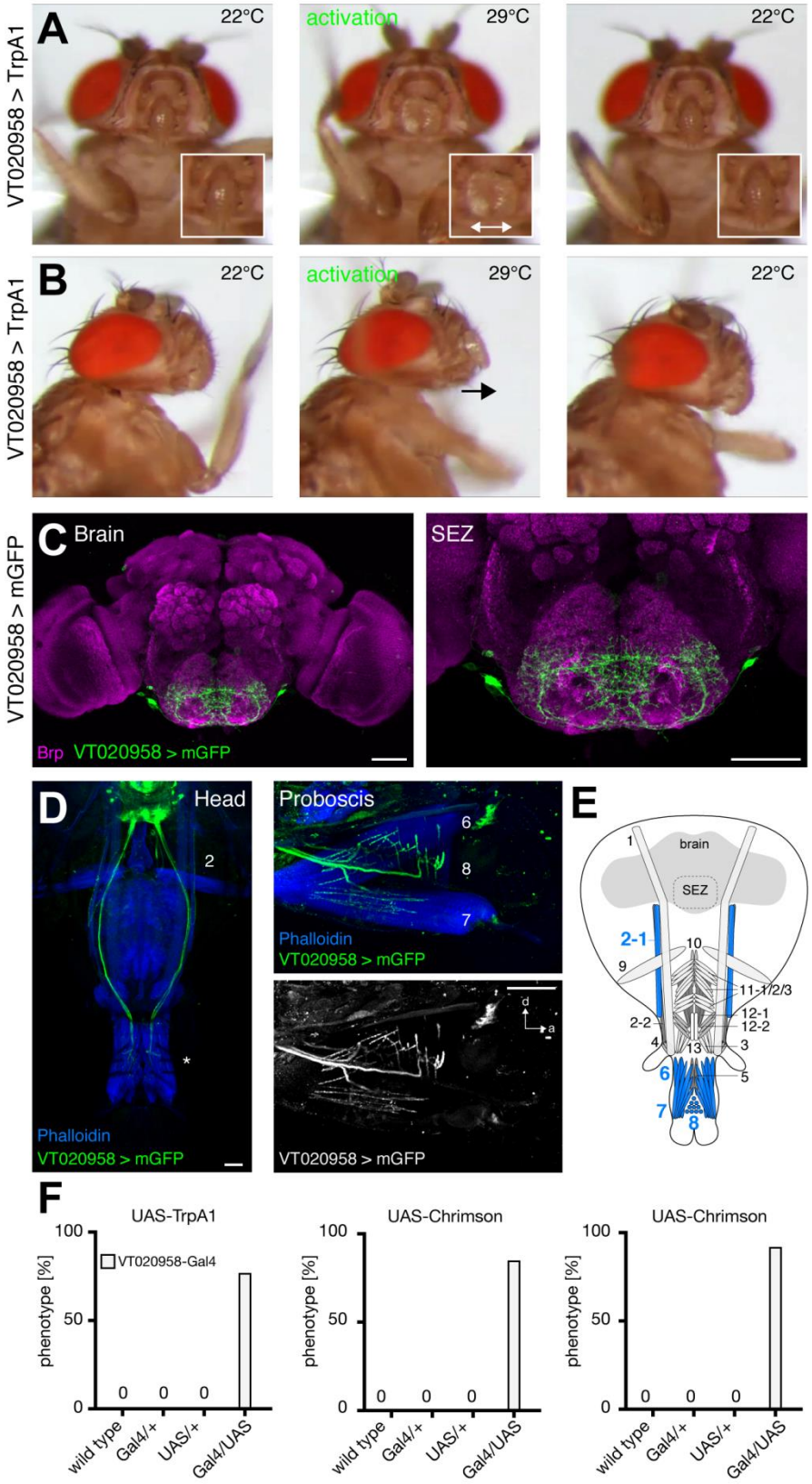

Schwarz et al. Figure 10-figure supplement 1

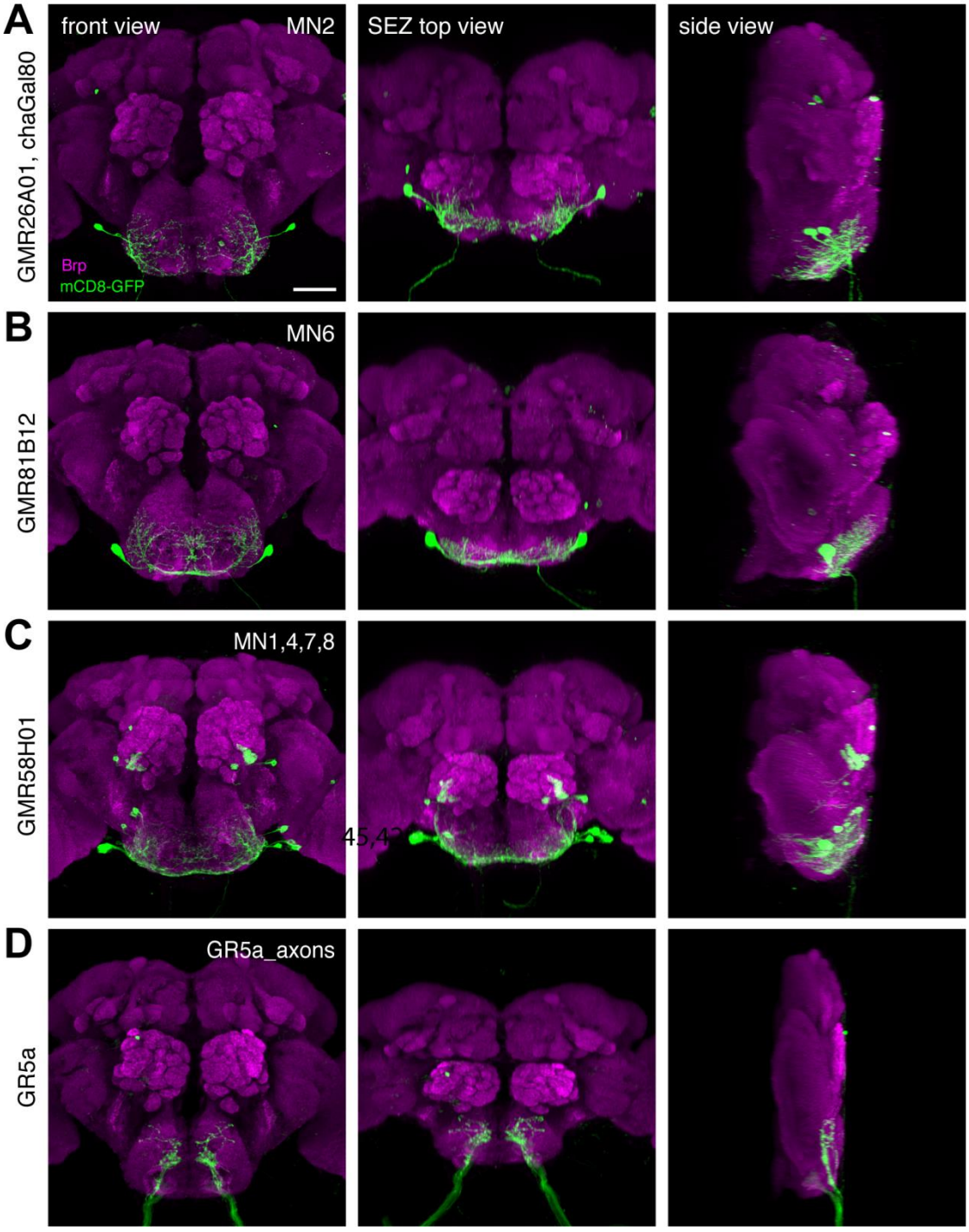

Schwarz et al. Figure 10-figure supplement 2

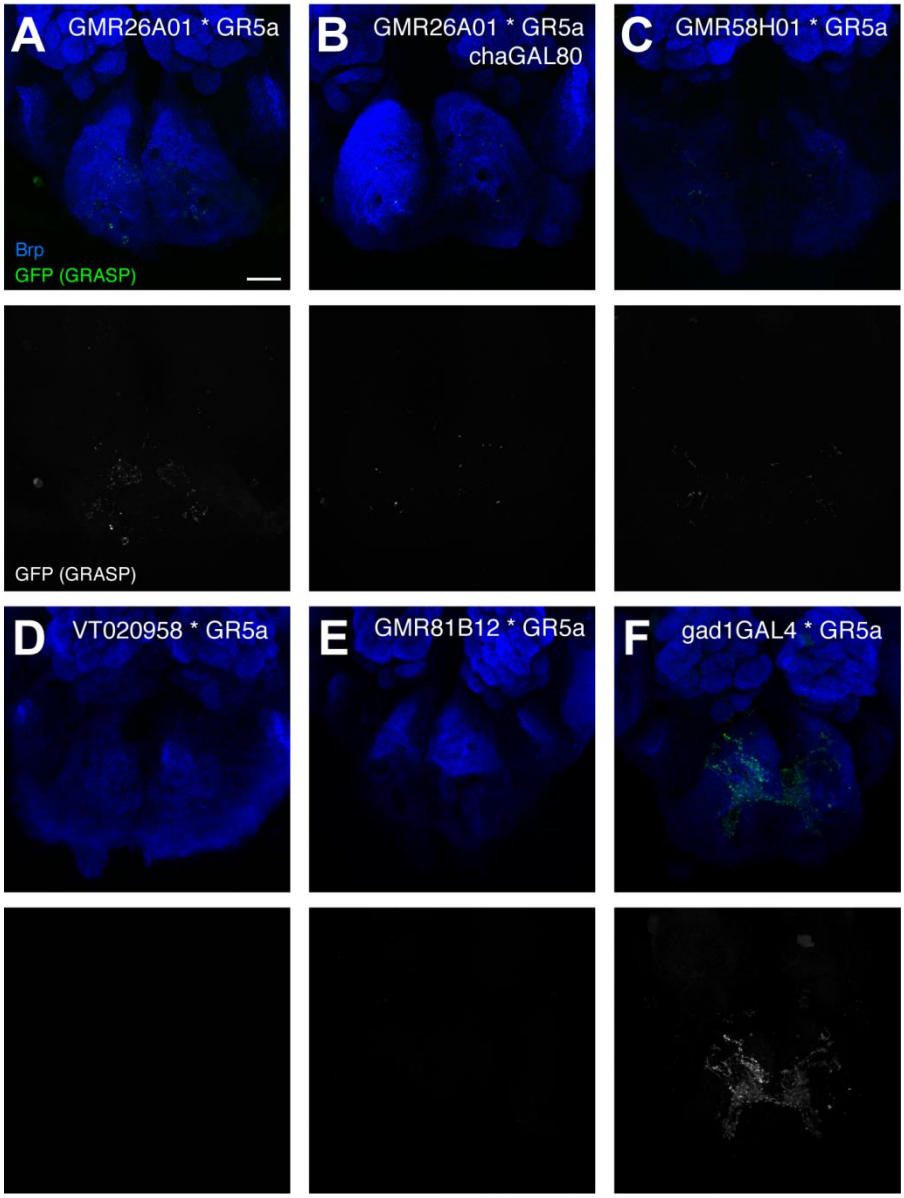

Schwarz et al. Supplementary file 1

Figure	Genotype	Gal4-line	UAS-line		
			TrpA1	Chrimson	shibire^{ts}
Figure 5	wildtype	GMR18B07	0/24	0/20	0/10
	Gal4 / +		0/25	0/22	
	Gal4, repo-Gal80 / +		0/22	0/22	0/11
	UAS / +		0/23	0/31	0/10
	Gal4 / UAS		30/33 p<0.0001	43/45 p<0.0001	
	Gal4, repo-Gal80 / UAS		27/28 p<0.0001	55/55 p<0.0001	15/15 p<0.0001
Figure 6	wildtype	GMR26A01	0/24	0/20	0/10
	Gal4 / +		0/22	0/19	0/12
	Gal4, cha-Gal80 / +		0/21	0/22	
	UAS / +		0/23	0/31	0/10
	Gal4 / UAS		38/53 p<0.0001	37/49 p<0.0001	24/25 p<0.0001
	Gal4, cha-Gal80 / UAS		0/24	4/67* p=0.125	0/12
Figure 7	wildtype	GMR81B12	0/24	0/20	0/10
	Gal4 / +		0/26	0/23	0/10
	UAS / +		0/23	0/31	0/10
	Gal4 / UAS		46/47 p<0.0001	70/70 p<0.0001	15/16 p<0.0001
			46/47 p<0.0001	70/70 p<0.0001	15/16 p<0.0001
Figure 8	wildtype	GMR58H01	0/24	0/20	
	Gal4 / +		0/23	0/21	
	UAS / +		0/23	0/31	
	Gal4 / UAS		27/38 p<0.0001	45/49 p<0.0001	0/12
			27/38 p<0.0001	45/49 p<0.0001	
Figure 9	wildtype	VT020958	0/24	0/20	
	Gal4 / +		0/24	0/24	
	UAS / +		0/23	0/31	
	Gal4 / UAS		33/43 p<0.0001	39/46 p<0.0001	0/12
			33/43 p<0.0001	39/46 p<0.0001	

3.3 Studying the PER Motor Program by Identifying Interneurons

3.3.1 Introduction

The stereotyped temporal ordering of the motor steps underlying the proboscis extension response is an ideal model to study how neuronal ensembles produce a sequential behavior. Through the previously performed Gal4-based behavioral activation screen we were able to gain genetic control over 5 different motoneurons, each one innervating one specific muscle and each one controlling one specific step within the PER motor program. This implies that the temporal sequence of these steps is represented by the temporal sequence of motoneuron activity executing these steps. Based on the artificial neuronal activation and inhibition data we could exclude that the activation of a motoneuron controlling a preceding step is a requirement or the trigger for the initiation of the following step. This led us to the conclusion that interneurons control the precise temporal orchestration of motoneuron activity.

At the moment, there is no interneuron known, that is directly connected to proboscis motoneurons. However, a recent study identified a single pair of command interneurons, also called 'feeding neuron' or 'Fdg neuron', that induce the entire feeding sequence when artificially activated (Flood et al., 2013). Based on colocalization experiments, these neurons are neither connected to sensory neurons nor to motoneurons. This suggests, that one or more levels of interneurons connect proboscis motoneurons to the upstream command feeding interneuron. To address this, we aimed to identify and characterize motor-related interneurons, that are downstream of the command feeding interneurons, mainly focusing on premotor interneurons. The term *premotor interneuron* is not strictly defined, however, for my thesis, this term exclusively includes interneurons that are directly connected to motoneurons. So far, information on premotor interneurons controlling proboscis motoneurons is completely lacking. But considering the successful implementation of the behavioral activation screen to identify and characterize motoneurons, it might be possible to identify premotor interneurons using a similar strategy. In addition, the acquired knowledge about the exact position of motoneuron dendrites enabled us to focus the search on interneurons arborizing within this specified region and therefore facilitates preselection of candidate lines that might express in neurons directly connected to motoneurons.

Our goals are to identify and characterize proboscis premotor interneurons in order to understand how the stereotyped temporal ordering of the motor steps underlying the proboscis extension

response is achieved and to shine light onto general principles of neuronal circuits to generate sequential movements.

3.3.2 Results

We browsed through the GMR-Gal4 expression database with the focus on sparse lines expressing in neurons arborizing within the anteroventral SEZ. Based on these criteria, 20 lines

	Line	Brain Expression with mCD8GFP	TrpA1 Behavior
1	51E06	1 pair of SEZ neurons, OL, MB	12/12 rRL, + LE and LO
2	56G04	dominant IPCs and medio-ventral SEZ	no reaction
3	77C10	strong medial SEZ arborizatin, 1 cell pair	6/6 eye grooming; 1/6 rRL
4	79C11	weak medial SEZ	no reaction
5	84B09	weak in SEZ	no reaction
6	86D02	weak SEZ + strong IPCs + CC	12/12 rRL
7	78G05	dorsal SEZ + CB	no reaction
8	95H11	no expression	no reaction
9	15F09	no expression	no reaction
10	21C11	7 pairs of SEZ neurons + 10 pairs in CB	6/6 rCE + grooming
11	10H05	probocerebral bridge + glia	6/6 fast leg movements
12	11A12	no expression	2/6 twitch
13	78A03	weak in SEZ	no reaction
14	94G09	weak in medial SEZ	no reaction
15	14G09	2 pairs SEZ neurons + 6 pairs EB	no reaction
16	18E06	some SEZ expression covered with glia	2/6 twitch + LE
17	32D08	1 lateral + 6 medial pair of SEZ neurons	6/6 stiff leg position
18	33H10	no expression	no reaction
19	44A01	3 SEZ pairs + 1 pair in higher brain, MNs	6/6 LE and LO; 2 had drop
20	47G08	very weak in SEZ and CC	2/6 HE

Table 1. Summary of the behavioral activation screen to identify premotor interneurons
Each row represents one line. The brain expression pattern and the behavior of each line are described. Abbreviations to describe the brain expression pattern: SEZ, Suboesophageal Zone; OL, Olfactory Lobe; MB, Mushroom Body; IPCs, Insulin-Producing Cells; CC, Central Complex; CB, Central Brain; EB, Ellipsoid Body
Abbreviations to describe the TrpA1 mediated behavior: rRL, repetitive Rostrum Lifting; LE, Labellum Extension; LO, Labellum Opening; rCE, repetitive Complete Extension; HE, Haustellum Extension

were selected and analyzed in a behavioral activation screen using TrpA1 in the same way as it was already done to identify the motoneurons. The only exception is that the flies were glued with their wings on a coverslip instead of being immobilized in a pipett tip. In parallel, these lines were also crossed to UAS-mCD8GFP to visualize the targeted neurons. The behavior and morphology datasets are summarized in Table 1. Out of these 20 lines, 10 showed no behavioral phenotype upon temperature increase. Nine of the remaining 10 lines were excluded from further investigations for different reasons. Two showed no expression in the SEZ, 1 is expressed in motoneurons, 2 are too broadly expressed, 3 only had a phenotype with a low penetrance (2 or less out of 6 flies), and 1 line showed a leg phenotype. However, the remaining line, GMR51E06-Gal4 (Line 1 in Table 1), fullfills all criteria to be a highly promising premotor interneuron candidate. In the screen, it showed a fully penetrant behavioral phenotype (12/12), namely the repetitve lifting of the rostrum at a rate of about 1 Hz. All lifting events are accompanied by the extension and opening of the labellum when the rostrum is maximally lifted (Figure 9, Movie 3). The behavioral phenotype could be reproduced by optogenetic activation using Chrimson, except that the frequency of extension events was lower. However, heat-induced silencing of GMR51E06 neurons using shibire^{ts} did not reveal any defects of the proboscis extension response towards a positive gustatory stimuli.

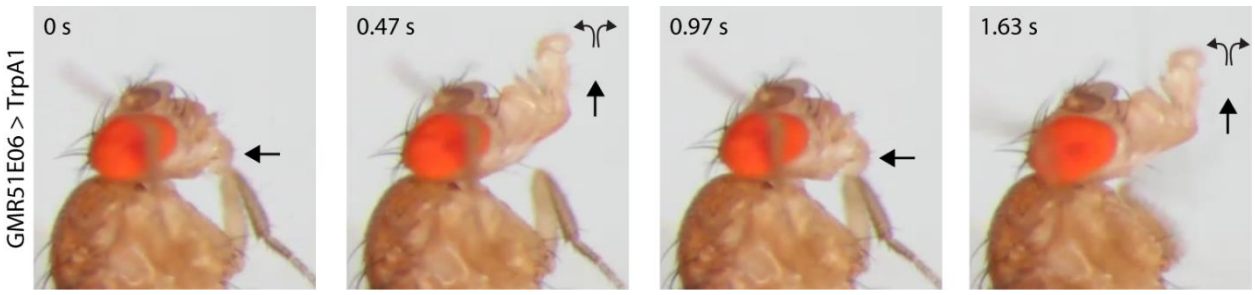

Figure 9. GMR51E06 neurons are sufficient to elicit 3 steps of the PER sequence
Artificial activation of GMR51E06 using TrpA1 induces repetitive rostrum lifting that is accompanied by the extension and opening of the labellum at the end of each lifting event. All snapshots are taken at 29°C. The timepoint of each snapshot is indicated at the top left corner. Arrows indicate movement directions.

The expression pattern of this line was initially hard to resolve. Even though the cells in the optic lobe could be visualized very clearly using the mCD8-GFP reporter-line, the expression in the SEZ was very weak and only one cell pair could be detected. After crossing GMR51E06-Gal4 flies to a variety of different reporter-lines, we could successfully identify one line, 20xUAS-hexamericGFP, that greatly increased signal intensity. High-resolution imaging clearly showed that the expression of this line within the central brain is very sparse and only two types of neurons are located within the SEZ (Figure 10A). One type consists of two bilateral clusters of four neurons on each side, which mainly arborize outside of the SEZ. The other type consists of

only one bilateral pair of neurons that mainly projects to the anteromedial and anteroventral SEZ (Figure 10B). Whole-head preparation showed no expression in sensory neurons or motoneurons.

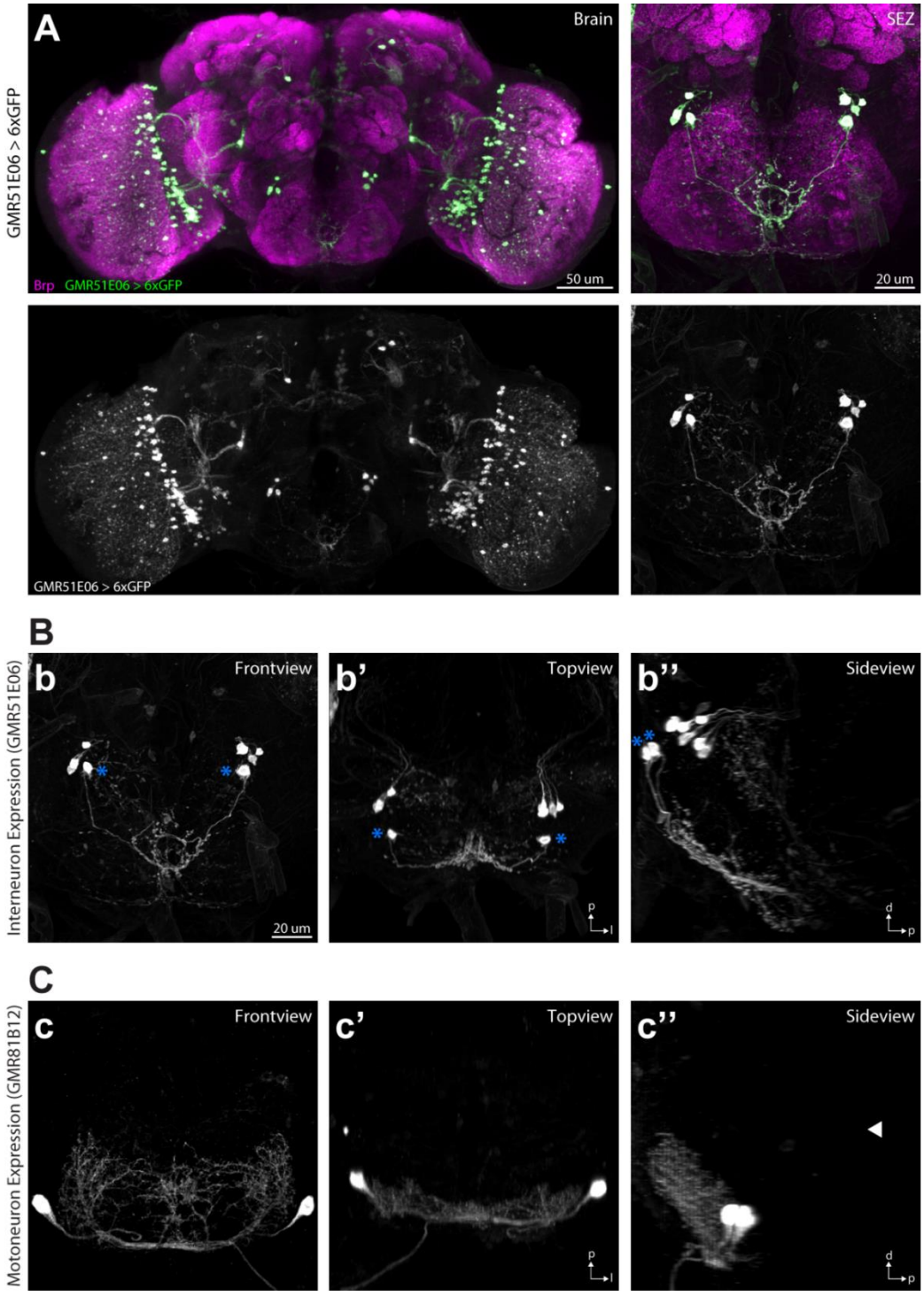

Figure 10. Expression of GMR51E06 in the adult brain
(A) Neurons are marked by the expression of 20xUAS-hexamericGFP (green) and the neuropil is visualized using the presynaptic active zone marker Brp (magenta). (B) The expression of GMR51E06 in the SEZ is shown as a frontview (b), topview (b'), and sideview (b''). Blue asterisks indicate the bilateral pair of neurons that arborize within the anteromedial and anteroventral SEZ. (C) The SEZ expression of GMR81B12 > mCD8-GFP in a pair of motoneurons innervating muscle 6 is shown as a frontview (c), topview (c'), and sideview (c'').

4. General Discussion and Outlook

4.1 Identification of Proboscis Motoneurons and Taste Interneurons

The functional behavioral screen of preselected GMR-Gal4 lines using TrpA1 to artificially activate targeted neurons was very well suited to identify essential control elements of the *Drosophila* taste circuitry. We successfully identified different, higly interesting interneuron lines, that are characterized in detail in Xinyu Liu's PhD thesis and a variety of motoneuron lines which together cover the whole proboscis extension sequence. It is important to note that this screen does not enable the identification of neurons belonging to the aversive pathways, as activating those neurons would not result in an extension of the proboscis. To identify bitter circuit elements, it would require to simultaneously apply an attractive stimulus to the GSNs and examine if the PER score is decreased at the restrictive temperature compared to the permissive temperature.

To choose the settings for the screen we initially tested wildtype flies in the heating chamber and observed that at high temperature starved flies showed some artificial behaviors, including *twitching* of the proboscis, *constant extension of the haustellum* or *repetitive complete extensions* of the proboscis. These three groups most likely represent behaviors that are not related to the taste system and occur as defence behaviors in response to the restriction of wing and leg movements through the pipet tip and the uncomfortably high temperature. Interestingly, the frequency of these behaviors was reduced in fed flies (data not shown). This might be due to better physical conditions and, as a result, the increased robustness of these flies. Therefore, we decided to perform the screen with fed flies to avoid any masking by behaviors that are not specifically elicited by the activation of the targeted neurons. However, as the three mentioned behaviors were the most abundant behaviors observed in the screen, it its likely, that not taste-related behaviors may have been categorized as false positives.

Many different aspects of the motor output of the taste circuitry were observed upon artificial activation of Gal4 expressing neurons. The repetitive extensions of the proboscis most likely occur through activation of upstream neurons since artificial activation of all the sweet sensory neurons leads to similar, repetitive full extensions of the proboscis (Movie 4). Repetitive extensions of the proboscis are naturally observed in flies feeding on a substrate. It was shown that flies feed in feeding bursts where each burst consists of about six sips with the proboscis

being retracted and extended between each sip (Itskov et al., 2014). Thus, lines maintaining this facet of the feeding program might control expression in neurons upstream in the taste circuitry, as they are sufficient to induce general aspects of the natural feeding behavior.

As already mentioned, the screen was not designed to identify elements of the aversive pathways. However, also the identification of neurons conveying attractive signals is not always straightforward. Several different internal and external stimuli can inhibit the PER (Chatterjee and Hardin, 2010; Dethier, 1976; Masek and Scott, 2010; Menda et al., 2011; Shiraiwa, 2008; Shiraiwa and Carlson, 2007). In a situation where neurons from the attractive pathway are artificially activated it is still possible that inhibitory signals decrease or abolish a potential response if these signals are integrated downstream of the genetically targeted neurons. In the screen, we were particularly successful in identifying motoneuron-lines and, as hypothesized, they were all included within the *constant extension* and *labellum spreading* group. The main reason for the high efficacy to identify motoneurons might be due to the fact that the proboscis motoneurons are the very last neurons of the taste circuitry and thus, presumably downstream of all inhibitory signals that may impinge on it.

4.2 The Proboscis Motor Program is Controlled by Independent Motor Units

Our work on different aspects of the proboscis motor system set the basis to thouroughly analyze the generation of a serial behavior. First, we have carefully dissected the proboscis extension response sequence into five steps, that are rostrum lifting, haustellum extension, labellum extension, labellum opening, and proboscis retraction. Second, we developed a new dissection method that allowed the description of the anatomy of all the proboscis muscles in fine details in an intact head. In addition this method opened the door to visualize a complete motoneuron, i.e the cell body, dendritic arborization, axonal projection, and muscle innervation in a single preparation. Third, we gained genetic access to the motoneurons controlling the four steps of the motor sequence and identified the muscles executing these steps. Thus, we have the control over the taste circuitry on three different levels, namely on a behavioral, muscular, and motoneuronal level. Together, this bears an immense potential to thoroughly analyze the generation of a complex serial behavior in an intact animal.

Moreover, these three levels are linked to each other into units in a very straightforward manner. One of the four behavioral step is controlled by one bilateral pair of muscles which is innervated by one or more bilateral pairs of motoneurons. In addition, based on our thermo- and optogenetic

activation and silencing experiments, we could clearly demonstrate that these units act completely independently of each other, meaning that the activation of one unit is neither required nor the trigger for the execution of the following unit. This independent regulation of the different units enables a high degree of freedom to produce different proboscis movements. This would not be possible if the units were linked to each other in a reflex chain like falling domino stones.

In addition to its main role in feeding behavior, the extension of the proboscis is also part of two other behaviors. First, the proboscis is extended to perform courtship licking of the female genitalia to taste pheromones (Hall, 1994; Nichols et al., 2012). The proboscis movement for courtship licking behavior has never been described in details. We hypothesize, that the proboscis of the male fly has to make an upwards movement in order to reach the female genitalia from below and that the labellum is extended and open to expose all GSNs. Second, the proboscis is also extended during grooming to clean it (Hampel et al., 2015; Seeds et al., 2014). There, the proboscis is extended in a more straight manner and rubbed between the two anterior legs, suggesting that this behavior only requires the lifting of the rostrum and the extension of the haustellum. Feeding, licking and grooming all involve the extension of the proboscis but all three behaviors require a different proboscis motor program. Bearing in mind the independent regulation of the different motor units, the motor output can be varied simply by recruiting different units.

If we consider *pumping* as the fifth behavioral unit, the feeding-related proboscis extension response recruits all five motor units. In contrast, courtship licking seems to require rostrum lifting, labellum extension, and labellum opening, even though we can not exclude that also the haustellum is partially extended. On the other side, grooming of the proboscis requires the lifting of the rostrum and the extension of the haustellum. Thus, we suggest, that the three different proboscis motor programs for feeding, licking, and grooming are controlled by three different, independent, and context-specific central circuits, that generate three different motor unit recruitment profiles (Figure 11).

A previous study showed the existence of a command interneuron that induces all behavioral steps required for feeding (Flood et al., 2013). Thus, it is very likely, that also the licking PER and the grooming PER have their own command interneuron, comparable to the Fdg-neuron that induces feeding. We suggest, that the different command interneurons induce the appropriate,

context-related PER motor sequence by recruiting the right sets of motor units. A similar scenario was recently described for wing movements. Whereas flight requires the activation of a specific set of dopaminergic interneurons, these neurons do not control the production of the courtship song consisting of unilateral wing extension and vibration (Sadaf et al., 2015).

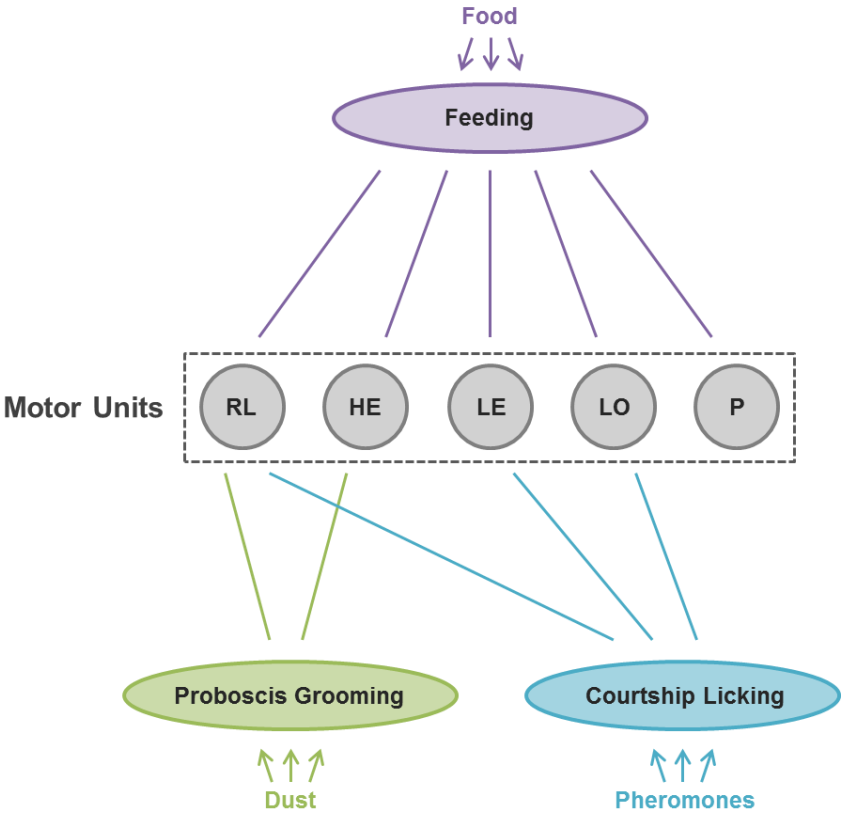

Figure 11. Schematic illustration showing the three different proboscis motor programs
Palatable food sources induce feeding that recruits all five motor units. In contrast, proboscis grooming, that is elicited by dust or other particles on the proboscis, only requires two motor units. In addition, courtship licking, induced by the presence of a reproductive female, only requires three motor units. Abbreviations: RL, rostrum lifting; HE, haustellum extension; LE, Labellum extension; LO, labellum opening; P, pumping.

4.3 Control of the Temporal PER Sequence

Interestingly, activation of a single Fdg neuron induced asymmetric proboscis extension to the ipsilateral side (Flood et al., 2013). This suggests that Fdg interneurons are rather downstream in the gustatory sensory-motor circuit as they selectively control proboscis muscle contraction on the ipsilateral side of the body. But whether these neurons are directly connected to motoneurons remains to be determined. If direct excitatory connections of the command interneurons to the specific set of motoneurons would be the basis for motoneuron activity, the temporal orchestration of motor unit activation would be difficult to achieve, since there seems to be no crosstalk on the level of the motor units. Longer or thinner axons to motoneurons controlling later steps in the PER sequence would be the only way to achieve the temporal ordering. But as the latest step (labellum opening) of the feeding PER sequence is elicited several hundred

milliseconds after the initial step (rostrum lifting), it is very unlikely that this type of themporal orchestration can account for this delay.

It might be the case, that we can find a premotor interneuron on top of each motor unit, which directly activates the corresponding motoneuron. In addition, it might activate the premotor interneuron of the subsequent step, either directly or indirectly via disinhibition. Thereby it would be possible to explain the temporal ordering of the sequence. Thus, we suggest a model where different command interneurons recruit different sets of premotor interneurons which in turn activate the corresponding motoneurons and regulate the temporal ordering of the behavior (Figure 12). This model would also explain why artificial activation of any motoneuron does not lead to a progression in the motor sequence and why inhibition of a single motoneuron does not disturb the execution of the rest of the sequence.

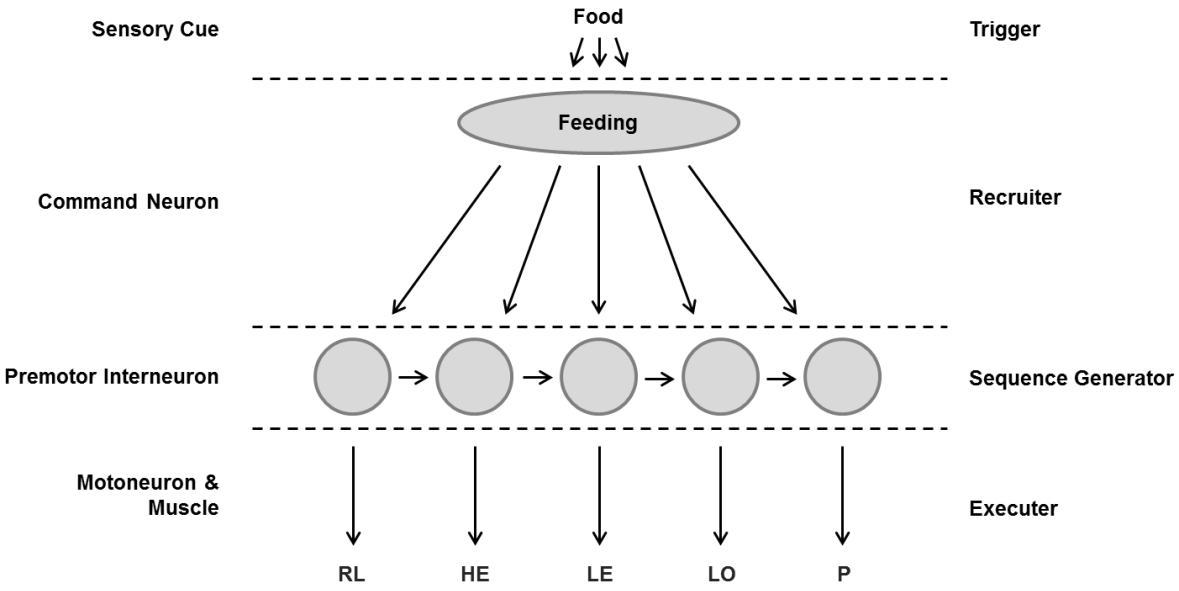

Figure 12. Schematic model showing how the feeding PER motor sequence is generated
Sensory cues in palatable food sources trigger the PER by activating the feeding command interneurons. They, in turn, recruit the right set of motor units (in case of feeding, all five) by activating premotor interneurons which are on top of each motor unit. Premotor interneurons directly activate the corresponding motoneuron which executes the motor unit and generate the temporal sequence by activating or disinhibiting the premotor interneuron of the subsequent step.

In our second behavioral activation screen we identified a line, GMR51E06, that shows repetitive lifting of the rostrum upon thermo-or optogenetic activation. The lifting events end with the extension and opening of the labellum. Interestingly, The unit recruitment profile of the behavior, that is artificially elicited in line GMR51E06 corresponds to the one that is naturally used for courtship licking. Thus, it is possible that command licking interneurons are targeted in this line and are responsible for the behavioral phenotype. Consistently, shi^{ts}-mediated silencing

of these neurons did not lead to any defects of the PER in response to a sweet gustatory stimuli. Assuming that the inhibition was complete, these neurons are not required to execute the feeding PER. This strengthens the idea, that these neurons are indeed command licking interneurons exclusively required in this context.

Another possibility is, that the targeted interneurons are not command licking interneurons but premotor interneurons that are used for feeding and/or licking PER, since both behaviors require all three motor units that are elicited in this line. Given that Gal4 expression levels in the SEZ neurons in this line are low, it is possible that shi^{ts}-mediated silencing was not complete and therefore, we can not exclude, that these neurons may also be required for the feeding motor program. This would also explain the observation that the behavior is produced in a repetitive manner. This feature has only been observed during feeding, but not during licking or grooming. But whether the repetitive execution of these three motor units resulted from the intrinsic, characteristic properties of these neurons or whether it is an artifact due to the artificial activation is not yet clear.

Even though the TrpA1 mediated behavior could be reliably elicited in all tested flies, it was not possible to visualize the neurite arborization of the targeted neurons with the commonly used GFP-reporters, most likely due to low Gal4 expression levels. Stronger GFP-reporter lines clearly showed that there is only one pair of interneurons that arborize within the SEZ. Thus we suggest that this bilateral pair of neurons are sufficient to induce the behavior. More specifically, these cells arborize within the anteromedial and anteroventral SEZ, i.e. the region, where proboscis motoneurons spread their dendritic arborizations (compare Figure 10B and 10C). Thus, these neurons may indeed represent premotor interneurons connected to motoneurons. Further experiments, including GRASP, are necessary to evaluate the precise role of these interneurons in different behavioral paradigms.

4.4 Outlook

It will be of high interst to determine the exact function and connectivity of the newly identified interneuron and whether it indeed represents a crucial element of the taste circuitry between the command interneuron and the motoneurons. Identification of additional interneurons downstream of the PER command interneurons would allow to test the hypothesized model and to gain insight into motor control and the production of a stereotypic serial behavior.

Once we know more about further interneuron types, it might be possible to create a closed circuit from sensory neurons, via command interneurons, to proboscis motoneurons with genetically targeted neurons. This would have an enormous potential to shine light onto fundamental neuroscientific questions including the specificity of the connectivity, the plasticity of the synapses, and the integration of learning and other sensory stimuli.

Motoneurons of *Drosophila* larvae are intensively used to study the principles underlying the formation, function, and stability of neuromuscular junctions (NMJs) (Enneking et al., 2013; Pielage et al., 2011; Pielage et al., 2008; Pielage et al., 2005; Stephan et al., 2015). The genetic targeting of individual proboscis motoneurons in combination with the newly developed dissection method to visualize motoneurons and neuromuscular junction simultaneously in an intact had open the possibility to study motoneuron disease models in an adult organsim. In addition, motoneuron disfunction might be displayed by an obvious failure in the proboscis extension response which would allow to correlate motoneuron dysfunction to a behavioral defect.

5. Materials and Methods

Fly Stocks

Fly stocks were maintained on standard fly food at 25°C. Crosses for Immunohistochemistry were kept at 25°C, while crosses for neuronal activation and silencing experiments were kept at 22°C. Enhancer-Gal4 lines were obtained from the Bloomington Stock Center (Jenett et al., 2012) and the Vienna *Drosophila* Resource Center (Dickson and Stark). In addition, the following strains were used in this study: w^{1118}, OK371-*Gal4*, *FRT19A/FM7c*, *FRT19A,hsFLP,*Tubulin-*Gal80;* *OK371-Gal4,*UAS-*mCD8::GFP/CyO*, Gr5a-*LexA*;UAS-*tdTomato::LexAop-CD4::spGFP11*;*UAS-CD4::spGFP1-10* (Feinberg et al., 2008; Gordon and Scott, 2009), Gad1-Gal4 (Sakai et al., 2009), MHC-GFP (Chen and Olson, 2001) UAS-*mCD8::GFP*, 10XUAS-*mCD8::GFP*, 20XUAS-*6XGFP*, UAS-*DenMark* (Nicolai et al., 2010), UAS-*TrpA1* (Hamada et al., 2008), UAS-Chrimson (Klapoetke et al., 2014), UAS-$shibire^{ts}$ (Kitamoto, 2001), cha-*Gal80* (Kitamoto, 2002), repo-*Gal80* (Awasaki et al., 2008).

Immunohistochemistry and Microscopy

2-10 days old male and female flies were incubated in fixative (4% PFA (Paraformaldehyde) in PBS (Phosphate-Buffered Saline), 0.2% Triton-X 100) for 3 hrs at 4°C and washed with PBST (PBS, 0.2% Triton-X 100) 3x 30 min. Brain, proboscis, and head dissections were performed in PBST.

Brain dissection: Brains were dissected and transferred to a tube with ice cold PBST. Primary antibodies were incubated for 3 days at 4°C and secondary antibodies for 2 days at 4°C.

Proboscis and Head dissection: Flies were decapitated with a razor blade. For the proboscis dissection the part of interest was cut. For the head dissection the head was left completely intact with the exception of a few holes that were pierced into the cuticle on the ventral side of the proboscis (26-gauge needle) to allow antibody penetration. Primary antibodies were incubated for 5 days at RT and secondary antibodies for 3 days at RT.

Antibodies were diluted in PBST and used at the following concentrations: mouse anti-Bruchpilot (nc82) 1:200, mouse anti-Synapsin (3c11) 1:100 (both obtained from Developmental Sudies Hybridoma Bank, IA), rat anti-CD8 (Caltag Laboratories) 1:500, rabbit anti-Discs large (Pielage et al., 2011) 1:1,000, rabbit anti-GFP (A6455, Life technologies) 1:1,000, mouse anti-mCherry (632543, Clontech) 1:1,000, phalloidin Alexa647 (Life technologies) 1:1,000. Alexa488, 555, and 647 coupled secondary antibodies (Life technologies) were used at 1:1,000.

Brains, proboscises, and heads were mounted in Vectashield (Vector Laboratories) and images were acquired with a Zeiss LSM 700/710 laser scanning confocal microscope with either a 10x (NA 0.3) objective, a 20x (NA 0.7) oil immersion objective, or a 40x (NA 1.25-0.75) oil immersion objective. Images were processed using Imaris (Bitplane) and Adobe Photoshop software.

GFP Reconstitution Across Synaptic Partners (GRASP)

Enhancer-*Gal4* lines were crossed to *Gr5a-LexA;* UAS-*tdTomato::LexAop-CD4::spGFP11;* UAS-*CD4::spGFP1-10* and the offspring flies with the genotype *Gr5a-Lexa*/+; UAS-*tdTomato::LexAop-CD4::spGFP11/+;* UAS-*CD4::spGFP1-10/*enhancer-*Gal4* were dissected in ice cold PBST. Brains were incubated in fixative for 20 min at 4°C and washed with PBST 3x 30 min. Primary and secondary antibodies were incubated overnight at 4°C.

Artificial Activation Using TrpA1

Enhancer-Gal4 lines were crossed to UAS-TrpA1 at 22°C. We used 2-10 days old male and female flies. Flies were mounted on a glass coverslip 30 min prior to testing. The behavior, with and without gustatory stimulation, was analyzed in a custom-made heating chamber and monitored (Canon EOS 60D) at control (22°C) and activation (28°C - 32°C) temperature.

Artificial Activation Using Chrimson

Enhancer-Gal4 lines were crossed to UAS-Chrimson at 25°C and kept in the dark. Crosses were raised on standard food mixed with 200 uM all-trans retinal. We used 2-10 days old male and female flies. Flies were mounted on a glass coverslip 30min prior to testing. The behavior, with and without gustatory stimulation, was analyzed and monitored (Canon EOS 60D) under control (475nm) and activation wavelength (633nm) in an otherwise dark room.

Artificial Silencing Using shibirets

Enhancer-Gal4 lines were crossed to UAS-shibire^{ts} at 22°C. 2-10 days old male and female flies were starved for 24 hrs and mounted on a glass coverslip 30min prior to testing. The behavior was analyzed and monitored (Canon EOS 60D) in a custom-made heating chamber. To elicit PER a positive stimulus (200 mM Sucrose) was applied to the anterior legs. First, PER was observed at 22°C. Flies that showed no or only incomplete PER were excluded. Second, after the chamber was heated to 30°C flies were repeatedly stimulated to analyze PER at the restrictive

temperature. Third, after the chamber was cooled down to 22°C flies that showed no or only incomplete PER were excluded.

Quantification of proboscis displacement

Enhancer-Gal4 lines were crossed to UAS-Chrimson at 25°C and kept in the dark. Crosses were raised on standard food mixed with 200 uM all-trans retinal. We used 2-10 days old male and female flies that were starved for 24 hrs. Flies were mounted on a glass coverslip 30min prior to testing. The behavior was analyzed and monitored (Canon EOS 60D) in a dark room. The maximum proboscis extension (MPE) is defined as the distance between the most posterior part of the eye and the tip of the labellum when the proboscis is maximally extended. One dataset consist of four MPE data points: Two at blue light with ($blue^+$) and without ($blue^-$) sucrose stimulation and two at red light with (red^+) and without stimulation (red^-). The data points at blue light and red light for one dataset are from two consecutive stimulations. In all quantifications for Figure 8A-E the values are normalized to ($blue^+$-$blue^-$) which represents 100% proboscis extension distance. The values for Figure 8A-E are calculated the following: $\frac{\text{blue+ (−) blue−}}{\text{blue+ (−) blue−}} * 100\%$ for grey bars, $\frac{\text{red− (−) blue−}}{\text{blue+ (−) blue−}} * 100\%$ for green bars and $\frac{\text{red+ (−) blue−}}{\text{blue+ (−) blue−}} * 100\%$ for green+blue bars. In Figure 8F the values are normalized to [($blue^+$-$blue^-$) – (red^--$blue^-$)] which represents 100% proboscis extension distance and are calculated the following: $\frac{(\text{red+ (−) blue−}) - (\text{red− (−) blue−})}{(\text{blue+ (−) blue−}) - (\text{red− (−) blue−})} * 100\%$

6. Appendix

6.1 Supplementary Data

GMR/VT Gal4-line	Constant Extensions			Repetitive Extensions			Twitching	Labellum Opening	Pumping	Drop	No Reaction
	C	H	R	C	H	R					
09F06				xx					x		
10A11		x		x				x			
10B11		x					xx				
10D09											x
10G09											x
11A06		x									
11G09		x				x					
11H11		x								x	
12B12				x							
12D05		x					x	x			
12D06		x		x							
12D09		x									
12F05											x
12G06											x
13B12											x
13E04											x
14B04		x					xx				
14C10											x
14G08										x	
14G09				x			x				
15A08							xxx				
15D07											x
16C03											x
16D02		x					x				
16E11		x		x			xx		x		
16F06							xxx		x		
17A04	x	xx									
17B03							xx				
17B12							x				
17C02											x
17H12		x									
18B07			xxx								
18G08											x
19B03											x
19E09											x
19F08											x
19F11						xxx					
19G10							xxx		xx		
19H06		x					x			x	

GMR/VT Gal4-line	Constant Extensions			Repetitive Extensions			Twitching	Labellum Opening	Pumping	Drop	No Reaction
	C	H	R	C	H	R					
20A07											x
20C04		x		x					x		
20C08				xx							
20C12				x							
20D04							x				
20D07		x					x			x	
20E04		x									
20E06							xxx		x		
20G07		x					x				
21D07		xxx								x	
21E06		x					x				
21H04				x			x				
22A12				x			x				
22B05	x					x			x		
22B10	xx	x					x			x	
22F08				++							
22H09						xx					
23A12											x
23C06											x
23E04				x			x	x			
23E10		x					xx				
23H04	x			x			xx				
24D02	xxx										
24H08	x	x									
25A07											x
25B01				x							
25F04	xxx								x	x	
25G04											x
25G05		xx									
25H02		x					xxx				
25H08				xx							
26A01		x					x				
26B04				xx							
26B10							x				
26E09				x							
27B01							x			x	
27E07							x				
28D11		x		x			xx				
29H12				x					x		
30A06	xxx								xxx		
30C01											x
30F04		x									
30G05		x		x							
31A02				x							
31B01		x									
31F03		x		x			x				

GMR/VT Gal4-line	Constant Extensions			Repetitive Extensions			Twitching	Labellum Opening	Pumping	Drop	No Reaction
	C	H	R	C	H	R					
31F06	x						xx			x	
31F09		x									
31G06											x
32E04				x							
33B02		x		x			x				
33F11							x				
33G04				x						x	
34B02											x
35A03		x		xx			x				
35C12	xx										
36C10											x
36F08				xx			xx		x	x	
37G08		x					x			x	
38B09		x					x				
38C04				x		x				x	
38G08	x						xx				
39F10						x					
40A12				x							
41A01		x		x							
43E05							x				
43G04											x
44D09											x
44E04		x					x				
44E06											x
44G02							x				
45H01											x
46C10		xx					x				
46G12		x									
47A09				xx			xx				
47G08											x
48B01											x
48B06		x					x				
48G01						x					
50C10		x					x				
51F01		x				x				x	
52G12		x					x				
54H01	x						x				
55D04		x					x				
57B04				x		x	x				
58H01			x				x	x			
60G05		x					x				
61C11				xxx			xx		x		
69H10		x		x			xx		x		
70C06		xx									
70C07		x		x			x		xx	x	
70E10											x

GMR/VT Gal4-line	Constant Extensions			Repetitive Extensions			Twitching	Labellum Opening	Pumping	Drop	No Reaction
	C	H	R	C	H	R					
70E11		x					x				
70G07											x
76B10	x	x									
77C10		x					x				
80A01		x									
80H05											x
81B12			x								
81E08		x		x			x		x		
83C03											x
85C03											x
86A08				x		x					
86C01				x							
86D08							xxx				
87C05				x			x				
88F08											x
88G07		x									
89F06											x
VT007688		x					x				
VT020958								x			
VT022100		x					x				
VT026174											x
VT037488				xxx							
VT037534				xxx					x	x	
VT039465							xx			x	
VT040022											x
VT040980					x		x				
VT047645				xx			xx				
VT047747				x			xx				
VT050245						xx					
VT056866				x							
VT058682											x
VT059228				x							
VT059427				x			x			x	

Supplementary Table 1. Summary of the behavioral activation screen
Each column represnts one behavioral phenotype. The strength of an observed behavior is indicated (x, low; xx, middle; xxx, strong) Each row represents one line. The number of each line is indicated on the left.
Abbreviations: C, complete; H, only haustellum; R, only rostrum

6.2 Abbreviations

CPG	Central Pattern Generator
DNA	Deoxyribonucleic acid
Flp	Flippase
FRT	Flippase Recognition Target
GABA	Gamma-Aminobutyric acid
GCaMP	GFP, Calmodulin, M13 Peptide
GECI	Genetically Encoded Calcium Indicator
GFP	Green Fluorescent Protein
GR	Gustatory Receptor
GRASP	GFP Reconstitution Across Synaptic Partners
GSN	Gustatory Sensory Neuron
GTPase	Guanosine Triphospate hydrolase
HVC	Higher Vocal Center
MN	Motoneuron
NMJ	Neuromuscular Junction
PER	Proboscis Extension Response
SEZ	Subesophageal Zone
TrpA1	Transient receptor potential channel A1
UAS	Upstream Activation Sequence

6.3 References

Adams, M.D., S.E. Celniker, R.A. Holt, C.A. Evans, J.D. Gocayne, P.G. Amanatides, S.E. Scherer, P.W. Li, R.A. Hoskins, R.F. Galle, R.A. George, S.E. Lewis, S. Richards, M. Ashburner, S.N. Henderson, G.G. Sutton, J.R. Wortman, M.D. Yandell, Q. Zhang, L.X. Chen, R.C. Brandon, Y.H. Rogers, R.G. Blazej, M. Champe, B.D. Pfeiffer, K.H. Wan, C. Doyle, E.G. Baxter, G. Helt, C.R. Nelson, G.L. Gabor, J.F. Abril, A. Agbayani, H.J. An, C. Andrews-Pfannkoch, D. Baldwin, R.M. Ballew, A. Basu, J. Baxendale, L. Bayraktaroglu, E.M. Beasley, K.Y. Beeson, P.V. Benos, B.P. Berman, D. Bhandari, S. Bolshakov, D. Borkova, M.R. Botchan, J. Bouck, P. Brokstein, P. Brottier, K.C. Burtis, D.A. Busam, H. Butler, E. Cadieu, A. Center, I. Chandra, J.M. Cherry, S. Cawley, C. Dahlke, L.B. Davenport, P. Davies, B. de Pablos, A. Delcher, Z. Deng, A.D. Mays, I. Dew, S.M. Dietz, K. Dodson, L.E. Doup, M. Downes, S. Dugan-Rocha, B.C. Dunkov, P. Dunn, K.J. Durbin, C.C. Evangelista, C. Ferraz, S. Ferriera, W. Fleischmann, C. Fosler, A.E. Gabrielian, N.S. Garg, W.M. Gelbart, K. Glasser, A. Glodek, F. Gong, J.H. Gorrell, Z. Gu, P. Guan, M. Harris, N.L. Harris, D. Harvey, T.J. Heiman, J.R. Hernandez, J. Houck, D. Hostin, K.A. Houston, T.J. Howland, M.H. Wei, C. Ibegwam, et al. 2000. The genome sequence of Drosophila melanogaster. *Science*. 287:2185-2195.

Ando, R., H. Hama, M. Yamamoto-Hino, H. Mizuno, and A. Miyawaki. 2002. An optical marker based on the UV-induced green-to-red photoconversion of a fluorescent protein. *Proc Natl Acad Sci U S A*. 99:12651-12656.

Asahina, K., K. Watanabe, B.J. Duistermars, E. Hoopfer, C.R. Gonzalez, E.A. Eyjolfsdottir, P. Perona, and D.J. Anderson. 2014. Tachykinin-expressing neurons control male-specific aggressive arousal in Drosophila. *Cell*. 156:221-235.

Awasaki, T., S.L. Lai, K. Ito, and T. Lee. 2008. Organization and postembryonic development of glial cells in the adult central brain of Drosophila. *J Neurosci*. 28:13742-13753.

Bailey, D.L., T.D. W., V. P.E., and M. M.N. 2005. Positron Emission Tomography: Basic Sciences.

Baines, R.A., J.P. Uhler, A. Thompson, S.T. Sweeney, and M. Bate. 2001. Altered electrical properties in Drosophila neurons developing without synaptic transmission. *J Neurosci*. 21:1523-1531.

Baird, G.S., D.A. Zacharias, and R.Y. Tsien. 1999. Circular permutation and receptor insertion within green fluorescent proteins. *Proc Natl Acad Sci U S A*. 96:11241-11246.

Bautista, D.M., J. Siemens, J.M. Glazer, P.R. Tsuruda, A.I. Basbaum, C.L. Stucky, S.E. Jordt, and D. Julius. 2007. The menthol receptor TRPM8 is the principal detector of environmental cold. *Nature*. 448:204-208.

Bellen, H.J., C.J. O'Kane, C. Wilson, U. Grossniklaus, R.K. Pearson, and W.J. Gehring. 1989. P-element-mediated enhancer detection: a versatile method to study development in Drosophila. *Genes Dev*. 3:1288-1300.

Bellen, H.J., C. Tong, and H. Tsuda. 2010. 100 years of Drosophila research and its impact on vertebrate neuroscience: a history lesson for the future. *Nat Rev Neurosci*. 11:514-522.

Bier, E., H. Vaessin, S. Shepherd, K. Lee, K. McCall, S. Barbel, L. Ackerman, R. Carretto, T. Uemura, E. Grell, and et al. 1989. Searching for pattern and mutation in the Drosophila genome with a P-lacZ vector. *Genes Dev*. 3:1273-1287.

Bischof, J., R.K. Maeda, M. Hediger, F. Karch, and K. Basler. 2007. An optimized transgenesis system for Drosophila using germ-line-specific phiC31 integrases. *Proc Natl Acad Sci U S A*. 104:3312-3317.

Boyden, E.S., F. Zhang, E. Bamberg, G. Nagel, and K. Deisseroth. 2005. Millisecond-timescale, genetically targeted optical control of neural activity. *Nat Neurosci*. 8:1263-1268.

Brand, A.H., and N. Perrimon. 1993. Targeted gene expression as a means of altering cell fates and generating dominant phenotypes. *Development*. 118:401-415.

Chatterjee, A., and P.E. Hardin. 2010. Time to taste: circadian clock function in the Drosophila gustatory system. *Fly (Austin)*. 4:283-287.
Chatterjee, A., S. Tanoue, J.H. Houl, and P.E. Hardin. 2010. Regulation of gustatory physiology and appetitive behavior by the Drosophila circadian clock. *Curr Biol*. 20:300-309.
Chen, E.H., and E.N. Olson. 2001. Antisocial, an intracellular adaptor protein, is required for myoblast fusion in Drosophila. *Dev Cell*. 1:705-715.
Clyne, P.J., C.G. Warr, and J.R. Carlson. 2000. Candidate taste receptors in Drosophila. *Science*. 287:1830-1834.
Cremona, O., and P. De Camilli. 1997. Synaptic vesicle endocytosis. *Curr Opin Neurobiol*. 7:323-330.
Crone, S.A., K.A. Quinlan, L. Zagoraiou, S. Droho, C.E. Restrepo, L. Lundfald, T. Endo, J. Setlak, T.M. Jessell, O. Kiehn, and K. Sharma. 2008. Genetic ablation of V2a ipsilateral interneurons disrupts left-right locomotor coordination in mammalian spinal cord. *Neuron*. 60:70-83.
Davis, R.L. 2005. Olfactory memory formation in Drosophila: from molecular to systems neuroscience. *Annu Rev Neurosci*. 28:275-302.
Delcomyn, F. 1980. Neural basis of rhythmic behavior in animals. *Science*. 210:492-498.
Dethier, V.G. 1976. The Hungry Fly: A Physiological Study of the Behavior Associated with Feeding.
Dimitrov, D., Y. He, H. Mutoh, B.J. Baker, L. Cohen, W. Akemann, and T. Knopfel. 2007. Engineering and characterization of an enhanced fluorescent protein voltage sensor. *PLoS One*. 2:e440.
Dunipace, L., S. Meister, C. McNealy, and H. Amrein. 2001. Spatially restricted expression of candidate taste receptors in the Drosophila gustatory system. *Curr Biol*. 11:822-835.
Enneking, E.M., S.R. Kudumala, E. Moreno, R. Stephan, J. Boerner, T.A. Godenschwege, and J. Pielage. 2013. Transsynaptic coordination of synaptic growth, function, and stability by the L1-type CAM Neuroglian. *PLoS Biol*. 11:e1001537.
Enriquez, J., L. Venkatasubramanian, M. Baek, M. Peterson, U. Aghayeva, and R.S. Mann. 2015. Specification of individual adult motor neuron morphologies by combinatorial transcription factor codes. *Neuron*. 86:955-970.
Falk, R.B.-A., N.; Atidia, J. 1976. Labellar taste organs of Drosophila melanogaster. *Journal of Morphology*. 150:327-341.
Feinberg, E.H., M.K. Vanhoven, A. Bendesky, G. Wang, R.D. Fetter, K. Shen, and C.I. Bargmann. 2008. GFP Reconstitution Across Synaptic Partners (GRASP) defines cell contacts and synapses in living nervous systems. *Neuron*. 57:353-363.
Fischer, J.A., E. Giniger, T. Maniatis, and M. Ptashne. 1988. GAL4 activates transcription in Drosophila. *Nature*. 332:853-856.
Flood, T.F., S. Iguchi, M. Gorczyca, B. White, K. Ito, and M. Yoshihara. 2013. A single pair of interneurons commands the Drosophila feeding motor program. *Nature*. 499:83-87.
Gao, Q., B. Yuan, and A. Chess. 2000. Convergent projections of Drosophila olfactory neurons to specific glomeruli in the antennal lobe. *Nat Neurosci*. 3:780-785.
Gilbert, C.D., and T.N. Wiesel. 1979. Morphology and intracortical projections of functionally characterised neurones in the cat visual cortex. *Nature*. 280:120-125.
Golic, K.G., and S. Lindquist. 1989. The FLP recombinase of yeast catalyzes site-specific recombination in the Drosophila genome. *Cell*. 59:499-509.
Gordon, M.D., and K. Scott. 2009. Motor control in a Drosophila taste circuit. *Neuron*. 61:373-384.
Gosgnach, S., G.M. Lanuza, S.J. Butt, H. Saueressig, Y. Zhang, T. Velasquez, D. Riethmacher, E.M. Callaway, O. Kiehn, and M. Goulding. 2006. V1 spinal neurons regulate the speed of vertebrate locomotor outputs. *Nature*. 440:215-219.

Gray, J. 1950. The role of peripheral sense organs during locomotion in the vertebrates. *Physiological Mechanisms in Animal Behaviour*:112-126.
Grewe, B.F., and F. Helmchen. 2009. Optical probing of neuronal ensemble activity. *Curr Opin Neurobiol*. 19:520-529.
Grienberger, C., and A. Konnerth. 2012. Imaging calcium in neurons. *Neuron*. 73:862-885.
Griesbeck, O. 2004. Fluorescent proteins as sensors for cellular functions. *Curr Opin Neurobiol*. 14:636-641.
Groth, A.C., M. Fish, R. Nusse, and M.P. Calos. 2004. Construction of transgenic Drosophila by using the site-specific integrase from phage phiC31. *Genetics*. 166:1775-1782.
Grynkiewicz, G., M. Poenie, and R.Y. Tsien. 1985. A new generation of Ca2+ indicators with greatly improved fluorescence properties. *J Biol Chem*. 260:3440-3450.
Halfon, M.S., S. Gisselbrecht, J. Lu, B. Estrada, H. Keshishian, and A.M. Michelson. 2002. New fluorescent protein reporters for use with the Drosophila Gal4 expression system and for vital detection of balancer chromosomes. *Genesis*. 34:135-138.
Hall, J.C. 1994. The mating of a fly. *Science*. 264:1702-1714.
Hamada, F.N., M. Rosenzweig, K. Kang, S.R. Pulver, A. Ghezzi, T.J. Jegla, and P.A. Garrity. 2008. An internal thermal sensor controlling temperature preference in Drosophila. *Nature*. 454:217-220.
Hammer, T.J., C. Hata, and J.C. Nieh. 2009. Thermal learning in the honeybee, Apis mellifera. *J Exp Biol*. 212:3928-3934.
Hampel, S., R. Franconville, J.H. Simpson, and A.M. Seeds. 2015. A neural command circuit for grooming movement control. *Elife*. 4.
Han, D.D., D. Stein, and L.M. Stevens. 2000. Investigating the function of follicular subpopulations during Drosophila oogenesis through hormone-dependent enhancer-targeted cell ablation. *Development*. 127:573-583.
Harris, D.T., B.R. Kallman, B.C. Mullaney, and K. Scott. 2015. Representations of Taste Modality in the Drosophila Brain. *Neuron*. 86:1449-1460.
Hayashi, S., K. Ito, Y. Sado, M. Taniguchi, A. Akimoto, H. Takeuchi, T. Aigaki, F. Matsuzaki, H. Nakagoshi, T. Tanimura, R. Ueda, T. Uemura, M. Yoshihara, and S. Goto. 2002. GETDB, a database compiling expression patterns and molecular locations of a collection of Gal4 enhancer traps. *Genesis*. 34:58-61.
Heim, N., and O. Griesbeck. 2004. Genetically encoded indicators of cellular calcium dynamics based on troponin C and green fluorescent protein. *J Biol Chem*. 279:14280-14286.
Hiroi, M., N. Meunier, F. Marion-Poll, and T. Tanimura. 2004. Two antagonistic gustatory receptor neurons responding to sweet-salty and bitter taste in Drosophila. *J Neurobiol*. 61:333-342.
Hori, S., H. Takeuchi, and T. Kubo. 2007. Associative learning and discrimination of motion cues in the harnessed honeybee Apis mellifera L. *J Comp Physiol A Neuroethol Sens Neural Behav Physiol*. 193:825-833.
Horowitz, L.F., J.P. Montmayeur, Y. Echelard, and L.B. Buck. 1999. A genetic approach to trace neural circuits. *Proc Natl Acad Sci U S A*. 96:3194-3199.
Hubel, D.H., and T.N. Wiesel. 1959. Receptive fields of single neurones in the cat's striate cortex. *J Physiol*. 148:574-591.
Huber, D., D.A. Gutnisky, S. Peron, D.H. O'Connor, J.S. Wiegert, L. Tian, T.G. Oertner, L.L. Looger, and K. Svoboda. 2012. Multiple dynamic representations in the motor cortex during sensorimotor learning. *Nature*. 484:473-478.
Huettel, S.A., A.W. Song, and G. McCarthy. 2009. Functional Magnetic Resonance Imaging (2 ed.).
Inagaki, H.K., S. Ben-Tabou de-Leon, A.M. Wong, S. Jagadish, H. Ishimoto, G. Barnea, T. Kitamoto, R. Axel, and D.J. Anderson. 2012. Visualizing neuromodulation in vivo:

TANGO-mapping of dopamine signaling reveals appetite control of sugar sensing. *Cell*. 148:583-595.
Inagaki, H.K., Y. Jung, E.D. Hoopfer, A.M. Wong, N. Mishra, J.Y. Lin, R.Y. Tsien, and D.J. Anderson. 2014. Optogenetic control of Drosophila using a red-shifted channelrhodopsin reveals experience-dependent influences on courtship. *Nat Methods*. 11:325-332.
Ito, K., K. Shinomiya, M. Ito, J.D. Armstrong, G. Boyan, V. Hartenstein, S. Harzsch, M. Heisenberg, U. Homberg, A. Jenett, H. Keshishian, L.L. Restifo, W. Rossler, J.H. Simpson, N.J. Strausfeld, R. Strauss, L.B. Vosshall, and G. Insect Brain Name Working. 2014. A systematic nomenclature for the insect brain. *Neuron*. 81:755-765.
Itskov, P.M., J.M. Moreira, E. Vinnik, G. Lopes, S. Safarik, M.H. Dickinson, and C. Ribeiro. 2014. Automated monitoring and quantitative analysis of feeding behaviour in Drosophila. *Nat Commun*. 5:4560.
Jefferis, G.S., E.C. Marin, R.J. Watts, and L. Luo. 2002. Development of neuronal connectivity in Drosophila antennal lobes and mushroom bodies. *Curr Opin Neurobiol*. 12:80-86.
Jenett, A., G.M. Rubin, T.T. Ngo, D. Shepherd, C. Murphy, H. Dionne, B.D. Pfeiffer, A. Cavallaro, D. Hall, J. Jeter, N. Iyer, D. Fetter, J.H. Hausenfluck, H. Peng, E.T. Trautman, R.R. Svirskas, E.W. Myers, Z.R. Iwinski, Y. Aso, G.M. DePasquale, A. Enos, P. Hulamm, S.C. Lam, H.H. Li, T.R. Laverty, F. Long, L. Qu, S.D. Murphy, K. Rokicki, T. Safford, K. Shaw, J.H. Simpson, A. Sowell, S. Tae, Y. Yu, and C.T. Zugates. 2012. A GAL4-driver line resource for Drosophila neurobiology. *Cell Rep*. 2:991-1001.
Kampa, B.M., W. Gobel, and F. Helmchen. 2011. Measuring neuronal population activity using 3D laser scanning. *Cold Spring Harb Protoc*. 2011:1340-1349.
Katona, G., G. Szalay, P. Maak, A. Kaszas, M. Veress, D. Hillier, B. Chiovini, E.S. Vizi, B. Roska, and B. Rozsa. 2012. Fast two-photon in vivo imaging with three-dimensional random-access scanning in large tissue volumes. *Nat Methods*. 9:201-208.
Kitamoto, T. 2001. Conditional modification of behavior in Drosophila by targeted expression of a temperature-sensitive shibire allele in defined neurons. *J Neurobiol*. 47:81-92.
Kitamoto, T. 2002. Conditional disruption of synaptic transmission induces male-male courtship behavior in Drosophila. *Proc Natl Acad Sci U S A*. 99:13232-13237.
Kitamura, K., B. Judkewitz, M. Kano, W. Denk, and M. Hausser. 2008. Targeted patch-clamp recordings and single-cell electroporation of unlabeled neurons in vivo. *Nat Methods*. 5:61-67.
Klapoetke, N.C., Y. Murata, S.S. Kim, S.R. Pulver, A. Birdsey-Benson, Y.K. Cho, T.K. Morimoto, A.S. Chuong, E.J. Carpenter, Z. Tian, J. Wang, Y. Xie, Z. Yan, Y. Zhang, B.Y. Chow, B. Surek, M. Melkonian, V. Jayaraman, M. Constantine-Paton, G.K. Wong, and E.S. Boyden. 2014. Independent optical excitation of distinct neural populations. *Nat Methods*. 11:338-346.
Komischke, B., M. Giurfa, H. Lachnit, and D. Malun. 2002. Successive olfactory reversal learning in honeybees. *Learn Mem*. 9:122-129.
Krashes, M.J., S. DasGupta, A. Vreede, B. White, J.D. Armstrong, and S. Waddell. 2009. A neural circuit mechanism integrating motivational state with memory expression in Drosophila. *Cell*. 139:416-427.
Kuffler, S.W. 1953. Discharge patterns and functional organization of mammalian retina. *J Neurophysiol*. 16:37-68.
Lai, S.L., and T. Lee. 2006. Genetic mosaic with dual binary transcriptional systems in Drosophila. *Nat Neurosci*. 9:703-709.
LaJeunesse, D.R., S.M. Buckner, J. Lake, C. Na, A. Pirt, and K. Fromson. 2004. Three new Drosophila markers of intracellular membranes. *Biotechniques*. 36:784-788, 790.
Lanuza, G.M., S. Gosgnach, A. Pierani, T.M. Jessell, and M. Goulding. 2004. Genetic identification of spinal interneurons that coordinate left-right locomotor activity necessary for walking movements. *Neuron*. 42:375-386.

Lee, A.K., I.D. Manns, B. Sakmann, and M. Brecht. 2006. Whole-cell recordings in freely moving rats. *Neuron*. 51:399-407.
Lee, T., and L. Luo. 1999. Mosaic analysis with a repressible cell marker for studies of gene function in neuronal morphogenesis. *Neuron*. 22:451-461.
Long, M.A., D.Z. Jin, and M.S. Fee. 2010. Support for a synaptic chain model of neuronal sequence generation. *Nature*. 468:394-399.
Luan, H., N.C. Peabody, C.R. Vinson, and B.H. White. 2006. Refined spatial manipulation of neuronal function by combinatorial restriction of transgene expression. *Neuron*. 52:425-436.
Luo, L., E.M. Callaway, and K. Svoboda. 2008. Genetic dissection of neural circuits. *Neuron*. 57:634-660.
Manzo, A., M. Silies, D.M. Gohl, and K. Scott. 2012. Motor neurons controlling fluid ingestion in Drosophila. *Proc Natl Acad Sci U S A*. 109:6307-6312.
Marder, E., and D. Bucher. 2001. Central pattern generators and the control of rhythmic movements. *Curr Biol*. 11:R986-996.
Marder, E., D. Bucher, D.J. Schulz, and A.L. Taylor. 2005. Invertebrate central pattern generation moves along. *Curr Biol*. 15:R685-699.
Marder, E., and R.L. Calabrese. 1996. Principles of rhythmic motor pattern generation. *Physiol Rev*. 76:687-717.
Marder, E., and V. Thirumalai. 2002. Cellular, synaptic and network effects of neuromodulation. *Neural Netw*. 15:479-493.
Masek, P., and K. Scott. 2010. Limited taste discrimination in Drosophila. *Proc Natl Acad Sci U S A*. 107:14833-14838.
McGuire, S.E., P.T. Le, A.J. Osborn, K. Matsumoto, and R.L. Davis. 2003. Spatiotemporal rescue of memory dysfunction in Drosophila. *Science*. 302:1765-1768.
Meinertzhagen, I.A. 2010. The organization of invertebrate brains: cells, synapses and circuits. *Acta Zoologica*. 91:64-71.
Menda, G., H.Y. Bar, B.J. Arthur, P.K. Rivlin, R.A. Wyttenbach, R.L. Strawderman, and R.R. Hoy. 2011. Classical conditioning through auditory stimuli in Drosophila: methods and models. *J Exp Biol*. 214:2864-2870.
Mendes, C.S., I. Bartos, T. Akay, S. Marka, and R.S. Mann. 2013. Quantification of gait parameters in freely walking wild type and sensory deprived Drosophila melanogaster. *Elife*. 2:e00231.
Miesenböck, G., D.A. De Angelis, and J.E. Rothman. 1998. Visualizing secretion and synaptic transmission with pH-sensitive green fluorescent proteins. *Nature*. 394:192-195.
Miller, A. 1950. Biology of Drosophila.
Miyawaki, A., J. Llopis, R. Heim, J.M. McCaffery, J.A. Adams, M. Ikura, and R.Y. Tsien. 1997. Fluorescent indicators for Ca2+ based on green fluorescent proteins and calmodulin. *Nature*. 388:882-887.
Montell, C. 2009. A taste of the Drosophila gustatory receptors. *Curr Opin Neurobiol*. 19:345-353.
Nagai, T., A. Sawano, E.S. Park, and A. Miyawaki. 2001. Circularly permuted green fluorescent proteins engineered to sense Ca2+. *Proc Natl Acad Sci U S A*. 98:3197-3202.
Nagel, G., M. Brauner, J.F. Liewald, N. Adeishvili, E. Bamberg, and A. Gottschalk. 2005. Light activation of channelrhodopsin-2 in excitable cells of Caenorhabditis elegans triggers rapid behavioral responses. *Curr Biol*. 15:2279-2284.
Nakai, J., M. Ohkura, and K. Imoto. 2001. A high signal-to-noise Ca(2+) probe composed of a single green fluorescent protein. *Nat Biotechnol*. 19:137-141.
Nichols, C.D., J. Becnel, and U.B. Pandey. 2012. Methods to Assay Drosophila Behavior.e3795.

Nicolai, L.J., A. Ramaekers, T. Raemaekers, A. Drozdzecki, A.S. Mauss, J. Yan, M. Landgraf, W. Annaert, and B.A. Hassan. 2010. Genetically encoded dendritic marker sheds light on neuronal connectivity in Drosophila. *Proc Natl Acad Sci U S A*. 107:20553-20558.
Nitabach, M.N., and P.H. Taghert. 2008. Organization of the Drosophila circadian control circuit. *Curr Biol*. 18:R84-93.
Nusbaum, M.P., and M.P. Beenhakker. 2002. A small-systems approach to motor pattern generation. *Nature*. 417:343-350.
Nusbaum, M.P., D.M. Blitz, A.M. Swensen, D. Wood, and E. Marder. 2001. The roles of co-transmission in neural network modulation. *Trends Neurosci*. 24:146-154.
O'Kane, C.J., and W.J. Gehring. 1987. Detection in situ of genomic regulatory elements in Drosophila. *Proc Natl Acad Sci U S A*. 84:9123-9127.
Paradis, S., S.T. Sweeney, and G.W. Davis. 2001. Homeostatic control of presynaptic release is triggered by postsynaptic membrane depolarization. *Neuron*. 30:737-749.
Peabody, N.C., J.B. Pohl, F. Diao, A.P. Vreede, D.J. Sandstrom, H. Wang, P.K. Zelensky, and B.H. White. 2009. Characterization of the decision network for wing expansion in Drosophila using targeted expression of the TRPM8 channel. *J Neurosci*. 29:3343-3353.
Pfeiffer, B.D., A. Jenett, A.S. Hammonds, T.T. Ngo, S. Misra, C. Murphy, A. Scully, J.W. Carlson, K.H. Wan, T.R. Laverty, C. Mungall, R. Svirskas, J.T. Kadonaga, C.Q. Doe, M.B. Eisen, S.E. Celniker, and G.M. Rubin. 2008. Tools for neuroanatomy and neurogenetics in Drosophila. *Proc Natl Acad Sci U S A*. 105:9715-9720.
Pfeiffer, B.D., T.T. Ngo, K.L. Hibbard, C. Murphy, A. Jenett, J.W. Truman, and G.M. Rubin. 2010. Refinement of tools for targeted gene expression in Drosophila. *Genetics*. 186:735-755.
Pielage, J., V. Bulat, J.B. Zuchero, R.D. Fetter, and G.W. Davis. 2011. Hts/Adducin controls synaptic elaboration and elimination. *Neuron*. 69:1114-1131.
Pielage, J., L. Cheng, R.D. Fetter, P.M. Carlton, J.W. Sedat, and G.W. Davis. 2008. A presynaptic giant ankyrin stabilizes the NMJ through regulation of presynaptic microtubules and transsynaptic cell adhesion. *Neuron*. 58:195-209.
Pielage, J., R.D. Fetter, and G.W. Davis. 2005. Presynaptic spectrin is essential for synapse stabilization. *Curr Biol*. 15:918-928.
Poodry, C.A. 1990. shibire, a neurogenic mutant of Drosophila. *Dev Biol*. 138:464-472.
Potter, C.J., and L. Luo. 2011. Using the Q system in Drosophila melanogaster. *Nat Protoc*. 6:1105-1120.
Rajashekhar, K.P., and R.N. Singh. 1994. Organization of Motor-Neurons Innervating the Proboscis Musculature in Drosophila-Melanogaster Meigen (Diptera, Drosophilidae). *Int J Insect Morphol*. 23:225-242.
Ramón y Cajal, S. 1888. Estructura de los centros nerviosos de las aves. *Rev. Trim. Histol. Norm. Pat*. 1:1-10.
Ramón y Cajal, S. 1899. Estudios sobre la cortexa cerebral humana. *Corteza visual. Rev. Trim. Microgr.* 4:1-63.
Reichert, H.W.J.J.H., G. 1981. Crayfish Escape Behavior: Neurobehavioral Analysis of Phasic Extension reveals Dual Systems for Motor Control. *Journal of Comparative Physiology*. 142:687-717.
Ritzenthaler, S., E. Suzuki, and A. Chiba. 2000. Postsynaptic filopodia in muscle cells interact with innervating motoneuron axons. *Nat Neurosci*. 3:1012-1017.
Riveros, A.J., and W. Gronenberg. 2009. Olfactory learning and memory in the bumblebee Bombus occidentalis. *Naturwissenschaften*. 96:851-856.
Romoser, V.A., P.M. Hinkle, and A. Persechini. 1997. Detection in living cells of Ca2+-dependent changes in the fluorescence emission of an indicator composed of two green fluorescent protein variants linked by a calmodulin-binding sequence. A new class of fluorescent indicators. *J Biol Chem*. 272:13270-13274.

Rosenzweig, M., K.M. Brennan, T.D. Tayler, P.O. Phelps, A. Patapoutian, and P.A. Garrity. 2005. The Drosophila ortholog of vertebrate TRPA1 regulates thermotaxis. *Genes Dev*. 19:419-424.

Rosenzweig, M., K. Kang, and P.A. Garrity. 2008. Distinct TRP channels are required for warm and cool avoidance in Drosophila melanogaster. *Proc Natl Acad Sci U S A*. 105:14668-14673.

Sadaf, S., O.V. Reddy, S.P. Sane, and G. Hasan. 2015. Neural control of wing coordination in flies. *Curr Biol*. 25:80-86.

Sakai, R., V. Repunte-Canonigo, C.D. Raj, and T. Knopfel. 2001. Design and characterization of a DNA-encoded, voltage-sensitive fluorescent protein. *Eur J Neurosci*. 13:2314-2318.

Sakai, T., J. Kasuya, T. Kitamoto, and T. Aigaki. 2009. The Drosophila TRPA channel, Painless, regulates sexual receptivity in virgin females. *Genes Brain Behav*. 8:546-557.

Sankaranarayanan, S., and T.A. Ryan. 2000. Real-time measurements of vesicle-SNARE recycling in synapses of the central nervous system. *Nat Cell Biol*. 2:197-204.

Schroll, C., T. Riemensperger, D. Bucher, J. Ehmer, T. Voller, K. Erbguth, B. Gerber, T. Hendel, G. Nagel, E. Buchner, and A. Fiala. 2006. Light-induced activation of distinct modulatory neurons triggers appetitive or aversive learning in Drosophila larvae. *Curr Biol*. 16:1741-1747.

Scott, K., R. Brady, Jr., A. Cravchik, P. Morozov, A. Rzhetsky, C. Zuker, and R. Axel. 2001. A chemosensory gene family encoding candidate gustatory and olfactory receptors in Drosophila. *Cell*. 104:661-673.

Seeds, A.M., P. Ravbar, P. Chung, S. Hampel, F.M. Midgley, Jr., B.D. Mensh, and J.H. Simpson. 2014. A suppression hierarchy among competing motor programs drives sequential grooming in Drosophila. *Elife*. 3:e02951.

Shiga, Y., M. Tanaka-Matakatsu, and S. Hayashi. 1996. A nuclear GFP/ beta-galactosidase fusion protein as a marker for morphogenesis in living Drosophila. *Development, Growth and Differentiation*. 38:99-106.

Shiraiwa, T. 2008. Multimodal chemosensory integration through the maxillary palp in Drosophila. *PLoS One*. 3:e2191.

Shiraiwa, T., and J.R. Carlson. 2007. Proboscis extension response (PER) assay in Drosophila. *J Vis Exp*:193.

Siegel, M.S., and E.Y. Isacoff. 1997. A genetically encoded optical probe of membrane voltage. *Neuron*. 19:735-741.

Sineshchekov, O.A., K.H. Jung, and J.L. Spudich. 2002. Two rhodopsins mediate phototaxis to low- and high-intensity light in Chlamydomonas reinhardtii. *Proc Natl Acad Sci U S A*. 99:8689-8694.

Singh, R.N. 1997. Neurobiology of the gustatory systems of Drosophila and some terrestrial insects. *Microsc Res Tech*. 39:547-563.

Sperry, R.W. 1943. Effect of 180 Degree Rotation of the Retinal Field on Visuomotor Coordination. *Journal of Experimental Zoology*. 92:263-279.

Stephan, R., B. Goellner, E. Moreno, C.A. Frank, T. Hugenschmidt, C. Genoud, H. Aberle, and J. Pielage. 2015. Hierarchical microtubule organization controls axon caliber and transport and determines synaptic structure and stability. *Dev Cell*. 33:5-21.

Stocker, R.F. 1994. The organization of the chemosensory system in Drosophila melanogaster: a review. *Cell Tissue Res*. 275:3-26.

Stockinger, P., D. Kvitsiani, S. Rotkopf, L. Tirian, and B.J. Dickson. 2005. Neural circuitry that governs Drosophila male courtship behavior. *Cell*. 121:795-807.

Struhl, G., and K. Basler. 1993. Organizing activity of wingless protein in Drosophila. *Cell*. 72:527-540.

Sweeney, S.T., K. Broadie, J. Keane, H. Niemann, and C.J. O'Kane. 1995. Targeted expression of tetanus toxin light chain in Drosophila specifically eliminates synaptic transmission and causes behavioral defects. *Neuron*. 14:341-351.

Thorne, N., S. Bray, and H. Amrein. 2005. Function and expression of the Drosophila gr genes in the perception of sweet, bitter and pheromone compounds. *Chem Senses*. 30 Suppl 1:i270-272.

Thorne, N., C. Chromey, S. Bray, and H. Amrein. 2004. Taste perception and coding in Drosophila. *Curr Biol*. 14:1065-1079.

Tissot, M., N. Gendre, and R.F. Stocker. 1998. Drosophila P[Gal4] lines reveal that motor neurons involved in feeding persist through metamorphosis. *J Neurobiol*. 37:237-250.

van der Bliek, A.M., and E.M. Meyerowitz. 1991. Dynamin-like protein encoded by the Drosophila shibire gene associated with vesicular traffic. *Nature*. 351:411-414.

Venken, K.J., J.H. Simpson, and H.J. Bellen. 2011. Genetic manipulation of genes and cells in the nervous system of the fruit fly. *Neuron*. 72:202-230.

Vosshall, L.B., A.M. Wong, and R. Axel. 2000. An olfactory sensory map in the fly brain. *Cell*. 102:147-159.

Wagh, D.A., T.M. Rasse, E. Asan, A. Hofbauer, I. Schwenkert, H. Durrbeck, S. Buchner, M.C. Dabauvalle, M. Schmidt, G. Qin, C. Wichmann, R. Kittel, S.J. Sigrist, and E. Buchner. 2006. Bruchpilot, a protein with homology to ELKS/CAST, is required for structural integrity and function of synaptic active zones in Drosophila. *Neuron*. 49:833-844.

Wang, J.W., A.M. Wong, J. Flores, L.B. Vosshall, and R. Axel. 2003. Two-photon calcium imaging reveals an odor-evoked map of activity in the fly brain. *Cell*. 112:271-282.

Wang, L., and D.J. Anderson. 2010. Identification of an aggression-promoting pheromone and its receptor neurons in Drosophila. *Nature*. 463:227-231.

Wang, L., H. Dankert, P. Perona, and D.J. Anderson. 2008. A common genetic target for environmental and heritable influences on aggressiveness in Drosophila. *Proc Natl Acad Sci U S A*. 105:5657-5663.

Wang, Z., A. Singhvi, P. Kong, and K. Scott. 2004. Taste representations in the Drosophila brain. *Cell*. 117:981-991.

White, J.G., E. Southgate, J.N. Thomson, and S. Brenner. 1986. The structure of the nervous system of the nematode Caenorhabditis elegans. *Philos Trans R Soc Lond B Biol Sci*. 314:1-340.

Wickersham, I.R., D.C. Lyon, R.J. Barnard, T. Mori, S. Finke, K.K. Conzelmann, J.A. Young, and E.M. Callaway. 2007. Monosynaptic restriction of transsynaptic tracing from single, genetically targeted neurons. *Neuron*. 53:639-647.

Wilson, C.J., and P.M. Groves. 1981. Spontaneous firing patterns of identified spiny neurons in the rat neostriatum. *Brain Res*. 220:67-80.

Wing, J.P., L. Zhou, L.M. Schwartz, and J.R. Nambu. 1998. Distinct cell killing properties of the Drosophila reaper, head involution defective, and grim genes. *Cell Death Differ*. 5:930-939.

Yarmolinsky, D.A., C.S. Zuker, and N.J. Ryba. 2009. Common sense about taste: from mammals to insects. *Cell*. 139:234-244.

Yasunaga, K., K. Saigo, and T. Kojima. 2006. Fate map of the distal portion of Drosophila proboscis as inferred from the expression and mutations of basic patterning genes. *Mech Dev*. 123:893-906.

Yeh, E., K. Gustafson, and G.L. Boulianne. 1995. Green fluorescent protein as a vital marker and reporter of gene expression in Drosophila. *Proc Natl Acad Sci U S A*. 92:7036-7040.

Zhang, F., M. Prigge, F. Beyriere, S.P. Tsunoda, J. Mattis, O. Yizhar, P. Hegemann, and K. Deisseroth. 2008a. Red-shifted optogenetic excitation: a tool for fast neural control derived from Volvox carteri. *Nat Neurosci*. 11:631-633.

Zhang, F., L.P. Wang, E.S. Boyden, and K. Deisseroth. 2006. Channelrhodopsin-2 and optical control of excitable cells. *Nat Methods*. 3:785-792.
Zhang, J., G.M. Lanuza, O. Britz, Z. Wang, V.C. Siembab, Y. Zhang, T. Velasquez, F.J. Alvarez, E. Frank, and M. Goulding. 2014. V1 and v2b interneurons secure the alternating flexor-extensor motor activity mice require for limbed locomotion. *Neuron*. 82:138-150.
Zhang, Y., S. Narayan, E. Geiman, G.M. Lanuza, T. Velasquez, B. Shanks, T. Akay, J. Dyck, K. Pearson, S. Gosgnach, C.M. Fan, and M. Goulding. 2008b. V3 spinal neurons establish a robust and balanced locomotor rhythm during walking. *Neuron*. 60:84-96.
Zhang, Y.Q., C.K. Rodesch, and K. Broadie. 2002. Living synaptic vesicle marker: synaptotagmin-GFP. *Genesis*. 34:142-145.
Zhao, G., and M. Hortsch. 1998. The analysis of genomic structures in the L1 family of cell adhesion molecules provides no evidence for exon shuffling events after the separation of arthropod and chordate lineages. *Gene*. 215:47-55.
Zhou, L., A. Schnitzler, J. Agapite, L.M. Schwartz, H. Steller, and J.R. Nambu. 1997. Cooperative functions of the reaper and head involution defective genes in the programmed cell death of Drosophila central nervous system midline cells. *Proc Natl Acad Sci U S A*. 94:5131-5136.

6.4 Curriculum Vitae

PERSONAL DATA

Name	Olivia Schwarz
Date of Birth	3rd October 1985
Place of Birth	Baden, Switzerland
Address	Sonnenbergstrasse 18, 4127 Birsfelden

EDUCATION

2011 – now **Ph.D. in Neuroscience, Friedrich Miescher Institute, Basel, Switzerland**
Ph.D. thesis: „Identification and characterization of the motor program controlling the proboscis extension response"

2008 – 2010 **Master in Neurosciences, ETH Zürich, Switzerland**
Master thesis: „Effect of neuronal Nogo-A on neurite outgrowth in vitro"

2005 – 2008 **ETH Zürich, Switzerland**
Bachelor degree in Biology

2001 – 2005 **Gymnasium, Baden, Switzerland**
Matura

RESEARCH AND WORK EXPERIENCE

2011 – now Friedrich Miescher Institute for Biomedical Research, Basel, Switzerland
Ph.D. student, Department for Neurosciences, group of Dr. Jan Pielage

2010 – 2011 Brain Research Institute, University and ETH Zürich, Switzerland
Technician, group of Prof. Dr. Martin E. Schwab
Main project: „Nogo-A upregulation in injured neurons of the central nervous system positively modulates their regenerative response"

2009 – 2010 Brain Research Institute, University and ETH Zürich, Switzerland
Master thesis „Effect of neuronal Nogo-A on neurite outgrowth in vitro"
Group of Prof. Dr. Martin E. Schwab

2009 Brain Research Institute, University and ETH Zürich, Switzerland
Semester thesis „Characterization of a new genetically encoded calcium indicator by viral delivery into the adult mouse barrel cortex"
Group of Prof. Dr. Fritjof Helmchen

ADDITIONAL COURSES

April 2014 **Kavli Institute meets Friedrich Miescher Institute**, Copenhagen, Denmark
Workshop for the communication between different neuroscientific fields of research

June – July 2012 **Summer school at Cold Spring Harbor Laboratory**, New York, USA
Drosophila Neurobiology: Genes, Circuits & Behavior

PRESENTATIONS AND POSTERS (SELECTION)

September 2015 — **European Symposium for Insect Taste and Olfaction (ESITO)**, Villasimius, Italy
„Identification of the Neuronal Circuitry Controlling *Drosophila* Taste Behavior"
Presentation

September 2014 — **FMI annual meeting**, Pontresina, Switzerland
„The Adult Taste Circuitry of *Drosophila*"
Presentation

June 2014 — **Swiss Fly meeting**, Fribourg, Switzerland
„Identification of the Neuronal Circuitry Controlling *Drosophila* Taste Behavior"
Presentation

April 2014 — **Federation of European Neuroscience Societies (FENS) conference**, Copenhagen, Denmark
„Identification of the Motor Program Controlling *Drosophila* Taste Behavior"
Poster

HOBBIES AND INTERESTS

Captain of a National League A Basketball Team

Enjoy the mountains by snowboarding and downhill biking

Jigsaw Puzzles

PUBLICATIONS

Schwarz O, Asgar Bohra A, Liu X, Reichert H, VijayRaghavan K, Pielage J
„Neuroanatomical and Functional Characterization of Motoneurons Controlling the proboscis extension response motor sequence"
In preparation

Pernet V, Joly S, Dalkara D, Jordi N, **Schwarz O**, Christ F, Schaffer DV, Flannery JG, Schwab ME
„Long-distance axonal regeneration induced by CNTF gene transfer is impaired by axonal misguidance in the injured adult optic nerve"
Neurobiology of Disease, 2013

Pernet V, Joly S, Dalkara D, **Schwarz O**, Christ F, Schaffer D, Flannery JG, Schwab ME
„Neuronal Nogo-A upregulation does not contribute to ER stress-associated apoptosis but participates in the regenerative response in the axotomized adult retina"
Cell Death and Differentiation, 2011

6.5 Acknowledgement

This work would not have been possible without the support of many people.

Most importantly, I would like to thank Jan for the excellent supervision, the helpful support, and the open door for inspiring scientific discussions throughout the last four years. Thank you for giving me the opportunity to do my PhD in your lab on the exciting and challenging *Drosophila* taste project. It was just a fantastic time!

I am very grateful to Prof. Dr. Heinrich Reichert, Prof. Dr. Silvia Arber, and Prof. Dr. Andreas Lüthi for joining my PhD committee and for their helpful advices and support.

A special thank goes to the whole Pielage lab, especially to Dominique for the time at the bench and on the balcony and on different sports areas around Basel. In particular, I also want to thank Xinyu for performing the screen together with me and for the funny German teaching sessions.

I would also like to thank the whole FMI for generating this inspiring, fruitful, and friendly working atmosphere. Big thanks go to Steve Bourke from the FAIM facility for the kind and patient instructions and for making the nicest image of a Drosophila head.

An dieser Stelle möchte ich mich ganz besonders bei meiner Familie bedanken, die mich während meines Studiums und der Doktorarbeit bedingungslos unterstützt haben und auf die ich mich immer verlassen konnte.

Ich möchte Dominic für die starke Schulter, die beruhigenden Worte und das grosse Verständnis von Herzen danken.

Ein spezieller Dank gilt meinen Freunden und meinem Korbball-Team in Bachs für all die erlebnisreichen und schönen Stunden neben der Arbeit, die ich gebraucht habe, um abzuschalten und wieder Energie zu tanken.

„ In science, one can learn the most by studying what seems the least”

Marvin Minsky